Characterization of a bacterial-like signal transduction phosphorelay in *Methanosarcina acetivorans*

"vom Fachbereich Biologie der Technischen Universität Kaiserslautern zur Verleihung des akademischen Grades Dr.rer.nat. genehmigte Dissertation"

angefertigt im

Fachbereich Biologie

Abteilung Mikrobiologie

vorgelegt von

Anne Sexauer

Referent: Prof. Dr. Nicole Frankenberg-Dinkel

Korreferent: Prof. Dr. Matthias Hahn

Vorsitz: Prof. Dr. Stefan Kins

D386

Kaiserslautern, den 2.7.2021

Eidesstattliche Erklärung

Ich erkläre hiermit an Eides statt, dass ich die vorliegende Dissertation selbständig und ohne Benutzung anderer als angegebenen Hilfsmittel angefertigt habe. Die aus fremden Quellen übernommenen Gedanken sind ausnahmslos als solche kenntlich gemacht. Die Promotionsordnung des Fachbereichs Biologie der TU Kaiserslautern ist mir in der derzeit gültigen Fassung bekannt. Die Ergebnisse anderer Mitarbeiter sowie anderer Autoren wurden klar gekennzeichnet. Die Dissertation oder Teile daraus wurden in keinem anderen Fachbereich oder keiner anderen Fakultät als Prüfungsarbeit eingereicht. Ich habe zu keinem früheren Zeitpunkt an einer anderen Universität ein Promotionsverfahren beantragt.

City, date

Anne Sexauer Signature

Danksagung

An dieser Stelle möchte ich mich herzlich bei meiner Doktormutter Frau Prof. Dr. Nicole Frankenberg-Dinkel für die Betreuung über all die Jahre und das interessante Thema meiner Doktorarbeit bedanken. Vielen Dank für die Unterstützung auch in stürmischen Zeiten, die Motivation, wenn es mal schwer wurde und all das entgegengebrachte Vertrauen. Außerdem möchte ich mich für die Ermöglichung neue Methoden zu erlernen und die Teilnahme an internationalen Konferenzen bedanken.

Herrn Prof. Dr. Hahn danke ich sehr für die freundliche Übernahme des Korreferats bedanken.

Bei Herrn Prof. Dr. Kins möchte ich mich für die Bereitschaft den Vorsitz für die Promotionskommission zu übernehmen recht herzlich bedanken.

Ich möchte mich bei Prof. Dr. Neuhaus für die Bereitstellung der Geräte aus seinem Labor bedanken.

Ich möchte mich bei Frau Dr. Ilka Haferkamp sehr herzlich für die Problemlösung meiner Kinase Assays und für die regelmäßige Hilfe bei der Bestellung der Radioaktivität bedanken.

Mein herzlichster Dank gilt Herrn Dr. Oliver Trentmann. Danke lieber Olli für deine Ermutigungen, deine Hilfe und Rat. Wer dich als Freund hat, kann sich glücklich schätzen!

Bei dem Mibi-Team will ich mich herzlich bedanken. Danke für die oft so gute Stimmung, die vieles wett gemacht hat. Schön, dass ich in vielen von euch Freunde gefunden habe. Vielen lieben Dank auch an Susanne. Für ihre Aufmunterungen und die vielen guten Ratschläge. Danke liebe Christine Förster-Schorr für die Unterstützung beim Klonieren. Vielen Dank liebe Uti, dass du mich immer so gut versorgt hast, in Rat und Tat :)

Ohne Familie und Freunde wäre all das nicht möglich gewesen. Mein größter Dank gilt deshalb meiner Familie und meinen Freunden. Für die finanzielle Unterstützung, die Aufmunterungen und dafür dass ihr an mich geglaubt habt. Danke an alle dich mich im Gebet unterstützt haben, denn nur mit meinem Glauben konnte ich Hürden überwinden.

Widmung

Für meine liebste Mama

Table of contents

Abbreviation

ε	molar extinction coefficient
aa	amino acid
AU	absorbance unit
BCIP	5-bromo-4-chloro-3-indolyl phosphate
bp	base pair
CA	catalytic and ATP binding domain
CHASE	cyclases/histidine kinases associated sensory extracellular
DHp	dimerization and histidine phosphotransfer domain
DEPC	diethylpyrocarbonate
DNA	deoxyribonucleic acid
DTH	sodium dithionite
DTT	dithiothreitol
Fe(II)	Fe(II) heme complex, or hemin
Fe(III)	Fe(III) heme complex, or hemin
GAF	domain conserved in cyclic GMP-specific and stimulated phosphodiesterases, adenylate cyclases and *E. coli* formate hydrogen lyase transcriptional activator
h	hour
HAMP	present in histidine kinases, adenyl cyclases, methyl-accepting proteins and phosphatases
HPt	histidine phosphotransfer
HTH	helix-turn-helix
IPTG	isopropyl-β-thiolgalactosidase
LB	lysogeny broth
LMW	low molecular weight
Min	minute
MW	molecular weight
MWCO	molecular weight cut off
NBT	nitro blue tetrazolium chloride
OCS	one-component system
ORF	open reading frame
PAS	Per (Drosophila period clock protein)/Arnt (vertebrate aryl hydrocarbon receptor nuclear translocator)/Sim (Drosophila single-minded protein)
PCR	polymerase chain reaction
PVDF	polyvinylidene fluoride
R	receiver domain
RR	response regulator
RNA	ribonucleic acid
rpm	revolutions per minute
RT	room temperature
S	second
SDS	sodium dodecyl sulfate
SDS-PAGE	sodium dodecyl sulfate-polyacrylamide gel electrophoresis
SEC	Size exclusion chromatography
TCS	two-component system
TEMED	N,N,N',N'-tetramethylethane-1,2-diamine
UV/vis	Ultraviolet/visible
v/v	volume per volume
w/	with
w/o	without

w/v	weight per volume
wt	wild-type

1 Introduction

For the survival of all organisms, it is essential to react in a fast way to environmental changes by sensing a signal and responding to it. Variation, for example in pH values, temperature, light, or nutrition gradients can result in an adaptation of the organism by altering enzyme activity, modifying gene expression, or changing motile behavior. For achieving this cell response, cellular processes like protein modification are needed. The main mechanism of protein modification is the well-understood protein phosphorylation that ultimately results in modified gene expression or enzyme activity. Phosphorylation and dephosphorylation of the protein modification, improving signaling mechanism in the cell, is performed by proteins called kinases and phosphatases. Autophosphorylation activity of the kinases provides phosphorylation of specific amino acid residues, which results in activation of a cognate regulator after receiving the phosphoryl group. Most bacterial kinases involve two components, a histidine kinase and a cognate response regulator (RR) that is the most abundant form for such pathways compared to Hanks type kinases that get autophosphorylated at a Ser/Tyr/Thr residue (Rorbert B. Bourret et al., 1991; Rudolph and Oesterhelt, 1995; Stock et al., 1989b; Gao and Stock, 2009; Stock et al., 1995; Appleby et al., 1996; Stock et al., 2000; Steven Hanks and Tony Hunter, 1995).

1.1 Evolution of two-component systems

It is assumed that the first signal transduction system, possessed by a common ancestor of all three domains of life, was the one-component system (OCS). This system consists of a fused input and output domain. Sequence analysis provided cytoplasmatic located input domains and DNA binding HTH domains as output domains (Ulrich et al., 2005; Esser et al., 2016; Kennelly, 2003; Koretke et al., 2000).

The more complex two-component systems (TCS) evolved in Bacteria by co-evolution. The co-evolution model assumes this development by genome-wide duplication with following gene segregation, supported by the frequent occurrence of these systems (Koretke et al., 2000). TCS radiated to Archaea and Eukaryotes via horizontal gene transfer. Evidence is that mostly all Bacteria, except the genus Mycoplasma, possess two-component systems. Those systems are monophyletic which is not the case in Archaea. Also, not in all Archaea, TCS are available and their clusters are mostly related to bacterial ones. Eukaryotic TCS can only be found in protists and some fungi

but not in higher developed organisms (Esser et al., 2016; Koretke et al., 2000). One hypothesis for the origin of the Ser/Tyr/Thr kinases is that a common ancestor with a progenitor kinase gene existed before the partition of the eucaryotic kingdoms. Due to the identification of eukaryotic kinases in prokaryotes, it is suggested that a common ancestor possessed an ancestral kinase gene before the division of Prokaryotes and Eukaryotes (Steven Hanks and Tony Hunter, 1995). While it is more and more suggested that an ancestral kinase gene existed before the divergence of all three domains of life, radiating into all domains in equal shares (Stancik et al., 2018; Leonard et al., 1998).

1.2 Signal transduction of two-component systems

For accomplishing signal sensing and signal transduction inside the cell, typically structured histidine kinases possess a transmembrane signal domain and a cytoplasmic kinase catalytic core. The sensed signal leads to autophosphorylation of the kinase catalytic core with following phosphotransfer of the γ-phosphate to the cognate RR.

Depending on the organism, different sensor transmembrane domains evolved like the **C**a21 channels and **c**hemotaxis receptors (Cache) domain, binding amino acids, and the **c**yclases/**h**istidine kinases **a**ssociated **s**ensory **e**xtracellular (CHASE) domain that is predicted to bind small peptides and plant hormones and could therefore be involved in developmental processes. (Pas et al., 2004; Anantharaman and Aravind, 2000; Vivek Anantharaman and L. Aravind, 2001). Most transmembrane domains contain a ligand-binding domain, however, due to their big variety, these domains are not highly conserved. A well-characterized architecture for transmembrane signaling is the α-helical structure of periplasmic ligand-binding domains. Examples are the nitrate sensing kinase NarX (Cheung and Hendrickson, 2009) from *Escherichia coli* possessing a four-helical bundle that is similar to the aspartate sensor Tar (Gardina et al., 1998). Another structure of an extracellular ligand-binding domain is the PDC fold named after the kinases PhoQ (Cho et al., 2006), DcuS (Pappalardo et al., 2003), and CitA (Reinelt et al., 2003). The structural arrangement of the fold is a long N-terminal α-helix followed by a β-sheet enclosed by α-helices. The fold is similar to the sensor domain **P**er-**A**RNT-**S**im (PAS) in structure but not in function, as it shows no high dimerization affinity. Instead, the dimer subunits can be differently oriented subsequently affecting the signal state of the kinase (Cho et al., 2006; Gao and Stock,

2009). Another way of signal transduction is by indirect perception. In *Vibrio harveyi,* interaction of LuxQ with a periplasmic AI-2 binding protein LuxP leads to the sensing of the quorum-sensing signal autoinducer-2 (AI-2). This indirect perception results in an asymmetrical dimerization of the LuxPQ complex whereas the kinase catalytic core subsequently forms an asymmetrical dimer that inhibits kinase activity (Gao and Stock, 2009; Freeman et al., 2000).

For most kinases, the signal is still unknown and some kinases sense stimuli without binding a ligand. Removing for example the periplasmic sensor domain of the osmosensor EnvZ from *E. coli* has no inhibiting effect on kinase activity. This concludes that the kinase perceives stimuli most likely by interaction with other membrane proteins (Wolanin and Stock, 2003).

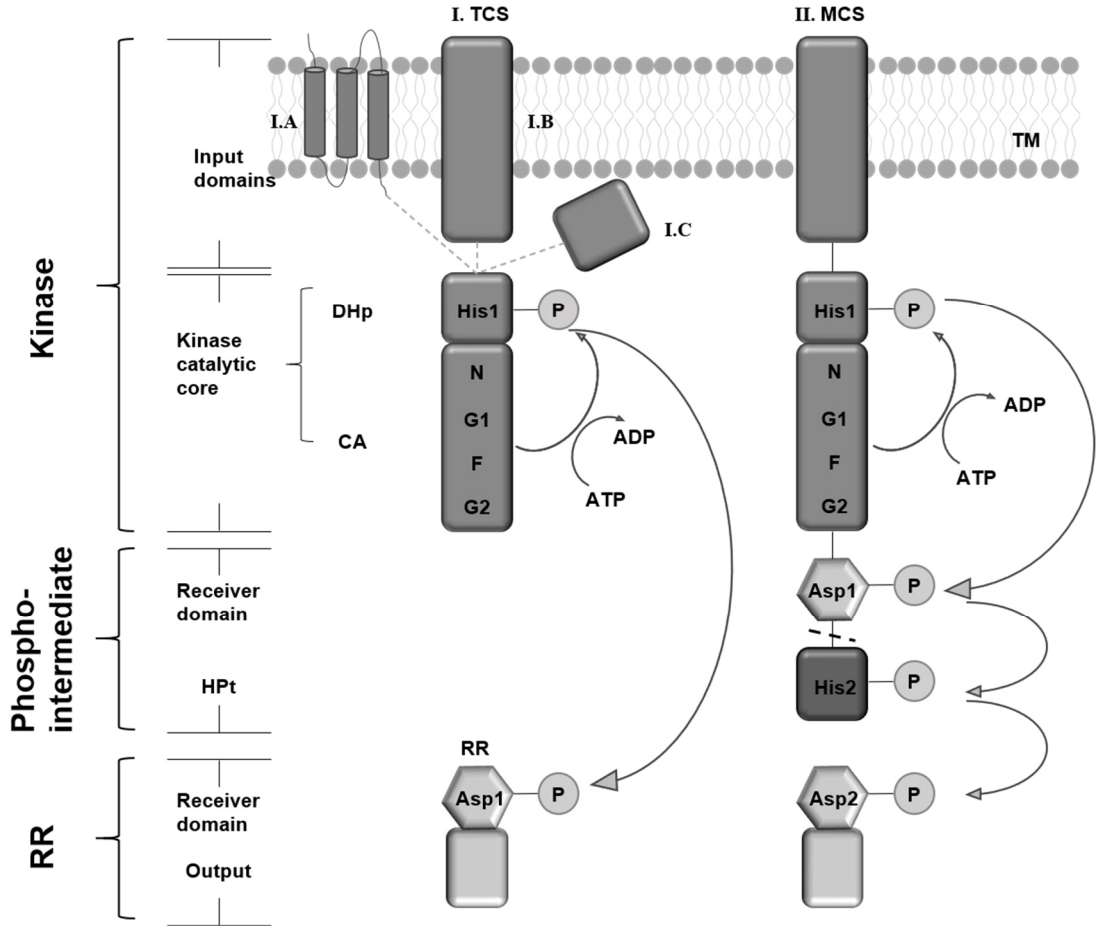

Figure 1.1. Domain organization and signal transduction of two- and multi-component systems. I. A classical two-component system consists of a histidine kinase (HK) and a response regulator (RR). The HK can be located in the transmembrane domain without sensing a stimulus, **I.A** sensing a signal with an extracytoplasmic sensor domain **I.B** or with a cytoplasmatic sensor domain **I.C**. The kinase catalytic core containing a DHp and CA domain hydrolyzes ATP in the CA domain and transfers the phosphate to a specific histidine (His1) residue in the DHp domain. The phosphate is transferred to a conserved aspartate (Asp1) located in the receiver domain of the RR possessing an output domain. **II.** In the MCS the hybrid histidine kinase autophosphorylates at a conserved histidine residue (His1) in the DHp domain subsequently the phosphoryl group gets transferred to a fused receiver domain (Asp1) and further to a histidine phosphotransfer (HPt) domain (His2) that can be fused or single standing (dashed line). The next phosphoacceptor in the phosphorelay is the RR with conserved aspartate (Asp2) in the receiver domain and the following output domain. Adapted from (Jung et al., 2012).

After a signal is detected, it has to be forwarded to the kinase catalytic core. C-terminal of the transmembrane domain mostly HAMP domains, named after its presence in **h**istidine kinases (HKs), **a**denylyl cyclases, **m**ethyl-accepting chemotaxis proteins (MCPs), and some **p**hosphatases, are located. Signal transmission is accomplished by rotation or piston movement of the HAMP domain (Gao and Stock, 2009; Parkinson, 2010). Kinases possessing no transmembrane domain are cytoplasmically localized like the kinase CheA from *E. coli* that is involved in chemotaxis signaling (Gao and Stock, 2009). Present in all kingdoms and the most common cytoplasmic sensor displays the PAS domain, named after a sequence similarity of proteins in *Drosophila* and vertebrates. PAS domains occur in cytoplasmic kinases but also in transmembrane located kinases that contain several sensor domains, where PAS is located in the cytoplasm. These domains can sense various physical and chemical signals by binding cofactors for the perception of light, redox state, and gases. An example is FixL from *Bradyrhizobium japonicum* and *Rhizobium meliloti*, possessing a heme cofactor enabling the perception of oxygen or ions and small ligands. In addition to its many functions, the PAS domain is responsible for the protein-protein interaction which mediates signal transduction in the case of the kinase KinA of *B. subtilis* (Lee et al., 2008; Taylor and Zhulin, 1999; Gilles-Gonzalez and Gonzalez, 2004; Möglich et al., 2009) Another widespread cytoplasmic sensor domain is the GAF domain named after its detection in c**G**MP-specific phosphodiesterases, **a**denylyl cyclases and the transcriptional activator **F**hlA (Aravind, L. and Ponting, C. P., 1997).

After perceiving the signal and transferring it inside the cell, it is activating the kinase catalytic core which consists of a dimerization and histidine phosphotransfer (DHp) domain and a catalytic and ATP binding (CA) domain (Zschiedrich et al., 2016; Bhate et al., 2015; Stock et al., 2000). The catalytic domain contains a conserved motif of N, G1, F, and G2 residues that form the ATP binding cavity. F and G2 residues are forming the ATP lid binding one molecule ATP together with two helices. The nucleotide gets hydrolyzed and the γ-phosphate subsequently transferred to the nitrogen atom of the catalytic histidine, located in the DHp domain (Bhate et al., 2015; Kim and Forst, 2001; Zhang and Shi, 2005; Appleby et al., 1996; Gao and Stock, 2009). The DHp domain includes two helices that are connected by a hairpin loop. Together they form a DHp bundle which functions as a binding interface of the RR (Zschiedrich et al., 2016; Capra and Laub, 2012; Podgornaia and Laub, 2013). The RR binds to the

interface and catalyzes its phosphorylation by transferring the phosphoryl group to the conserved aspartate residue in its N-terminal receiver domain. Phosphorylation triggers most receiver domains of the RR to dimerize as homo-dimer or multimer (Hong et al., 2007; Nguyen et al., 2000). This conformational change leads to the transformation of the input signal to a cellular output by activating the N-terminal effector domain of the RR. The effector domain can bind to DNA, RNA, proteins or it can be enzymatically active which might lead to a diverse cell response (Zschiedrich et al., 2016). After all, research revealed TCS not just as a simple input-output mechanism, in contrary as more complex systems that are involved in many cross-regulations (Jung et al., 2012).

1.3 Signal transduction in multi-component systems

The classical TCS consists of a two-step phosphorelay (His-Asp) including the histidine kinase and its RR. After receiving a signal, the autophosphorylated kinase gets phosphorylated at a histidine residue (His) subsequently the phosphate is transferred to a conserved aspartate (Asp) in the cognate RR (Rorbert B. Bourret et al., 1991). Through evolution multi-component systems (MCS) evolved which consist of an expanded two-component system and reveal a four-step phosphorelay (His1-Asp1-His2-Asp2). These systems possess a histidine kinase (His1) that transfers the phosphate after autophosphorylation to the C-terminal fused receiver domain (Asp1) referred to as hybrid kinase (His1-Asp1). The phosphate is transferred to a histidine phosphotransfer (HPt) domain (His2) that can be fused to the hybrid kinase domain. HPt domains serve as intermediates in the phosphorelay by getting phosphorylated at the conserved histidine residue (His2), located in a kinase-like structure but show no catalytic activity. Due to their high variability HPt domains are not easy to annotate as they show 20% sequence similarity (Kato et al., 1997; Mourey et al., 2001). Finally, the output RR in the phosphorelay is phosphorylated at a conserved aspartate (Asp2), causing a specific cell response to the detected stimuli (Appleby et al., 1996).

It is supposed that these systems evolved through gene duplication of one-component systems and further integrated components from other heterologous systems called the recruitment model. The assumption for this model is that kinases and regulators are not sharing the same cluster but are still able to conduct signal transduction as it is known from the kinases ArcB, TorS, and EvgS to phosphorylate RRs in non-cognate clusters (Koretke et al., 2000). There are different opinions if it is beneficial for

organisms to use hybrid kinases as a signal transduction system referring structurally to the fused input and output domain, relating to the one-component system (Ulrich et al., 2005). Otherwise, using a His1-Asp1-His2-Asp2 phosphorelay system allows a more complex signal transduction network by including an extra receiver and histidine phosphotransfer domain (HPt) which means an extra phosphate acceptor and donor that is exposed for cross-talk with phosphatases and kinases (Gao and Stock, 2009). Another potential benefit occurs by using hybrid systems that might transfer information more directly and therefore faster compared to signal cascades (Zhang and Shi, 2005; Esser et al., 2016; Cock and Whitworth, 2007; Koretke et al., 2000). The first described multi-phosphorelay includes four proteins involved in the sporulation of *Bacillus subtilis*. Receiving a signal, one of the three sensor kinases KinA, KinB, KinC autophosphorylates and transfers the signal to the receiver SpoOF (Asp1). The next phosphoacceptor SpoOB (His2) in the relay is a HPt domain and finally, the RR SpoOA (Asp2) containing the output function is phosphorylated (Burbulys et al., 1991). Later described hybrid systems including the TCS BvgSA involved in virulence of *Bordetella pertussis* details a phosphorelay in one protein (Uhl and Miller, 1996). Belonging to the BvgS family is the identified hybrid system ArcB (Iuchi, 1993), EvgS, and BarA in *E. coli* (Nagasawa et al., 1992; Mizuno, 1997). Here the receiver domain (Asp1) and the Hpt domain (His2) are fused C-terminal to the kinase domain (His1).

Multi-component systems are also found in Eukaryotes as it is described for the two-component system Sln1p-Ypd1p-Ssk1p that is involved in osmoregulation of *Saccharomyces cerevisiae*. In this phosphorelay, the kinase Sln1p (His1) involves the receiver domain (Asp1) and passes the phosphate to the single standing HPt domain Ypd1p (His2) (Posas et al., 1996). Hybrid kinases are also known to be involved in MCS of plants as Etr1 from *Arabidopsis thaliana*. The hybrid kinase contains a CHASE domain and is regulating ethylene response (Chang et al., 1993).

In Archaea hybrid kinases are less abundant as 22% occur in 18 analyzed archaeal genomes. Included are *Halobacterium sp*. NRC-1 possessing three hybrid-type HKs, *Methanosarcina mazei* Goe1 possessing two and *Archaeoglobus fulgidus* DSM 4304 possessing one. Interestingly, the methanogenic archaeon *Methanosarcina acetivorans* possesses five hybrid kinases (Zhang and Shi, 2005).

The function of these phosphorelay systems and the role of the hybrid kinases are still not known. As the amount of MCS is lower compared to bacterial genomes in Archaea and Eukaryotes it is suggested that phosphorelay systems originated in Bacteria and were spread to the other two domains via horizontal gene transfer (Koretke et al., 2000).

1.4 Signal-transduction in Archaea

The most commonly used signal transduction system in Archaea, the third domain of life, are one-component systems (OCS) (Ulrich et al., 2005) but also protein modification by phosphorylation was detected. Therefore, sensor kinases phosphorylated at a Ser/Tyr/Thr amino acid residue as well as at a histidine residue can be found in all archaeal phyla with few exceptions. The best-studied phyla of Archaea, the Euryarcheaota, and Crenarchaeota reveal a different use of signal transduction systems. Euryarchaeota utilize TCS for signal transmission including histidine and Ser/Tyr /Thr kinases in contrast to Crenarchaeota where only hank types kinases can be found (Eichler and Adams 2005; Ashby 2006; Galperin 2006, 2010).

In Archaea, the first protein phosphorylation was detected in 1980 in *Halobacterium salinarium* by Spudich and Stoeckenius (Spudich and Stoeckenius, 1980), and the first TCS CheA/CheY in *Halobacterium salinarium* was identified in 1995 where autophosphorylation of the kinase CheA was observed (Rudolph and Oesterhelt, 1995; Esser et al., 2016). Since then, constantly new insights of archaeal signal transduction were gained and reveal that even if possessing the same systems signal transduction is carried out distinctly. In comparison to Bacteria, a kinase to RR ratio of one to one is not given in Archaea where the interaction of the RR with various sensor kinases is supposed to take place (Krell, 2018). Also, the output of signal transduction is mainly regulated by protein-protein interaction or ligand binding as only 6% of all RR possess a helix-turn-helix domain (Krell, 2018; Galperin et al., 2018). An explanation for this suggestion is that archaeal genomes contain around 40% of alone standing receiver domains that are similar to CheY which is interacting with a protein influencing motility after phosphorylation (Galperin et al., 2018; Quax et al., 2018). These receiver domains can also be fused C-terminal of the kinase catalytic core referred to as hybrid kinase and are supposed to improve the complexity of signal transduction (Galperin et al., 2018). So far hybrid kinases are found but their phosphorelay system has not yet been described (Esser et al., 2016). Receiver domains are also found to be N-terminal

bound to PAS and/or GAF domains with or without the kinase catalytic core connected to them (Galperin et al., 2018).

Halobacteria and Methanomicrobia showed with 3-4% the highest amount of genes encoding for histidine kinases among archaea (Galperin et al., 2018). Therefore, the TCS like FilI-FilRs of *M. harundinacea* 6Ac was one of the first characterized TCS of methanogenesis. The kinase FilI involved in chemotaxis is regulating the RR FilR1 and FilR2 both possessing a receiver domain. FilR1 is binding to its promoter as well as to the promoter of FilR2 and additionally to the promoter regions of genes involved in methanogenesis (Esser et al., 2016; Li et al., 2014).

A further characterized TCS is LtrK/R from the antarctic strain *Methanococcoides burtonii* containing a thermo sensing kinase regulating the cognate RR LtrK (Najnin et al., 2016). Both described kinases possess a CHASE domain as extracytoplasmic sensor, whereas the CHASE4 domain is a specified sensor domain suggested to be only found in sensorkinases of *M. acetivorans* and *M. harundinacea* (Najnin et al., 2016).

1.5 The model organism *Methanosarcina acetivorans*

Methanosarcina acetivorans was isolated 1984 from methane-evolving sediments in an underwater canyon. It is classified as archaeum and belongs to the phylum *Euryarchaeota* and to the order Methanosarcinales where it is a member of the family *Methanosarcinaea* (Sowers et al., 1984). It is a methanogenic archaeon and therefore produces the greenhouse gas methane via its metabolism (Galagan et al., 2002). *M. acetivorans* is unique by using several ways to produce methane. It can reduce CO_2 with electrons during the carboxidotrophic pathway gained by hydrolyzing H_2, but is incapable to use H_2 for methanogenesis. In the acetoclastic pathway, an acetate group of activated acetate is cleaved, and the methyl group is reduced to methane. *M. acetivorans* is also able to utilize methylotrophic compounds and reduce them to CH_4. Through the reduction of different compounds an electrochemical gradient that is utilized for ATP synthesis is produced (Deppenmeier et al., 1999). Grown under anaerobic conditions in a medium containing acetate *M. acetivorans* forms single cocci that build cysts when reaching the late exponential phase. In the stationary phase the cysts are gathering as commune enclosed by an extracellular matrix (Sowers et al., 1984; Galagan et al., 2002). This matrix consists of the cell-wall component methanochondrin, a polymer of N-acetylgalactosamines (GalNAc), and one glucuronic

acid (GlcA). Single cells only produce the surface layer (S) that can be directly connected to the cytoplasmic membrane (Albers and Meyer, 2011). The single cocci are not motile but flagellar encoding genes are present as well as a complete genetic set for chemotaxis (Galagan et al., 2002).

The genome of *M. acetivorans* is completely sequenced and the largest among Archaea with 5.75 Mbp including ~4500 ORFs. The genome encodes for 64 histidine kinases, which mostly contain one or various PAS domains (Zhang and Shi, 2005; Galagan et al., 2002). Distinct to Bacteria, Archaea do not have a kinase to regulator relation in an equal amount. Therefore, it is not surprising that *M. acetivorans* contains 18 predicted RR receiver domains. Only one is a bacterial-like single RR with a bacterial effector domain. Seven of the receiver domains are fused to kinases, known as hybrid kinases. The remaining receiver domains are present as single protein domains (Galagan et al., 2002).

For investigations of archaeal biology and the metabolic pathway of methanogenesis *M. acetivorans* represents a beneficial model as genetic tools are developed for this organism. Powerful tools are transformation of plasmids (Metcalf et al., 1997), *in vivo* transposon mutagenesis (Zhang et al., 2000) as well as site-directed gene-specific mutagenesis (Zhang et al., 2002), CRISPR Cas system (Nayak and Metcalf, 2017), selectable markers (Boccazzi et al., 2000), reporter gene fusion and integration vectors (Conway de Macario et al., 1996). Protocols for growth on solid medium in anaerobic chambers for large-scale production are established as well (Metcalf et al., 1998)

1.6 Objectives of this work

As signal transduction is a vital tool for organisms to adapt to environmental changes understanding these mechanisms is of high importance. Research revealed a lot of new insights about the mechanisms of signal transduction in Eukaryotes and Bacteria. Despite that, less is known about the cell signaling in Archaea regarding two-component and phosphorelay systems. As Archaea diverged in an early state from a common ancestor investigation regarding the development of signal transduction systems and radiation via horizontal gene transfer from an evolutionary aspect are of interest. Additionally, Archaea have structurally a lot in common with Bacteria but resembling on a transcriptional level more with Eukaryotes. Learning from Archaea means also learning from the other domains. Investigations of *Methanosarcina*

acetivorans as model organism for methanogenesis is even more relevant as it bears interests for industrial uses.

Due to bioinformatic analysis, MA4377 was predicted to be a histidine hybrid kinase with two C-terminal fused receiver domains and containing three sensor domains. Based on the complex structure of the kinase, objective of this work was the characterization of the input domains as well as the function of the fused receiver domains. Additionally, the phosphorelay where the kinase is involved and its regulating effect should be determined. Biochemical analysis was used to reveal if the kinase coordinates a cofactor affecting kinase function. Furthermore, with generated versions, the phosphorylation site should be identified, and performing phosphotransfer assay with truncated version should disclose the phosphorelay inside of MA4377 and to the regulated proteins.

2 Material and Methods

2.1 Materials and Chemicals

The used chemicals were ACS grade or better and obtained through the purchase of AppliChem (Darmstadt), Carl Roth (Karlsruhe), Merck (Darmstadt) and Sigma-Aldrich (Munich) unless stated otherwise. Only autoclaved or sterile filtered solutions and lab ware was used for microbial cultivation. For the preparation of all buffers, growth-media and solutions water with a resistance of 18 MΩ was utilized.

2.1.1 Equipment

Table 1: Equipment used in this work.

Instrument	**Name**	**Manufacturer**
Autoclave	VX 150	Systec
Blotting system	Semidry Blot Trans-Blot®SD	BioRad
Cell disruption	LM10	Microfluidics
Centrifuges and rotors	5415D Rotor F-45-24-11	Eppendorf
	5810R Rotor A-4-62	Eppendorf
	Z32HK Rotor 12/002	Hermle
	Sorvall LYNX 6000 Rotors: T29-8 x 50 Fixed Angle Fiberlite F9-6x1000 LEX	ThermoFisher
Ultracentrifuge	L-80 XP	Beckman Optima
spectrometer		Leatherland, UK
Gel documentation	Gel iX20 Imager	Intas
Gel electrophoresis	Com Phor L Mini/Midi	Biozym
Incubator	Innova 44 Incubator Shaker Series	New Brunswick Scientific
	Innova 2300 Shaker	New Brunswick Scientific

	Polymax 1040	Heidolph
	SM 30 Control	Edmund Buehler
pH meter	Basic pH Meter P-11	Sartorius
PhosphoImager	Cyclone Typhoon FLA 7000	Perkin Elmer GE Healthcare
Photometers	8453 UV visible System	System Agilent
	NanodropTM Lite	Thermo Fisher
	Novaspec III	Amersham Bioscience
Power supplys	PowerPacTM Basic PowerPacTM 300 PowerPacTM HC	BioRad BioRad BioRad
SDS-page chamber	Mini-PROTEAN II System Mini-PROTEAN Tetra cell System	BioRad
SDS-page documentation	HP Scanjet 300	HP
Sonifier	UW 2200 with tip KE 76	Bandelin
Sonification bath	Sonorex RK 1028	Bandelin
Thermoblock	ThermoStat plus	Eppendorf
Thermocyler	T-Gradient	Biometra
	T-Personal	Biometra
Ultra-pure water system	MilliQ Integral Water Purification System	MerckMillipore
Vacuum pump	Laboport®	KNF
Vortex	Reax top	Heidolph

2.1.2 Kits, enzymes and consumable supplies

Table 2: Enzymes, Kits and other supply material used in this work.

Enzymes/Kits/Supplies	**Manufacturer**
Amicon® Ultra Centrifugal Filters	Merck
Centrifugal concentrators: Amicon Ultra-4 MWCO 10,000 Amicon Ultra-15 MWCO 50,000	 Merck Millipore Merck Millipore

Chromatography columns:	
− SuperoseTM 6 10/300 GL column	GE Healthcare
- Strep-Tactin® -Sepharose	IBA
- TALON® Metal Affinity Resin	Clontech
Desalting columns:	
PD MiniTrap TM G-25	GE Healthcare
PD MiniTrap TM G-10	GE Healthcare
illustra MicroSpin G-50 column	GE Healthcare
Dialysis Tubing (14.000 Da Cut-off)	Carl Roth
T4-DNA Ligase	Thermo Fisher
DNA loading dye:	
DNA Gel Loading Dye Purple (6x)	New England Biolabs
DNA Poylmerase:	
Phusionr HF DNA Polymerase	Thermo Fisher
Pfu Polymerase	From this lab
DreamTaq Green PCR Mastermix (2x)	Thermo Fisher
DNA size standard:	
GeneRulerTM DNA Ladder Mix	Thermo Scientific™
DNA stain:	
Gel Red	Biotium
Ethidiumbromid	Invitrogen
Kits:	
NucleoSpin® Gel and PCR Clean-up	Macherey-Nagel
NucleoSpin® Plasmid	Macherey-Nagel
Protein marker:	
Page Ruler™ Prestained Protein Ladder	Thermo Scientific™
PageRuler™ Unstained Protein Ladder	Thermo Scientific™
Roti®-PVDF-Membrane	Carl Roth
Standard protein for Size Exclusion Chromatography:	
β-Amylase	Sigma Aldrich
Albumin	Sigma Aldrich
Alcohol dehydrogenase	Sigma Aldrich
Apoferritin	Sigma Aldrich

Blue Dextran Carbonic anhydrase	Sigma Aldrich Sigma Aldrich
Sterile filter: PVDF 0.45 µm ∅ 25 mm	Diagonal

2.2 Microbial strains, plasmids and culture growth

All cloning steps employed *E. coli* JM83 or *E. coli* WM1788 except otherwise noted. Heterologous protein expression was performed in *E. coli* BL21(DE3). For homologous protein expression *M. acetivorans* WWM73 was used.

2.2.1 Microbial strains

Table 3: Used bacterial strain.

Strain	**Genotype**	**Reference**
E. coli DH5α	*F −1 −supE44D*(*argF-lac*) *U169 j80dlacZ ΔM15 hsdR17 recA1 endA1 gyrA96 thi-1 relA1*	(Grant et al., 1990)
E. coli BL21(λDE3)	*fhuA2 [lon] ompT gal* (*λ DE3*) *[dcm] ΔhsdS λ DE3 = λ sBamHIo ΔEcoRI-B int::*(*lacI:: PlacUV5::T7 gene1*) *i21 Δnin*	(Studier and Moffatt, 1986)
E. coli RP523	*F-, thr-1, leuB6*(*Am*), *fhuA21, lacY1, hemB220, glnX44* (*AS*), *e14-, rfbC1, glpR200*(*glpc*), *thiE1*	(Li et al., 1988)
E. coli Nissle 1917	serotype *O6:K5:H1*	(Grozdanov et al., 2004)
E. coli Walker (C43)	F^- *ompT gal dcm* $hsdS_B(r_B^- m_B^-)$(*DE3*)	(Miroux and Walker, 1996)

2.2.2 Plasmids

All plasmids used for this work were constructed by specific digested PCR products and following ligation into the desired target vector. The correctness of the generated construct was verified by DNA sequencing (Seq-IT, GATC).

Table 4: Vectors and plasmids constructs used and produced in this work.

Number	Plasmid	Description	Reference
1	pASK IBA3 plus	expression vector, C-terminal StrepII-tag, Amp^r	IBA GmbH
2	pASK-MA4377	pASK IBA3 plus with complete coding region of *MA4377*	this study
3	pASK-PKR1R2	1) with coding region of PAS domain, kinase catalytic core, receiver domain 1, receiver domain 2	this study
4	pASK-PKR1	1) with coding region of PAS domain, kinase catalytic core, receiver domain 1	this study
5	pASK-PK	1) with coding region of PAS domain, kinase catalytic core	this study
6	pASK-K	1) with coding region of kinase catalytic core	this study
7	pASK-PKH_{497}Q	5) with H_{497}Q mutation	this study
8	pASK-PKH_{538}Q	5) with H_{538}Q mutation	this study
9	pASK-PKH_{560}Q	5) with H_{560}Q mutation	this study
10	pASK-PK$H_{497, 538}$Q	5) with H_{497}Q, H_{538}Q mutation	this study
11	pASK-PK$H_{497, 560}$Q	5) with H_{497}Q, H_{560}Q mutation	this study
12	pASK-PK$H_{538, 560}$Q	5) with H_{538}Q, H_{560}Q mutation	this study
13	pASK-PK$H_{497, 538, 560}$Q	5) with H_{497}Q, H_{538}Q, H_{560}Q mutation	this study
14	pASK-K $C_{486, 631, 673}$S	6) with C_{486}S, C_{631}S, C_{673}S	this study
15	pET21a (+)	C-terminal His6-tag, Amp^r	Novagen
16	MA4376	15) with coding region of *MA4376*	this study
17	MA4376 D_{54}N	16) with D_{54}N mutation	this study

18	pACYC-Duet1	C-terminal His6-tag, Cm^r, T7-Promoter	Novagen
19	MA4375	18) with coding region for *MA4375*	this study

2.2.3 Oligonucleotides

Oligonucleotides are short, single-stranded DNA fragments that function as primers to mark the start of DNA-polymerase in a polymerase chain reaction (PCR). All primers for the construct of the MA4377, MA4376 and MA4375 variants and constructs are annotated.

Table 5: Oligonucleotides used in this work.

Primer	**Sequence (5'→3')**
pASKseqfwd	GAGTTATTTTACCACTCCCT
pASKseqrev	CGCAGTAGCGGTAAACG
pASK 4377 SacII fwd	GCTATCCGCGGCATGAATGTGAGTAGAAAAATTCT
pASK 4377 PAS rev	CGCCCATGGCCAATTTTGCTTGAAGCAGTTT
pASK 4377 PAS fwd	GCTATCCGCGGCAGGTTGAATTCCGATAAGGTTAA
HATPas-rev NocI	CGCCCATGGTGTGAGGGGAATTGTGAAC
Rec1 NocI rev	GCGCCATGGGATTTCTCTTAAGGAGTCC
PKR1 fwd	AAATGGGAGACCGCGGCGGCGGCAGGTTGAATT CCGATAAG
PKR1 rev	GTGGCTCCAAGCGCTGAGACTGATTTCTCTTAAGG AGTCCAG
H_{497}Q fwd	CCAATATGAGCCA**G**GAACTGCGGACG
H_{497}Q rev	CGTCCGCAGTTC**C**TGGCTCATATTGG
H_{538}Q fwd	GGAAGTGGAAAACA**G**CTCCTGGGGC
H_{538}Q rev	GCCCCAGGAG**C**TGTTTTCCACTTCC

H_{560}Q fwd	GGACCTGCA**A**TACAGTGAGTTTACTG
H_{560}Q rev	CAGTAAACTCACTGTA**T**TGCAGGTCC
MA4377 R1 DN fwd	GCCTGATGTTATCACTCTGG**ATTCAAC**GTTTTACTTCCCGATACC AGTGGC
MA4377 R1 DN rev	CGGGAAGTAAAAC**GTTGAAT**CCAGAGTGATAACATCAGGC
MA4377 R2 DN fwd	CCTCATCCTCG**AATTCA**ACCTGCTGATGCCGGAGATAAGTGG
MA4377 R2 DN rev	CCGGCATCAGCAGGTT**GAATTCC**GAGGATGAGGATATCCGGC
pACYC duett fwd	GGATCTCGACGCTCTCCCT
pACYC duett rev	GATTATGCGGCCGTGTACAA
MA4376 N His SacI fwd	GCGTCGAGCTCGAAAGAAATTCTTATTGTCG
MA4376 N His SalI rev	CCCTTAGTCGACTTCTCCCAGATATTTATCG
MA4376DN fwd	CGATATTATCCTCCTC**A**A**C**ATGCAACTTCCTAAAATGGACGGGC
MA4376DN rev	GCCCGTCCATTTTAGGAAGTTGCAT**G**T**T**GAGGAGGATAATATCG
pET21a fwd	TAATACGACTCACTATAGGG
pET21a rev	TGCTAGTTATTGCTCAGCGG
pET21a-MA4375-gb-fwd	CTTTAAGAAGGAGATATACAATGAAAATATCACTTA TTGACCTG
pET21a-MA4375-gb-rev	AGTGGTGGTGGTGGTG GTGCTTTATTTTGTCCAG CCGC

QC 4377 HisKa_C1 S fwd	GGCAGCCAGC**AGC**ACAAAGAGCGAGTTCC
QC 4377 HisKa_C1 S rev	GGAACTCGCTCTTTGT**GCT**GCTGGCTGCC
QC 4377 HisKa_C2 S fwd	GGGGGGTAGAGTCTCGGTCTAC**A**GCAAAAAGAGC
QC 4377 HisKa_C2 S rev	GCTTCCGCTCTTTTTGC**T**GTAGACCG
QC 4377 HisKa_C3 S fwd	CCTCCTCAGCCAGGCAGTAC**A**GCGGGACTGG
QC 4377 HisKa_C3 S rev	GCCCGAGCCCAGTCCCGC**T**GTACTGCCTGGC

The bold bases resemble the mutation in the oligonucleotide

2.2.4 Culture growth

E. coli cultures were cultivated in Luria Bertani (LB) medium or LB high salt medium (LB HS) at 37 ◦C with selection markers and supplements. Agar plates additionally contained 1.5 % (w/v) Agar-Agar.

LB medium

10 g/l	Tryptone
5 g/l	Yeast Extract
10 g/l	NaCl
(1.5 % (w/v) agar-agar)	

LB high salt medium

10 g/l	Tryptone

5 g/l	Yeast Extract
24.22 g/l	NaCl
(1.5 % (w/v) agar-agar)	

TB medium

24.0 g/l	yeast extract
12.0 g/l	Tryptone
4 ml/l	Glycerol
17 mM	KH_2PO_4
72 mM	K_2HPO_4
(1.5 % (w/v) agar-agar)	

Supplements and Selective markers

Supplement	**Stock concentration**	**Final concentration**
Ampicillin (Amp)	100 mg/ml	100 µg/ml
Anhydrotetracyclin (AHT)	2 mg/ml	200 µg/l
Chloramphenicol (Cmp)	34 mg/ml	34 µg/ml
Hemin	100 mM	10 µM
Isopropyl-β-D-thiogalactopyranoside(IPTG)	1 M	0.5-1 mM
Kanamycin (Kan)	50 mg/ml	50 µg/ml
Spectinomycin (Spc)	50 mg/ml	50 µg/ml

2.2.4.1 Cultivation of *E. coli* cells

E. coli pre-cultures under aerobic were grown overnight at 37°C, 160 rpm (Innova 2300 Shaker) in sterile flasks containing LB media with selection marker (1:1000). Pre-culture were inoculated 1:100 in LB medium or LB HS for cultivation in large-scale. Culturing *E. coli* under anaerobic conditions in TB media, sealed anaerobic flasks were used. To cultivate *E. coli* on agar-plates, 100-200 µl of the pre-culture were spread on a solid agar-plate containing selection marker (1:1000). The plates were incubated at 37°C.

2.2.5 Cultivation of *E. coli* cells

E. coli pre-cultures under aerobic were grown overnight at 37°C, 160 rpm (Innova 2300 Shaker) in sterile flasks containing LB media with selection marker (1:1000). Pre-culture were inoculated 1:100 in LB medium or LB HS for cultivation in large-scale. Culturing *E. coli* under anaerobic conditions in TB media, sealed anaerobic flasks were used. To cultivate *E. coli* on agar-plates, 100-200 µl of the pre-culture were spread on a solid agar-plate containing selection marker (1:1000). The plates were incubated at 37°C.

2.2.6 Storage of *E. coli* strains

Long-term storage of *E. coli* culture was conducted using a glycerol stock. 750 µl of the *E. coli* pre-culture were mixed 1:1 with autoclaved glycerol (86 % (v/v)). The culture was frozen with liquid nitrogen and stored at -80°C.

2.2.7 Determination of cell density

To determine the cell density of a *E. coli* culture the absorbance at a wavelength of λ = 600 nm (Optical density at 600 nm (OD_{600}) was measured using a photometer (Novaspec III). The value of 1 resembles 8x108 cells/ml. As reference the medium the measured culture was inoculated, was used.

2.3 Molecular Biological Techniques

2.3.1 Preparation of chemically competent cells

To transform extrinsic DNA into *E. coli* is a powerful tool. As *E. coli* cells do not possess natural competence it is important to achieve this facility of the cells by chemical treatment. The incubation with $CaCl_2$ leads to a porous membrane and improves the transfer of the hydrophilic DNA into the cell. 100 ml LB medium were inoculated with a pre-culture in a ratio of 1:100 and incubated at 37°C until the culture reached a OD_{595} of 0.5. The cells were aliquoted to 2x 50 ml in Falcon reaction tubes and harvested by centrifugation for 10 min, 4000 rpm at 4°C (Eppendorf 5810R, rotor A-4-62). After discarding the supernatant, the pellet was resuspended carefully in 50 ml of 50 mM $CaCl_2$ and incubated on ice for at least 45 - 60 min. Subsequent to the incubation time the cells were centrifuged at 4000 rpm, 4 °C for 10 min (Eppendorf 5810R, rotor A-4-62), and the supernatant discarded. Each pellet was resuspended in 2.5 ml of 50 mM $CaCl_2$ with 15 % glycerol (v/v) and aliquoted to 200 µl. The competent cell aliquots were frozen with liquid nitrogen and stored at -80°C. During all the steps contamination should be prevented. As a control one aliquot of the competent cell was transformed with water and plated on a LB-Agar plate with and without selection marker.

2.3.2 Transformation of chemically competent cells

For transforming external DNA into *E. coli* cells, aliquots of chemically competent cells were thawed on ice and 50-200 ng plasmid DNA were added. After resuspending the cells carefully with the fingertip, cells were incubated on ice for 15 min. The cell-plasmid-mix was gently mixed and further incubated on ice for 15 min. The $CaCl_2$ treated porous cell undergoes a heat-shock for 90-120 s at 42°C using a waterbath or thermoblock (ThermoStat plus, Eppendorf). The heat-shock depolarizes the membrane and lowers the negative inner-membrane potential and makes it therefore easier for the negatively charged DNA to enter the cell. Afterwards, the cells were incubated again on ice to recover. For phenotypical expression, 700 µl of LB medium were added and incubated for 1-1.5 h at 37°C, 160 rpm (Innova 2300 Shaker). The cells were then centrifuged for a few seconds and 700 µl of the supernatant were discarded. The remaining supernatant and pellet were homogenized and plated on selective agar plates and incubated at 37°C overnight.

2.3.3 Isolation and preparation of plasmid DNA

To isolate plasmid DNA, single colonies were picked with sterile toothpicks from transformed *E. coli* cells growing overnight on Agar plates. The colony sticking on the toothpick was inoculated in 5 ml of LB medium with selection marker (1:1000) and grown overnight at 37°C, 160 rpm (Innova 2300 Shaker). To yield the plasmids alkaline lysis was performed after the specification of the Plasmid DNA Miniprep kit (NucleoSpin®Plasmid EasyPure-Kit, Macherey-Nagel).

2.3.4 Determination of DNA concentration in aqueous solution

To determine the DNA/RNA concentration the NanoDrop Sepctrophotometer (NanodropTM Lite, ThermoFisher) was used. As reference 1 µl of water or elution buffer, depending in which solution the DNA was eluted, was used before the DNA sample was measured. With the NanoDrop Sepctrophotometer the concentration of DNA/RNA in ng/µl and the DNA/RNA (A260) versus protein (A280) ratio was obtained which shows the purity of the sample. After purification of the DNA, ethanol (EtOH) can remain in the sample which can disturb and lower the quality of the sequence analysis reactions. By opening the lid and heating the reaction tube up to 70-80°C in a thermoblock (ThermoStat plus, Eppendorf) EtOH evaporates.

2.3.5 DNA amplification by PCR

To amplify DNA the polymerase chain reaction (PCR) method is used by attaching specific, complementary oligonucleotides (primers) to the template DNA. The PCR methods consists of several steps. The reaction starts with the initial heating by rising temperatures to 95°C for 2-5 min to ensure that the template DNA does not longer occur as double-strand by disrupting the hydrogens-bonds. Then the cycle starts including several steps: denaturation, amplification, and elongation. These steps get repeated several times, depending on the polymerase enzyme facilities. To get a high yield the amplified DNA gets denatured to single strand DNA with 95°C in the denaturation step. The added primers are then promoted to attach to the template DNA during the annealing step. Therefore, the temperature is important and chosen to be 5 °C under the melting temperature of the primer. The polymerase is then extending the primer in the elongation step with an optimal temperature at 72°C. Every polymerase has its own time specific elongation rate.

PCR reaction mix for Pfu DNA polymerase:

X µl	Template DNA (0.5µg/50µl)
Each 1 µl	Primer (5-50 pmol/µl)
0.5 µl	Pfu DNA polymerase (2-3U/ µl)
1 µl	dNTP mix (10 mM each)
5 µl	Pfu DNA Polymerase 10x buffer with $MgSO_4$
X µl	Nuclease-free water to final volume of

PCR cycle for Pfu DNA polymerase:

Cycle	**Temp. [°C]**	**Duration**	
Initial denaturation	98	300 s	
Denaturation	98	60 s	30 cycles
Annealing	98	15 s	
Elongation	55	x s	
Final elongation	72	600 s	
Cooling	4	hold	

2.3.6 Site directed mutagenesis

To insert specific mutations into a DNA sequence, site directed mutagenesis was performed. Therefore, primers containing the mutations were designed and the plasmid with the desired mutation was used as template. A specific PCR cycle with reaction mixtures containing only the forward or the reverse primer was started and after few cycles the reactions were united to improve the insertion rate of the mutation. For site specific mutagenesis polymerase enzyme with proof reading, like Phusion®-HF polymerase or Pfu DNA polymerase are recommended.

First PCR-Set-up

Components	Set-up A	Set-up B
H_2O dest	35 µl	35 µl
5x buffer HF	10 µl	10 µl
Template (30 ng)	1 µl	1 µl

Primer forward	2.5 µl	-
Primer reverse	-	2.5 µl
DNTP-MIX (2.5mm/nucleotide)	1 µl	1 µl
Phusion ®polymerase (2U/µl)	0.5 µl	0.5 µl
Total volume	50 µl	50 µl

Second PCR-Set-up

Components	Set-up A
Set-up A	25 µl
Set-up B	25 µl
Phusion ®polymerase (2U/µl)	0.5 µl
Total volume	50.5 µl

First PCR program

Cycle	Temp. [°C]	Duration
1x	98	30 s
8x	98	15 s
	55	30 s
	72	3 min 30 s
1x	4	hold

Second PCR program

Cycle	Temp. [°C]	Duration
1x	98	30 s
18x	98	15 s
	55	30 s
	72	3 min 30 s
1x	72	10 min
1x	4	hold

After the PCR the reaction mixture contains plasmids with the inserted mutation which should get transferred into *E. coli* DH5α for replication. Before executing the transformation step, it is important to get rid of the parental plasmid. The parental plasmid is compared to the newly synthesized plasmids, methylated and can get

degraded by adding DpnI (New England Biolabs) at 37 °C following the manufacturers recommendation. The inserted mutations were verified by sequencing reaction.

2.3.7 Analysis of DNA by agarose gel electrophoresis

To analyze the size and amount of DNA, the method gel electrophoresis is used. DNA samples are mixed with a 6x loading dye that simplify loading and makes it possible to track DNA by containing tracking dyes. The mixture was loaded on an agarose gel which was covered with 1x TAE buffer inside the agarose gel chamber. The samples were then subjected to an electric field (100 V) and due to the negative charged DNA, the samples were running to the positive electrode. This results in a separation according to DNA size of the DNA fragments combined in the sample. The short fragments travel rapidly in the polymerized agarose compared to the larger fragments. Ethidium bromide that intercalates with the double helix of the DNA was used. The gel was therefore incubated in a water bath containing ethidium bromide (0.05 % (v/v)) for 15 min excluding light as the reagent is light sensitive. The DNA fragments were then visualized via fluorescence excitation with UV light. For documentation GelDoc (Intas) was used.

2.3.8 Restriction of DNA

For cloning techniques specific restricted DNA ends are necessary. Therefore, specific restriction enzymes like FastDigest enzymes (Thermo Fisher) and restrictions enzymes from New England Biolabs (NEB) were utilized. The restriction mixture was composed according to manufacturer's instructions, as well as the incubation and heat inactivation time. To remove the restriction enzymes the sample could be purified with the DNA NucleoSpin Gel and PCR Clean-up kit (MachereyNagel).

2.3.9 Ligation of DNA molecules

For the ligation Vector DNA (10-100 ng) and PCR products were used in a molar ratio of 1:3. The T4 DNA Ligase (Thermo Fisher) was used as it was recommended from the manufacturer's instructions. The reaction mix was composed of a total volume of 20 µl and incubated 1h at RT or overnight at 16 °C. After ligation 1-2 µl of the ligation product were transformed into competent cells.

2.3.10 Construction of expression vectors

To construct expression vectors, coding regions of the desired insert were amplified by specific primers taking genomic DNA or Plasmid DNA as template. The insert and

the vector were cut with specific restriction enzymes, purified, ligated and transformed into competent cells. For cloning *E. coli* Dh5α were used and after plasmid isolation the accuracy was obtained by sequence analysis.

For construction of the PKR1 fragments the NEBuilder® HiFi and the belonging Master MIX was used. Reactions were performed as the manufacturer recommended.

2.4 Biochemical and Biophysical Techniques

2.4.1 Test expression of recombinant genes

To test the best condition regarding temperature and expression time of a recombinantly produced protein, a test expression was performed.

Therefore, three flasks with 100 ml of LB medium were inoculated (1:100). with a pre-culture containing selection marker The flasks were incubated at 37 °C until reaching an OD_{595} of 0.5 and for *E. coli* Nissle 1917 until an OD_{595} of 1. The cultures were then induced with AHT (200 ng/ml) or IPTG (0.25 mM) according to the expression plasmid and for expression in *E. coli* Nissle 1917 10 µl hemin (10 µM) were added. Then each flask was incubated at different temperatures like 17°C, 30°C and 37°C. A sample was taken after 1 h, 2h, 3h, and overnight as well as before induction. The samples were adjusted with medium to an OD_{595} of 0.5. The pellet was harvested by centrifugation for 2min at 13.2000 rpm (Eppendorf 5415D Rotor F-45-24-11) and resuspended in 50 µl of buffer W. The samples were sonicated in the sonification bath (Bandelin Sonorex RK 1028) and again centrifuged for 15 min at 13,200 rpm (Eppendorf 5415D Rotor F-45-24-11). The supernatant and the pellets were separated. The pellets were again resuspended in 30 µl of buffer W and in 10 µl of 10% SDS. All samples were loaded on a SDS-gel for SDS-PAGE.

Buffer W

100 mM	Tris/HCl pH 8.0
150 mM	NaCl
1 mM	EDTA

2.4.2 Production of recombinant proteins in *E. coli* BL21(DE3)

To produce recombinant proteins, chemically competent *E. coli* BL21 (DE3) cells were transformed with plasmids like all MA4377 constructs which are *tet*-promoter driven (pASK IBA 3 plus) and containing a C-terminal StrepII-tag. For production, a 1 l LB HS medium was inoculated with an overnight culture (1:100) and 100 µg/ml ampicillin as selection marker was added. For culture growth conditions with 37 °C and 100 rpm shaking were chosen and by reaching a OD_{595} of 0.5 the protein expression by adding AHT (200 ng/µl) was induced. AHT is binding the tet repressor that is attached to the

promoter of the coding region. Plasmids with T7 driven promoter (pET21a(+)), were induced with 0.25 mM IPTG.

The cell culture was cooled down to 17 °C and the growth continued overnight (~22 h) with 100 rpm stirring at 17°C. To harvest the culture, the cells were filled into 1 l bottles and centrifuged at 9000 rpm and 4 °C for 10 min (Thermo Fisher, Sorvall LYNX 6000, rotor F9). The supernatant was discarded, and the pellet was transferred into a falcon tube and stored at -20 °C.

2.4.3 Production of recombinant proteins in *E. coli* Nissle 1917

For the production of recombinant proteins determining incorporation of a heme cofactor, *E. coli* Nissle 1917 as expression system was used. The same procedure of production as described for *E. coli* BL21 (DE3) was used, except the addition of hemin directly after AHT (200 ng/µl) induction at a cell culture density of OD_{595} 1-1.5. Hemin (10 µM) was freshly prepared with DMSO. As hemin is in combination with light toxic for the cells, protein expression was performed in darkness.

2.4.4 Production of recombinant proteins in *E. coli* RP523

To produce the apo-protein, MA4377 without the heme cofactor the strain *E. coli* RP523 was used. *E. coli* RP523 needs due to its *hemB* mutation hemin or porphyrin homologs during aerobic growth. Culturing this strain under anaerobic conditions in 1 l serum bottle in TB medium and 1% glucose, *E. coli* RP523 needs no additional hemin. When the culture reached an OD_{595} of 0.5 protein expression was induced with AHT (200 ng/µl) using a syringe. The culture was cooled down to 17°C and then stirred at 100 rpm overnight.

2.4.5 Cell disruption of *E. coli* cells

To isolate the recombinant produced protein, cells have to get disrupted. The harvested pellets were therefore resuspended in 20 ml buffer W, 1 mM dithiothreitol (DTT), 0.25 mM 4-(2-aminoethyl)benzenesulfonyl fluoride hydrochloride (AEBSF), a spatula tip of Lysozym /(AppliChem) and a spatula tip of DNAse I (Carl Roth) and incubated on ice for 30 min. The cell suspension was homogenized by vortexing and adjusted with buffer W if it was to sticky. Depending on the pellets additional DNAseI was needed to get the solution fluid. For sonification a cup filled with ice water was taken and the falcon tube containing the cells placed into the ice bath using a floating foam tube rack. For cell disruption using the sonifier (Bandelin UW 2200 with tip KE

76), cells were sonicated in intervals of 15s at 50 % power output and 15 s break for 3 min.

Using the microfluidizer the resuspend pellet must be homogenized and be fluid like water. The device was first washed with the used buffer (5000 psi). Cells were added and disrupted using 3 times 15.000 psi. It is important to clean the device properly with water, 1M NaOH and 20% EtOH.

To separate the cell debris the lysate was centrifuged for 10 min at 4000 rpm (Eppendorf 5810R, rotor A-4-62. The supernatant was transferred to centrifuge tubes and centrifuged for at least 40 min at 19.000 (SorvallTM LYNXTM 6000 centrifuge, rotor T29). The supernatant was filtered using a syringe with a filter tip (45 µM PVDF).

2.4.6 Purification via affinity chromatography

To purify StrepII-tagged proteins affinity-chromatography was used. A column containing Strep-Tactin ® that is a derivative to the very stable protein streptavidin (2CV) was equilibrated with buffer W (10 CV). The filtered lysate was added onto the column and the flow through was collected. At this step, the tagged protein is bound to the streptavidin beads. To get rid of all remaining lysate debris the column was washed with buffer W (10 CV). The washing fraction was collected in an extra tube. To elute the bound protein buffer E was prepared and three times a fraction of 2 ml was added onto the column and collected in 2 ml Eppendorf tubes. Buffer W is containing desthiobiotine (2.5 mM) which is a derivative of biotin, the natural ligand of streptavidin, and therefore replacing the strep tagged protein. From each collected fraction samples for SDS-PAGE were prepared. After determination of the SDS-gel, elution fractions containing the protein were combined and dialyzed against Tris buffer pH 8.0.

The column was regenerated with buffer R until the Strep-Tactin beads turned into a strong orange color.

Buffer E (buffer W with desthiobiotine)

100 mM	Tris/HCl pH 8.0
150 mM	NaCl
1 mM	EDTA
2.5 mM	desthiobiotine

Buffer R

	Buffer W
1 mM	Hydroxy-azophenyl-benzoic acid (HABA)

His-tagged proteins were purified with ÄktAprime (GE healthcare) device after manufacturer recommendation. The column (HisTrap™ High Performance) was equilibrated with bufferW_{His}. After loading 10 ml of the lysate using the superloop the protein was eluted with buffer$E_{His.}$

bufferW_{His}

50 mM	Tris
300 mM	NaCl
10 mM	Imidazol
pH 7.5 (HCl)	

bufferE_{His}

	bufferW_{His}
150 mM	Imidazol

2.4.7 Purification of membrane proteins

To purifiy membrane proteins, it was first important to test the best conditions for expression by test expression. Protein samples were prepared as described and 15 ml of the culture was centrifuged for 10 min, 4000 rpm (Eppendorf 5810R Rotor A-4-62) at 4°C after two hours of shaking (160 rpm). The supernatant was discarded, and the pellet was resuspended in 2 ml breaking buffer for membranes (BBF) containing the protease inhibitor phenylmethylsulfonylfluoride, buffer.

The samples were sonicated with a small sonifier tip until the solution was clear. The sample was transferred into a 2 ml reaction tube and centrifuged at 10.000 g for 2 min at 4°C. 800 µl of the supernatant was transferred to a new thick-walled ultracentrifugation tube and centrifuged at 4°C for 10 min at 200.000 g in the mini ultracentrifuge (Beckman Optima L-80 XP Ultracentrifuge). This step can be repeated.

The soluble protein should then be located in the membrane pellet, visible as a light brownish dot. The membrane pellets of all samples were solubilized in 100 -200 µl BBM buffer by pipetting gently up and down. 30 µl of the sample were analyzed by SDS-PAGE.

BBF buffer

10 mM	Tris
1 mM	EDTA
20 µl	PMSF (100 mM in ethanol)
pH 8.0 (HCl)	

2.4.8 SDS-polyacrylamide gel electrophoresis (SDS-PAGE)

For separation of protein size gel matrix Sodium dodecyl sulfate polyacrylamide gel electrophoresis (SDS-PAGE) was determined after Laemmli (1970). Sodium dodecyl sulfate (SDS) is a detergent that linearizes the protein structure together with reducing agents in the 4x SDS sample buffer. Furthermore, SDS charges protein negatively and the negative charge of the protein correlates with its molecular weight. Applying it to an electric field the charged protein can move through the uncharged acrylamide gel to the positive anode in the electric field. A SDS gel consist out of two gels, the stacking gel with a pH of 6.8 and containing a low amount of acryl amide and the separation gel with a pH value of 8.8 and containing 10 % acrylamide. The acrylamide amount correlates with the size of the protein which is to be separated. The buffer used for this system contains glycine and has a pH value of 8.3. The mentioned pH values play a big role in this method because it influences the charge state of glycine. In the electric field glycine is moving into the stacking gel and turns into a zwitterionic form due to the pH value of 6.8 which leads to a loss of charge and to a slow migration. At the same time Cl- ions that are also present in the buffer are moving very fast. Tris and Cl- building two fronts and the applied proteins, which have their own motility, got stacked in between.

Reaching the separation gel with a pH value of 8.8 which leads to a negative charge and fast movement of the glycine. The proteins are then not stacked anymore and got separated by entering the high arylamide concentration.

Protein samples were incubated with 4x SDS sample buffer and heated up to 95 °C for 5 min and centrifuged for 1 min centrifuged at 13.200 rpm (Eppendorf 5415D, Rotor F-45-24-11) before loading on the polyacrylamide gel. To determine the size of the protein bands, protein markers like protein marker mix Page Ruler™, Prestained Protein Ladder or PageRuler™ Unstained Protein Ladder (ThermoScientific™) were applied on the gel. The electrophoresis was performed with constant voltage of 200 V for 40 min. These conditions are not favorable, lower voltages and longer separation time should be considered. To visualize the proteins, the gel was colored in Coomassie Brilliant Blue G250 for 15 min. Coomassie Brilliant Blue G250 is a triphenylmethane dye that colors the protein blue by binding to positively charged amino acid residues. After staining Coomassie Brilliant Blue G250 was poured back, the polyacrylamide gel washed with water and incubated with destaining solution on a shaker (Heidolph Polymax 1040) to remove the background. In this work proteins were also separated by using gradient gels. The principle of gradient gels is the increasing amount of acrylamide from 4% to 20%. This leads to a sieving effect where proteins get separated due to their size. The benefit is that protein with a bigger and smaller size can get separated in one sample.

4x stacking gel buffer

0.5 mM	Tris/HCl pH 8.0
0.4% (w/v)	SDS pH 6.8 (HCl)

4x separation gel buffer

1.5 mM	Tris/HCl pH 8.0
0.4% (w/v)	SDS pH 8.8 (HCl)

Separation gel (10 %) for 4 gels

5.3 ml	Acrylamide (30 % (v/v) acrylamide 0.8 % (v/v) bisacrylamide)
4 ml	4x separartion gel buffer
6.7 ml	H_2Odest

120 µl	10 % APS
12 µl	TEMED

Stacking gel (5.25 %) for 4 gels

1.4 ml	Acrylamide (30 % (v/v) acrylamide 0.8 % (v/v) bisacrylamide)
2 ml	4x stacking gel buffer
64.6 ml	H_2Odest
30 µl	10 % APS
20 µl	TEMED

Gradient gel for 12 gels

	4%	20%
Acrylamide (30%)	7.3 ml	36.7 ml
Stacking buffer pH 6.8	13.70 ml	13.75 ml
Water	34 ml	4.55 ml
APS	302.5 ml	302.5 ml
TEMED	30.25 ml	30.25 ml

10 x SDS running buffer pH 8.8

250 mM	Tris pH 8.8 (HCl)
1.92 M	Glycerine 1 % (w/v)
1 % (w/v)	SDS

4 x SDS sample buffer

100 mM	Tris pH 8.8 (HCl)
110 mM	SDS
40 % (w/v)	Glycerine
3 mM	Bromphenol blue
2 mM	β-mercaptoethanol

Coomassie Brilliant Blue G250 staining solution

10 % (v/v)	Acetic acid
30 % (v/v)	Ethanol
1 % (w/v)	Coomassie Brilliant Blue G250

Destaining solution

30 % (v/v)	Ethanol
10 % (v/v)	Acetic acid

2.4.9 Dialyzation into different buffers

The transfer of a protein into another buffer for example to remove desthiobiotin or to change the buffer system dialysis was performed. Therefore, the protein is added into a dialysis tube (14 kDa molecular cut-off) into a new chilled buffer and stirred over night at 4°C. To work on with the protein at a desired concentration molecular weight cut off filter (50 kDa and 100 kDa) (MerckMillipore) were used.

Dialysis Buffer pH 7.0

50 mM	$Na_2HPO4 \times 2H_2O$
50 mM	$NaH_2PO4 \times H_2O$
100 mM	NaCl

Tris buffer pH 8.0

50 mM	Tris/HCl pH 8.0
150 mM	NaCl
5 mM	$MgCl_2$
50 mM	KCl

2.4.10 Immuno-detection of immobilized proteins (Western blot)

For specific detection and determination, a protein gets transferred to a membrane by an electric field. The membrane gets then incubated with a specific antibody that is detecting the protein.

Subsequent to the separation of a protein by SDS-PAGE the SDS gel got placed on a PVDF membrane. The gel and the membrane were covered from both sides with Whatman filter paper. This sandwich was soaked in Towbin transfer buffer and after placing the sandwich into a semi-dry blotting system (BioRad, Semidry-Blot Trans-Blotr SD), the protein got transferred onto the PVDF membrane trough an electric field (18 min, 15 V). The membrane then got incubated by shaking (Heidolph Polymax 1040) for 1 h at RT with blocking solution to block all free binding properties. The PVDF membrane was washed 3 times with PBS-T buffer. For StrepII-tagged proteins the anti-Strep-Tactin®-AP conjugate (1:4000, IBA GmbH) was applied for 1 h by shaking (Heidolph Polymax 1040). After incubation, the conjugate was stored at 4°C and the membrane was washed three times with PBS-T buffer and subsequently two times with PBS buffer. To visualize the detected protein a chromogen, light sensitive reaction mix consisting of 33 µl nitro blue tetrazolium chloride (NBT, 100 mg/ml) and 66 µl 5-bromo-4chloro-3-indolyl phosphate (BCIP, Material & Methods 28 50 mg/ml) dissolved in 10 ml AP buffer was added to the PVDF membrane. The reaction was stopped by holding the membrane under rinsed water. The membrane was then dried with normal tissues and documented by scanning with HP Scanjet 300 (HP).

PBS pH 7.4

5 mM	$Na_2HPO4 \times 2H_2O$
1.5 mM	$NaH_2PO4 \times H_2O$
137 mM	NaCl
2.7 mM	KCl

PBS-T pH 7.4

99.9 % (v/v)	PBS
0.1 % (v/v)	Tween-20

Blocking solution

97 % (v/v)	PBS
3 % (w/v)	BSA

Towbin-Buffer

25 mM	Tris pH 8.3 (HCl)
192 mM	Glycin

AP-Buffer

100 mM	Tris pH 9.5 (HCl)
100 mM	NaCl
5 mM	MgCl2

2.4.11 Determination of protein concentration

The protein concentration was determined by the absorption at 280 nm (A280) using the protein extinction coefficient (ε280) of the protein according to the estimation of Gill and von Hippel (Gill and Hippel, 1989).

$$\varepsilon 280 = (nTrp * 5690 + nTyr * 1280 + nCys * 120)\ M{-}1\ cm{-}1$$

with: nx = number of the specific amino acid in the protein molar extinction coefficient at 280 nm

Following the Lambeert-Beer's law the protein concentration was calculated.

c [mol l] = A280 ε280 · d

c : protein concentration in $mol\ l$

A280 : absorption at 280 nm

ε280 : molar extinction coefficient at 280 nm

d : pathlength of light trough the cuvette

The molecular weight of the protein was used to calculate the concentration in g/l, which was determined by the webtool ProteinCalculator v3.4 (http://protcalc.sourceforge.net).

2.4.12 Size exclusion chromatography

Size exclusion chromatography is a method to separate proteins based on their oligomerization state by filtrating trough a column packed with beads containing pores. When the proteins are entering the beads, they get included or excluded to the pores due to the molecular weight of the proteins. Small proteins remain in the pores compared to bigger proteins that are passing through the column. Therefore, proteins with a higher molecular mass elute first whereas small proteins have a longer retention time. Each protein has its specific elution volume (Ve) that correlates to its molecular weight. Due to the elution volume the oligomerization state of the protein can be calculated.

For this calculation, a standard curve using standard proteins was created. The logarithm of the standard proteins was plotted against the quotient of their Ve and void volume (V0). As standard proteins Apoferritin (MW = 443 kDa), β-Amylase (MW = 200 kDa), alcohol dehydrogenase (MW = 150 kDa), Albumin (MW = 66 kDa) and carbonic anhydrase (MW = 29 kDa) were used. For the calculation of the curve the void volume of the column is important. Therefore, the Ve of Blue Dextran (2000 kDa) was determined. The buffer creating this curve should be the same as for estimating the oligomerization state of the determined protein. For estimating SEC under anaerobic conditions oxygen was removed by incubating the buffer containing bottle with opened lid for 15 min in the ultrasonic bath chamber.

2.4.13 Optical absorption spectroscopy (UV/vis)

Ultra-Violet Spectroscopy is a technique to determine coordination of the heme cofactor. Chromophores like the heme cofactor absorb ultra-violet and visible light. For anaerobic conditions UV/vis spectra were performed using rubber-sealed cuvette containing 300 µl of the determined protein sample. To reduce the sample (Fe(III)), 5 mM sodium dithionate (DTH) was added and purged with N_2 gas for 10 min. To record the Fe(II)-CO complex, the sample was flushed with CO gas and inverted until a slight orange color appeared. All UV/vis spectra were performed at RT and recorded using a 8453 UV/visible spectrophotometer (Agilent Technologies).

2.4.14 Acidified butanone extraction

To determine if the heme cofactor is covalently attached to the protein an acidified butanone extraction was performed. Therefore, the protein sample was acidified with 1 M HCl. The pH value was observed with pH paper. After adding the same amount of ice-cold 2-butanone, the reagents were inverted and incubated on ice. The upper organic phase separates from the aqueous phase below by cooling down. The covalently bound heme cofactor remains in the aqueous phase whereas the non-covalently bound cofactor gets extracted and remains in the upper organic phase. Due to the localization of the heme cofactor the phase turns brown and the reaction tube can be documented by photographing.

2.4.15 Treatment with histidine residue masking reagent DEPC

The reagent diethylpyrocarbonat (DEPC) (Carl Roth) modifies histidine residues. Therefore, the phosphorylated amino acid residue of a kinase can be determined. The reagent was diluted in EtOH to the required concentration (1 mM) and incubated for 1 h at room temperature with the purified protein. The sample was autophosphorylated for 10 min. SDS-PAGE Proteins samples were mixed with 4x SDS sample buffer and then loaded without heating on a 10% SDS gel and separated by SDS-PAGE. To evaluate if the reagent is masking the histidine residue, the SDS gel was wrapped in plastic foil and exposed to a PhosphorImager screen in a cassette containing an enhancing screen overnight at room temperature. The signals were recorded using a PhosphorImager (GE Healthcare Perkin Elmer Cyclone Typhoon FLA 7000).

2.4.16 Acid-base treatment of phosphorylated protein

The proteins used in this work were phosphorylated, then separated via SDS-PAGE and transferred onto a PVDF membrane (18 min, 15 V) by Trans-Blot® SD semi-dry Western blot (BioRad). The membrane was exposed as described before overnight to a PhosphoImager screen. After the detection of the radioactive signals with a PhosphoImager (GE Healthcare Perkin Elmer Cyclone Typhoon FLA 7000), the membrane was incubated for 1 h at RT in 6 M HCl, 3 M NaOH and, as reference, in H_2O. Phosphorylation signals were again evaluated by exposing the membrane overnight as described above to a PhosphoImager screen and subsequently detected. To confirm protein transfer, the PVDF membrane was stained with Ponceau S to visualize the proteins.

Ponceau S

3 % (v/v)	Glacial acetic acid
0.33% (w/v)	Ponceau-S
25 % (v/v)	H_2Odest
Dissolve under constant stirring	

2.4.17 Pyridine hemochrome assay

Pyridine hemochrome assay is a technique to examine covalently binding of the heme cofactor to the purified protein measured spectrophotometrically. By adding pyridine to the protein sample, the reagent can replace the axial ligands of the cofactor which results in pyridine hemochrome that is detectable with UV/vis (Ultraviolet/visible spectroscopie) spectra.

For the procedure concentrated purified protein up to 10 µM in a total volume of 500 µl got reduced with potassium ferricyanide to ensure that the complete heme containing protein is in its oxidized Fe(III) state. To an amount of 500 µl protein solution 62.5 µl NaOH and 62.5 µl pyridine were added. After addition of DTH Fe(III) got reduced to Fe(II). NaOH keeps the reductant DTH in the solution stable, whereas pyridine can bind to the reduced protein. If pyridine is replacing the axial ligands like in case of hemoglobin it results in a spectrum of 556 nm.

2.4.18 Radioactive in vitro autophosphorylation and phosphotransfer assays

In order to investigate the autophosphorylation activity of the desired protein or protein variant a reaction mix of 10 µM of the purified protein, 2.5 µl of 5xTris-buffer pH 8.0 and ad. H_2O up to a total volume of 10 µl was combined in a sealed short thread vial (VWR). For reducing condition freshly prepared DTT was added to a final concentration of 2 mM. The reaction mix was flushed with N_2 using a cannula (Braun) for 15 sec whereas air bubbles were removed to create a reduced environment in the vial. To start the reaction 2.5 µl of the ATP Mix was added and samples were taken after different time points, and the reaction was stopped by the addition of 4x SDS sample buffer (2.4.8).

To investigate the phosphorelay inside the kinase MA4377, 10 µM of PK were autophosphorylated for 10 min. After removing excessive ATP with illustra™ MicroSpin™ G-25 Columns (GE healthcare), the protein was added to an extra vial containing 10 µM of the phosphate acceptor constructs (PKH_{497}QR1, PKH_{497}QR1D_{818}NR2, R, RD_{54}N and TF). All phosphate acceptor constructs were reduced with fresh DTT (2 mM) and flushed with N2 before phosphotransfer reaction.

To separate the phosphate acceptor construct from PK and to remove imidazole in the case of phosphorylated R, subsequent to affinity chromatography, Sephadex G-25 (GE) column were used.

All taken samples (10 µl) were quenched with 4x SDS sample buffer (2.4.8) and then loaded without prior heating on a 4-20% gradient polyacrylamide gel and separated by denaturing sodium dodecyl sulfate-polyacrylamide gel electrophoresis (SDS-PAGE) (BioRad). The gel was exposed to a PhosphorImager screen in a cassette containing an enhancing screen, overnight at room temperature. The signals were recorded using a PhosphorImager (GE Healthcare Perkin Elmer Cyclone Typhoon FLA 7000). To visualize the proteins, the same gel was stained in Coomassie Brilliant Blue G250, destained with a destaining solution (2.4.8) and documented by scanning with HP Scanjet 300 (HP).

To quantify the intensity of the increasing autophosphorylation activity of PK (10 µM) ImageJ (64-bit Java 1.8.0_172) Color_Pixel_Counter was used. The sample taken after 600 s referred as reference and was valued as 100% of signal intensity.

Kinase Assay Mix

x µl	10 µM of Protein
2.5 µl	5x Tris Buffer
2.5 µl	ATP-MIX
2 µl	H_2O

1xTris Buffer

50 mM	Tris pH 8.0
150 mM	NaCl
5 mM	$MgCl_2$
50 mM	KCl

ATP Mix

0.25 µl	ATP (10 mM)
0.25 µl	[γ-32P]-ATP (1850 kBq)
2 µl	H_2O

3 Results

Signal transduction is a mechanism to connect an environmental signal with a subsequent reaction to it and thereby provide the possibility of the organism to adapt to changing conditions. A very common mechanism is based on a two-component system (TCS) including autophosphorylation of a sensor histidine kinase resulting in a transfer of the phosphoryl group to the cognate RR leading to cell response. TCS were discovered in Bacteria and later also identified in Archaea and lower eukaryotes. It is supposed that these signal transduction systems were integrated into archaeal genomes via horizontal gene transfer. The hybrid kinase MA4377 seems to be structural of bacterial origin and draws with the C-terminal fused receiver attention to a more complex multi-component system (MCS) in Archaea. Therefore, it is interesting to examine MA4377 as a bacterial kinase in an archaeal system from an evolutionary aspect but also to gain more insights into archaeal signal transduction.

In order to investigate whether MA4377 acts like a bacterial histidine kinase *in vitro*, autophosphorylation studies were performed. To reveal its putative function in *M. acetivorans* in an MCS, truncated versions of the kinase were generated to analyze signal transduction inside the hybrid kinase and to probable adjacent phosphate acceptors.

3.1 Characterization of the hybrid kinase MA4377

Regarding its genetic localization, MA4377 is a stand-alone kinase in the genome of *M. acetivorans* and is annotated to encode a putative histidine kinase. Upstream of the kinase, genes encoding for a methyltransferase and an ATPase are located. Downstream a single receiver domain with its open reading frame is localized, overlapping with MA4377 by 29 nt. Adjacent to the receiver MA4376, a transcription factor (TF) belonging to the Msr family and a SAM dependent methyltransferase are positioned (Figure 3.1). The hybrid kinase is closely positioned to the kinases MsmS, which together with the kinase RdmS are involved in methylotrophic methanogenesis as they are encoded upstream of TFs. These TFs, structurally highly similar to MA4375, are regulating methyltransferases on a transcriptional level (Bose et al., 2009; Fiege and Frankenberg-Dinkel, 2019).

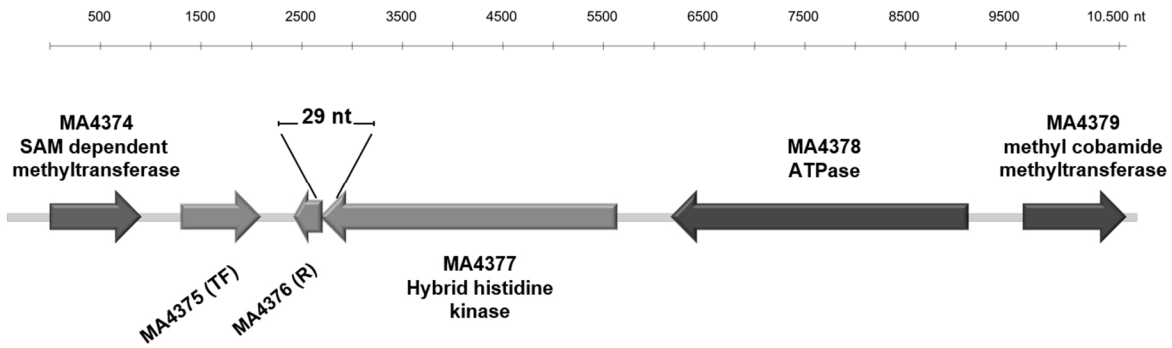

Figure 3.1. Genetic localization of MA4377. Schematic figure of MA4377, receiver MA4376 and transcription factor MA4375 (light grey arrows) arrangement in the genome of *M. acetivorans* drawn to scale (Galagan et al., 2002).

To get detailed information about the open reading frame (ORF) of MA4377, BLASTp (protein blast) analysis (NCBI; Phyre2; hhpred (MPI Bioinformatics Toolkit)) were performed to reveal the annotated domains and the similarity to other kinases supporting the characterization of MA4377. Subsequent amino acid sequence alignments (clustal omega) using matches with the lowest E-value and the highest identity (ID) with at least 30 % but also well-characterized bacterial histidine kinases, helping to identify conserved motifs, were performed (Supplementary Data 5.1) MA4377 encodes a predicted multidomain protein, consisting of three input domains (NCBI).

MA4377 encodes a predicted multidomain protein, consisting of three input domains: a membrane-anchored **c**yclases/**h**istidine kinases **a**ssociated **s**ensory **e**xtracellular 4 (CHASE4) domain (Mougel and Zhulin, 2001), followed by a cytoplasmic present domain in histidine kinases (HKs), **a**denylyl cyclases, **m**ethyl-accepting chemotaxis proteins (MCPs), and some **p**hosphatases (HAMP) (Parkinson, 2010)and **P**er-**A**RNT-**S**im (PAS) domain (Taylor and Zhulin, 1999). At the C-terminus of the kinase catalytic core a dimerization and histidine phosphotransfer (DHp) domain and a catalytic and ATP binding (CA) domain are located with terminally two successive receiver domains (Figure 3.2). Based on the domain structure, connecting the kinase catalytic core with the receiver domains and the highly conserved histidine residues in the DHp domain, MA4377 resembles a bacterial-like hybrid histidine kinase.

In order to determine whether MA4377 possesses kinase activity *in vitro* and to understand its putative function in *M. acetivorans*, truncated versions of the gene were cloned for heterologous expression in *Escherichia coli.*

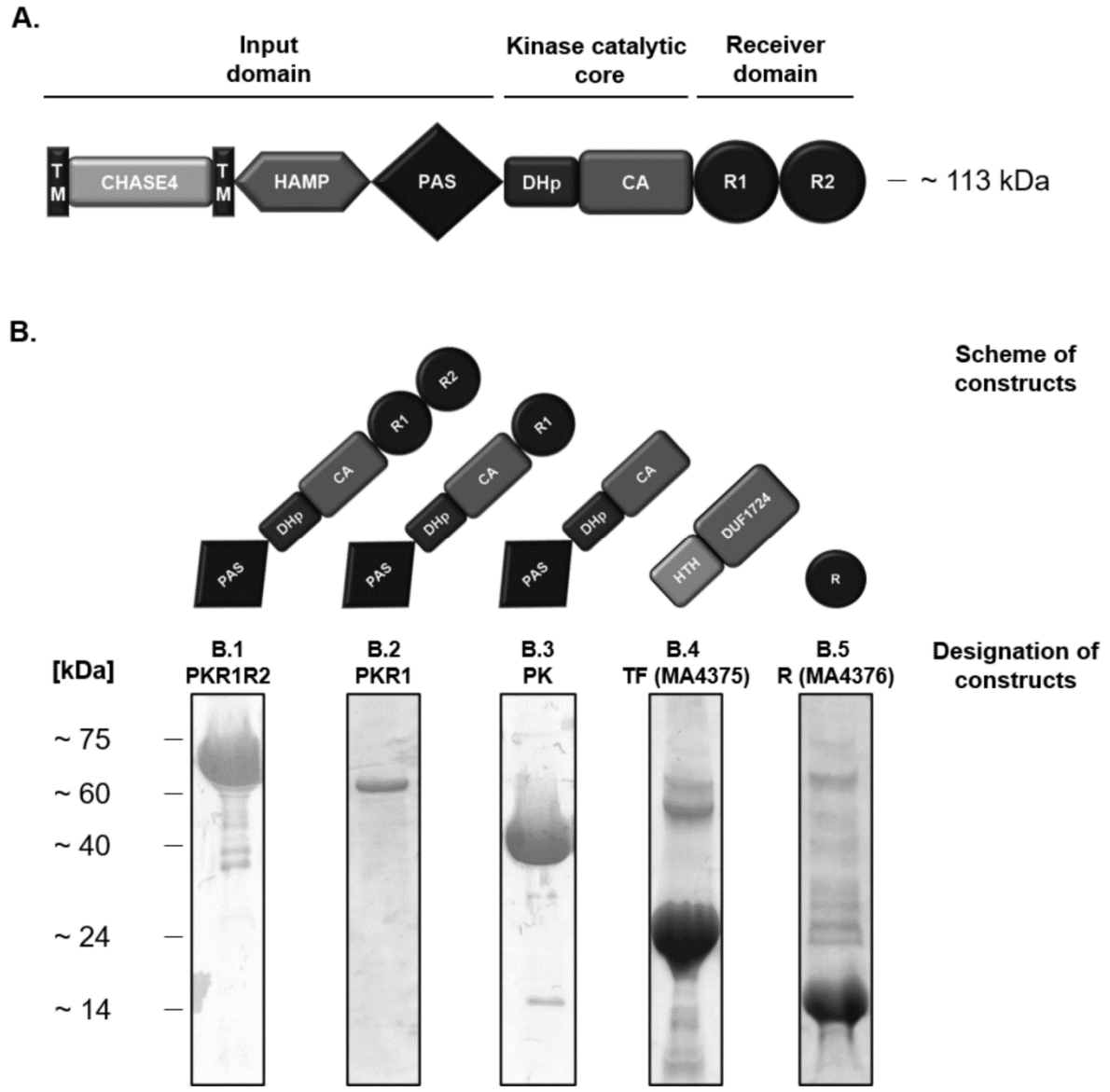

Figure 3.2. Schematic representation of the domain structure of hybrid histidine kinase MA4377 and purification of the indicated truncated versions of MA4377. **A.** Similar annotated domains of MA4377 analyzed by tools of NCBI (BLASTp; E-value: 0.05) and hhpred (MPI Bioinformatics Toolkit) (BLASTp; E-value of 1e-3). Single domains are divided into subgroups. CHASE-, HAMP- and PAS domain (blue) are associated with input domains. DHp and CA domain (red) belong to the kinase catalytic core and R1 and R2 (green) to receiver domains. **B.** Schematic and SDS-PAGE of purified truncated versions used. **B.1** PKR1R2 (~75 kDa) consisting of PAS domain, the kinase catalytic core and the receiver domains R1 and R2. **B.2** PKR1 (~60 kDa) consisting of a PAS domain, the kinase catalytic core and the receiver domains R1**. B.3** PK (~40 kDa) consisting of PAS domain, the kinase catalytic core. **B.4** TF (MA4375) (~24 kDa) consisting of a helix-turn-helix (HTH) motif and a domain of unknown function 1724 (DUF1724). **B5.** R (MA4376) (~14 kDa) consisting of a receiver domain

Initial to characterization experiments, the effect of the protein purification procedure at the bench exposing MA4377 to oxygen had to be determined, as MA4377 is originating from an anaerobic organism. Therefore, affinity chromatography at the bench with the construct PKR1R2 (Figure 3.2.B) produced in *E. coli* BL21 (DE3), using Tris buffer pH 8.0 containing DTT (250 mM), to create a reduced condition (Figure 3.3.A.1), was compared to protein purification in the anaerobic chamber (Figure 3.3.B.1). Purification under both conditions revealed a predominant protein of ~75 kDa

which resembles the mass of the protein of PKR1R2. Aerobic (Figure 3.3.A.2) and anaerobic (Figure 3.3.B.2) size exclusion chromatography (SEC) with Tris buffer pH 8.0 were performed to investigate the influence of oxygen on oligomeric state. Both proteins showed the same SEC profile with an elution volume of (~15.5 ml) resulting in a protein mass of ~ 240 kDa, indicating that oxygen does not influence the oligomeric state of the protein (Figure 3.4.A.2+B.2).

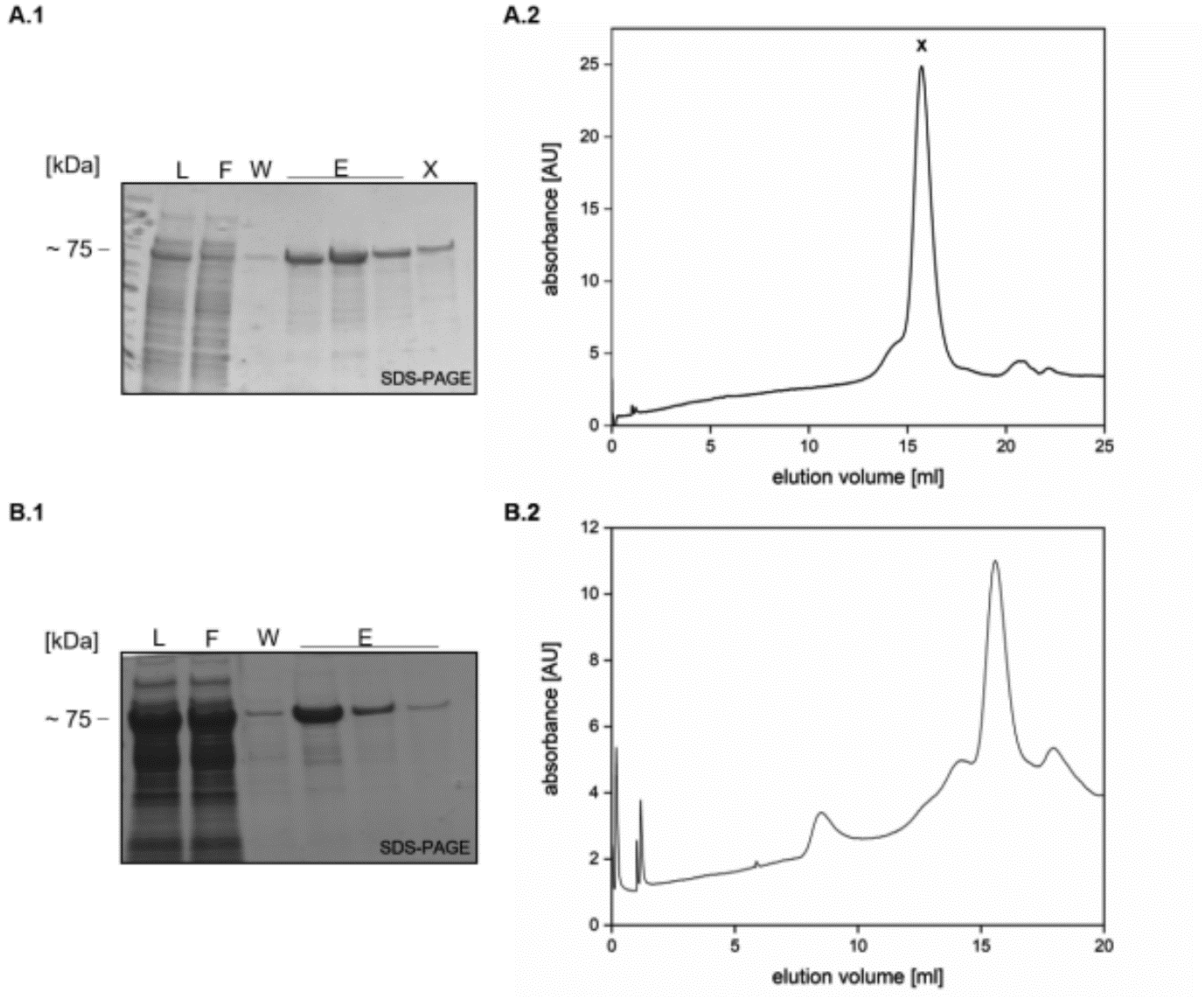

Figure 3.3. SDS-PAGE and SEC of PKR1R2 from *E. coli* BL21 (DE3) under anaerobic and aerobic conditions. **A.1** SDS PAGE of MA4377 PKR1R2 purified under anaerobic via affinity chromatography. L= lysate; F= flow-through fraction; W= washing fraction; E= elution fractions of PKR1R2 (MW=~75 kDa) from 2 l culture volume. **A.2** Elution profile of purified PKR1R2 under anaerobic conditions via SEC. The protein was separated via a Superose™ 6 10/300 GL column (GE Healthcare) and equilibrated with sonicated Tris buffer pH 8.0 containing no oxygen. Absorbance of the eluted protein at 15.6 ml was monitored at a wavelength of 280 nm. **B.1** SDS PAGE of MA4377 PKR1R2 purified under aerobic conditions via affinity chromatography. L= lysate; F= flow-through fraction; W= washing fraction; E= elution fractions of PKR1R2 (MW=~75 kDa) from 2 l culture volume. X= marks the SEC fraction of PKR1R2. **B.2** Elution profile of purified PKR1R2 via SEC under aerobic conditions. The protein was separated via a Superose™ 6 10/300 GL column (GE Healthcare) and equilibrated with Tris buffer pH 8.0. Absorbance of the eluted protein at 15.7ml (marked with a X) was monitored at a wavelength of 280 nm.

Overall these data indicate that anoxic condicitons are neither required for purification nor do they have an influence on the quaternary structure of the protein.

3.1.1 The hybrid kinase MA4377 displays autophosphorylation activity

To examine the autophosphorylation of MA4377 *in vitro* autophosphorylation assays were performed under reducing conditions (2 mM DTT). For these experiments, the PK construct (Figure 3.2.D) was used, containing the kinase catalytic core and the PAS domain, as this sensor domain is supposed to be important for protein-protein interaction (Taylor and Zhulin, 1999). Autophosphorylation activity steadily increased over 10 min, indicating that MA4377 possesses autokinase activity (Figure 3.4).

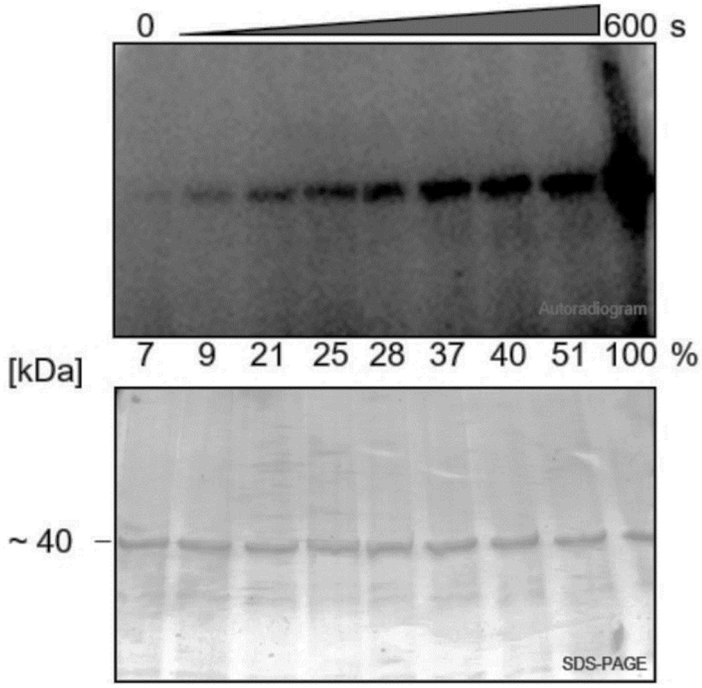

Figure 3.4. Autophosphorylation assay of truncated version PK of MA4377. 10 µM of purified PK was phosphorylated with [γ-^{32}P]-ATP. Reaction was stopped after different time points (30-600 s). Reaction contained DTT (2 mM), was flushed with N_2 and stopped with buffer containing β-mercaptoethanol. Samples (10 µl) were resolved on SDS-PAGE and subjected to autoradiography or Coomassie stained to show the protein amount. Intensities of the phosphorylation signals are given under the autoradiogram. Values were quantified with ImageJ Color_Pixel_Counter Plugin and normalized setting 600 s sample as 100%.

3.1.2 The kinase MA4377 is a bacterial–like histidine hybrid kinase

Signal transduction in bacteria is mostly implemented by histidine kinases that get autophosphorylated on a conserved histidine residue within the so-called H-box, located in the DHp domain (Figure 3.A) (Capra and Laub, 2012). However, also the so called Hanks type kinases are involved in some signal transduction systems that receive the phosphoryl group at a Ser/Thr/Tyr residue (Steven Hanks and Tony Hunter, 1995). Due to different characteristics of the chemical bond between amino acids and the phosphoryl group, acid base-treatment can be performed to identify the phosphorylation site. Phosphorylated Ser/Thr/Tyr kinases, which are more abundant in Archaea, form phosphoester bonds that show acid-stable and base-labile characteristics (Duclos et al., 1991). Whereas histidine kinases form a phosphoramidate bond with the N1 or N3 of the histidine imidazole ring that possesses a high negative free energy and makes it therefore suitable for phosphotransfer (Stock et al., 2000). To investigate the phosphorylation site of MA4377, which resembles a bacterial-like histidine kinase, an acid base-treatment was performed. Purified and phosphorylated MA4377 (PK) was incubated in water, base, and acid. No difference of the radioactive signal after incubation in water and base was observed, whereas the sample incubated in acid showed a significantly reduced signal suggesting histidine phosphorylation (Figure 3.5.A).

Further verification was obtained by treating the truncated versions PKR1R2 and PK (Figure 3.B1+B3) with the histidine modifying reagent diethylpyrocarbonate (DEPC) prior to the kinase assay (Figure 3.5.B). Upon autoradiography, no autophosphorylation signal was detected for the truncated versions PKR1R2 and PK used for this experiment confirming that MA4377 is a histidine kinase.

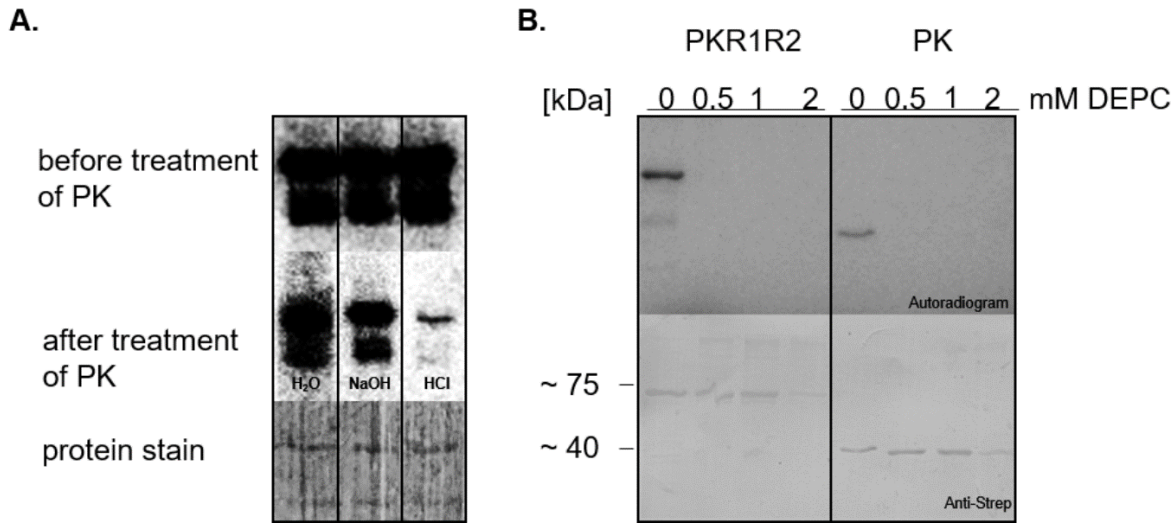

Figure 3.5. Analysis for identification of histidine phosphorylation. A. Acid-base treatment of hybrid kinase MA4377. Hydrolytic stability of phosphorylation site of autophosphorylated PK before and after treatment (autoradiogram) with water, 1M NaOH and 6M HCl. To verifiy protein amount, the PVDF membrane was stained with Ponceau S. **B.** Incubation of [γ-^{32}P]-ATP radiolabeled PKR1R2 and PK with increasing concentrations 0.5, 1, 2 mM of DEPC (Diethylpyrocarbonate). The samples (10 µl) were resolved on SDS-PAGE transferred to PVDF membrane, subjected to autoradiogram or antibody detection to show protein amount.

3.1.3 His$_{497}$ is the phosphorylation site in MA4377

Verifying the specific histidine residue of the kinase MA4377, amino acid sequence alignments of the DHp domain of MA4377 with other histidine kinases were performed. The aligned kinases were identified with BLASTp in *M. acetivorans* showing the lowest E-value and the highest ID with at least 30 %. This analysis revealed three conserved histidine residues at positions 497, 538 and 560 (5.1). The histidine at position 497 is located in the well-conserved H-Box (Figure 3.6.A) but for determination, histidine to glutamine variants of all three residues in all combinations were generated via site-directed mutagenesis (Figure 3.6.B).

A.

Residue number	1	2	3	4	5	6	7
AA sequences	H	(D/E)	(L/I)	(K/R)	(T/N)	P	L

B.

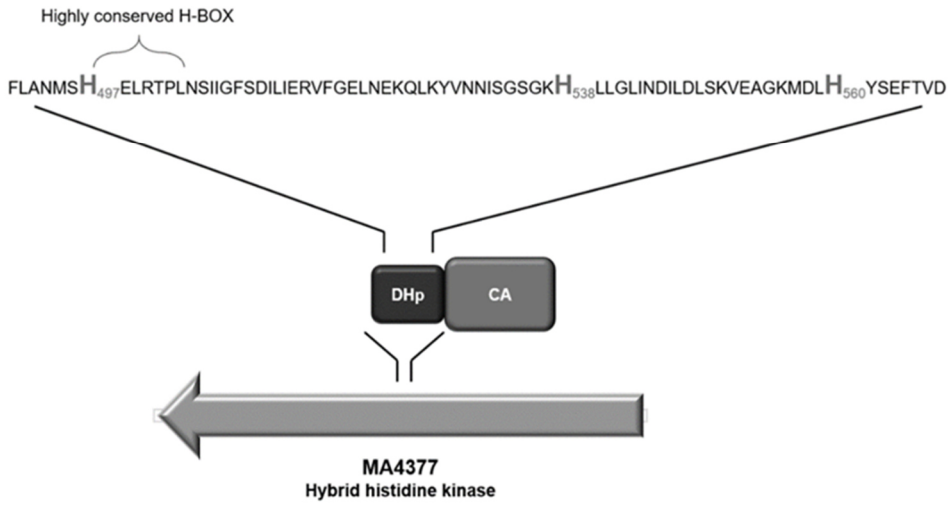

Figure 3.6. Conserved motif of H-Box and putative conserved histidine residues as phosphorylation site of MA4377. A. Conserved amino acid residues of H-Box after (Bhate et al., 2015). Part of the amino acid sequence of DHp of MA4377 shows conserved histidine residues at position 497, 538, and 560 and highlighted H-Box motif.

Purification of all variants via affinity chromatography revealed the same molecular weight of ~ 40 kDa as well as the same oligomerization state during SEC experiments (5.2). To determine the effect of the histidine variants on autophosphorylation activity, kinase assays were performed (Figure 3.7). Only protein variants lacking the histidine residue at position 497 showed no autophosphorylation activity and therefore identifying this residue as the specific phosphorylation site of the histidine hybrid kinase MA4377.

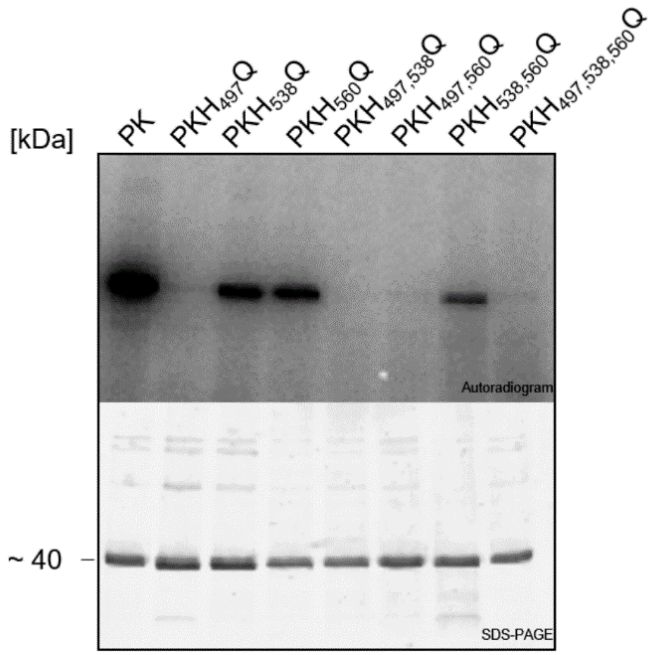

Figure 3.7. Identification of histidine phosphorylation site. Analysis of autophosphorylation activity of conserved histidine residue variants (10 µM) $PKH_{497}Q$, $PKH_{538}Q$, $PKH_{560}Q$, $PKH_{497,538}Q$, $PKH_{497,560}Q$, $PKH_{538,560}Q$, $PKH_{497,538,560}Q$. [γ-^{32}P]-ATP radiolabeled samples (10 µl) were separated by SDS-PAGE and the radioactive signals detected by PhosphoImager (Autoradiogram). The same SDS gel was stained with Coomassie (SDS-PAGE) to visualize the loaded protein.

3.1.4 Investigating whether MA4377 uses heme as a cofactor

The third sensor domain of MA4377, the PAS domain, is known to be mostly localized in the cytoplasm and N-terminally fused to histidine kinase catalytic core in Bacteria and Archaea as in the case of MA4377 (Figure 3.2.A). PAS domains can sense various physical and chemical signals by binding cofactors, like hemin (Lee et al., 2008; Gilles-Gonzalez and Gonzalez, 2004; Möglich et al., 2009; Taylor and Zhulin, 1999). Heme cofactors possess a central iron atom that is coordinated by six ligands. Four of these are displayed by the nitrogen atoms of the porphyrin ring. The remaining two axial ligands are represented by amino acids and small gases which influence the reactivity and function of the heme cofactor. Further roles of the heme cofactor relate to the oxidation state of the iron ion that enables oxidation and reduction of reactions as well as electron transport (Zhang, 2011). Another incidence for MA4377 containing a heme cofactor, next to possessing a PAS domain, is the genomic localization adjacent to the transcription factor MA4375 that belongs to the Msr family. The kinase MsmS as well as RdmS are directly upstream located to Msr transcription factors, that are involved in the regulation of methyltransferases. MsmS and RdmS contain the sensor domain

GAF, that binds a heme cofactor which influences the kinase activity (Fiege and Frankenberg-Dinkel, 2019).

3.1.4.1 Analysis of the heme cofactor in the full-length protein MA4377

To verify whether this is the case for MA4377, investigations were carried out, using *E. coli* Nissle 1917 as a heterologous expression system. This strain is mostly known for medical uses, but it was shown that it is useful for protein production and furthermore it possesses a heme-take-up system that leads to improved incorporation of heme due to its heme receptor ChuA (Fiege et al., 2018; Nissle, 1917). The full-length protein MA4377 which is predicted to a molecular weight of ~113 kDa was produced in *E. coli* Nissle 1917 with supplemental heme in the growth medium. Purification of the full-length protein (Figure 3.2.A) containing the transmembrane domain CHASE4 was carried out via affinity chromatography, neglecting membrane solubilization (Figure 3.8). To examine the cooperation of the heme cofactor and its coordination, UV/vis spectra analyses were performed (Figure 3.8.B).

The heme peak in the oxidized Fe(III) form at 412 nm resembles the Soret band for heme cofactors. The Fe(III) complex could be reduced by adding a spatula tip of DTH followed by a shift of the Soret band to 525 nm. After flushing the sample with CO gas for 15 s, the gas could bind to the porphyrin, resulting in a shifted band to 416 nm (Figure 3.8.B).

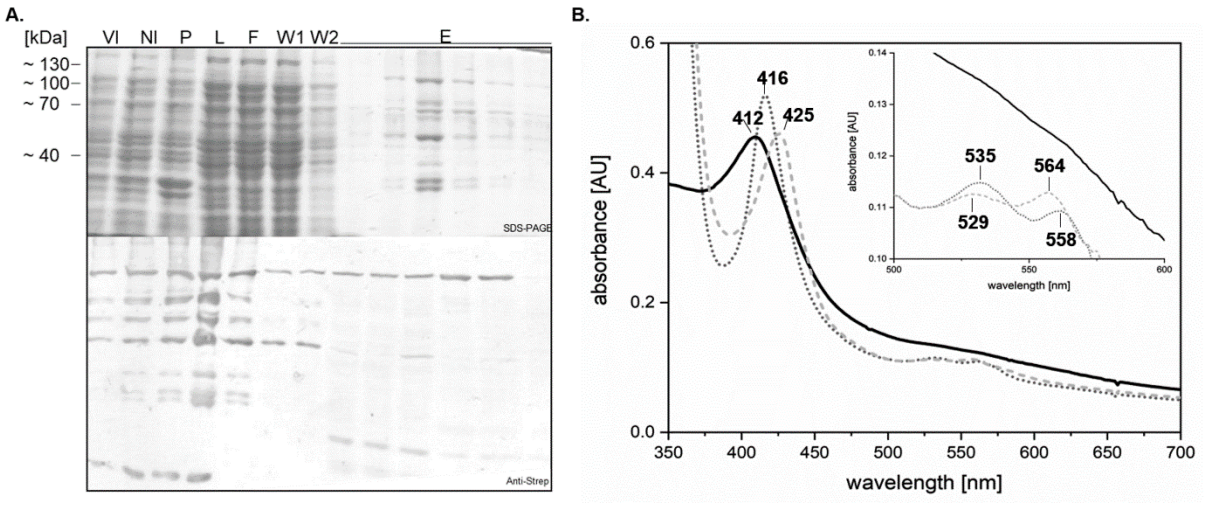

Figure 3.8. Coordination of heme cofactor of full-length protein MA4377 from *E. coli* Nissle 1917. A. SDS-PAGE of purified full-length MA4377 via affinity chromatography. L= lysate; F= flow-through fraction; W1= washing fraction 1; W2= washing fraction 2; E= elution fractions of MA4377 (MW=~113 kDa) from 2 l culture from *E. coli* Nissle 1917 volume. **B.** UV/vis spectra of full-length MA4377 produced in *E. coli* Nissle 1917 with heme shown as Fe(III) (black line), Fe(II) (light grey dashed line), Fe-CO (grey dotted line). The box in the right corner shows Q-bands by enlargement of the of absorbance [AU].

For further analysis of the full-length protein, repeated production and purification experiments were not successful.

Additional attempts for the purification of MA4377 were made using different expression systems. Overproduction of heterologous expressed transmembrane proteins can be limiting or toxic for the expression system. Using *E. coli* C43 a derivate from *E. coli* BL21(DE3) with mutations in the T7 RNA polymerase promoter LacUV5, leads to a decreased expression and therefore lower toxicity for the cell and supports protein production (Miroux and Walker, 1996; Wagner et al., 2008). Hence, *E. coli* Walker C43 was used for full-length expression of MA4377. Test expression in this system showed that MA4377 is only soluble when produced at 17°C and 37 °C in a time range from 1 to 3 hours and overnight at 37°C (Figure 3.9).

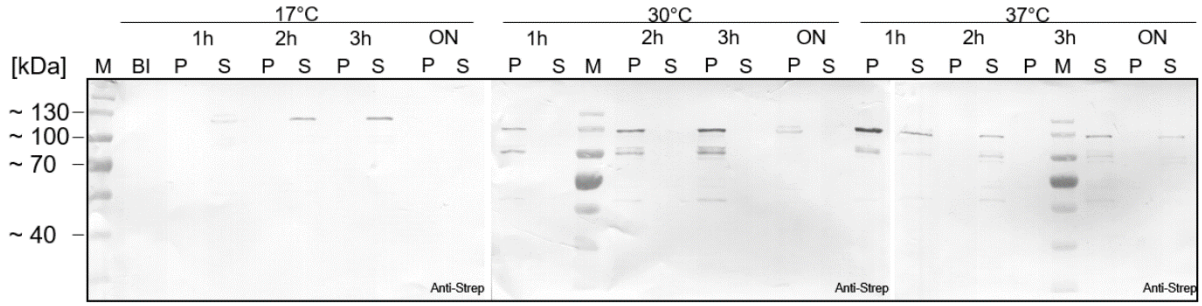

Figure 3.9. Test expression of MA4377 in *E. coli* Walker (C43). Protein expression of MA4377 was tested under varying temperatures of 17°C, 30°C and 37°C. Pellet (P) and supernatant (S) fraction of samples taken after 1h, 2h, 3h and overnight (ON) were resolved by SDS-Page. Protein samples were transferred to PVDF membrane and detected by anti-Strep-Tactin®-AP-conjugate.

Unfortunately, purification via affinity chromatography was not successful (data not shown).

An additional test expression was performed with 15 ml samples out of *E. coli* BL21(DE3) at 17 °C and 37°C (Figure 3.10.A). Comparison of the sample before induction (BI) and the samples after induction in the supernatant (S) fraction after 1h incubation at 17°C and overnight (ON) at 37 °C revealed a band with the desired molecular mass.

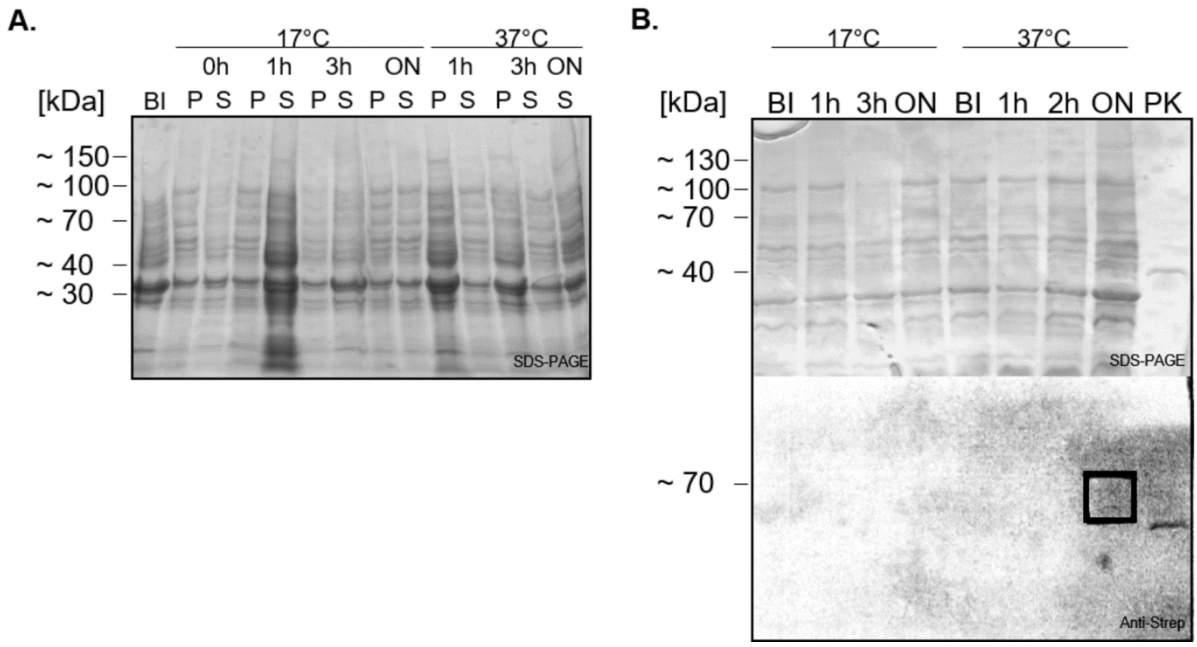

Figure 3.10. Test expression of MA4377 in *E. coli* BL21 (DE3) and solubilized membrane pellet. A. Samples of MA4377 protein production at 17°C and 37°C after different time points 1h, 3 h and overnight (ON) were sonicated. Subsequent centrifugation, pellet (P), and supernatant (S) fractions (12 µl) were loaded on the SDS gel (SDS-PAGE). A sample before induction (BI) served as a reference. **B.** Supernatant fractions were centrifuged by mini ultracentrifuge. Membrane pellet fractions were solubilized BBF buffer pH 8.0 and 12 µl of the samples were resolved by SDS-PAGE (SDS-PAGE). As reference a sample before induction (BI) and a truncated version of MA4377 (PK) were additionally loaded. Protein was transferred to PVDF membrane and detected by anti-Strep-Tactin®-AP-conjugate (Anti-Strep).

Preparation of the membrane fractions (Figure 3.10.B) did not reveal the soluble full-length protein, that was thought to be shown as a protein with a mass of ~100 kDa in the test expression (Figure 3.10.A).

3.1.4.2 Analysis of the heme cofactor in the truncated construct PK of MA4377

As the purification of the full-length protein was not successful the truncated version PK (Figure 3.2.D), was used to examine the coordination of the heme cofactor. PK was produced recombinantly in *E. coli* Nissle 1917 with the addition of hemin in the growth medium directly after inducing the gene expression by addition of AHT and was purified via affinity chromatography. The purified mass of the protein revealed 40 kDa (Figure 3.11.A). As heme cofactors can be differently coordinated and therefore influencing the protein function, UV/vis spectroscopy was performed (Figure 3.11.B). The peak in the oxidized Fe(III) state resulted at 409 nm and showed two slight shoulders in the Q-band region at 541 and 563 nm. The sample was reduced by the addition of DTH which led to a Soret band shift to 425 nm with a β-band at 564 nm that reveals a 5x

coordination of heme under these conditions. After flushing the sample with CO the peak shifted back to 414 nm and changes in the Q-band region by the formation of β and α at 537 and 566 nm resembled hexameric coordination by binding of CO). The UV/vis spectra analysis revealed that the heme cofactor binding to PK showed characteristically coordination.

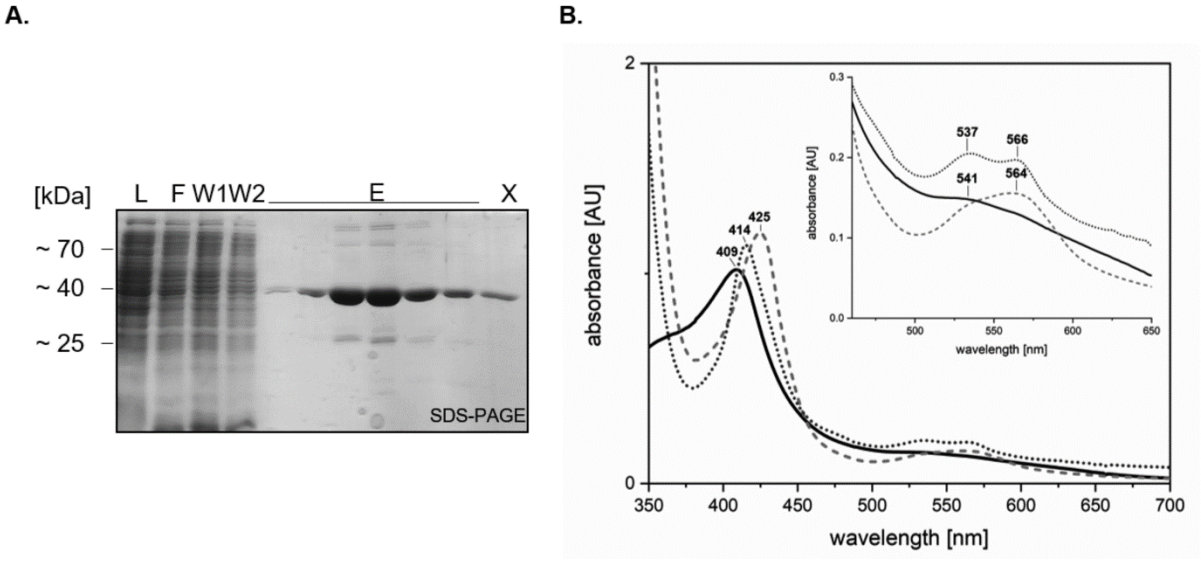

Figure 3.11. SDS-PAGE and UV/vis spectra of PK from *E. coli* Nissle 1917 with heme.
A. SDS-PAGE of purified PK via affinity chromatography. L= lysate; F= flow-through fraction; W1= washing fraction 1; W2= washing fraction 2; E= elution fractions of PK (MW=~40 kDa) from 2 l culture volume. X= marks the SEC fraction of PK. **B.** Shown as Fe(III) (black line), Fe(II) (light grey dashed line), Fe-CO (grey dotted line). The box in the right corner shows Q-bands by enlargement of the absorbance [AU].

To examine the oligomerization state of the truncated version size exclusion chromatography (SEC) was performed (Figure 3.12). PK produced with heme eluted at 16.9 ml that corresponded to a molecular mass of ~109 kDa and could therefore resemble a long-stretched dimer.

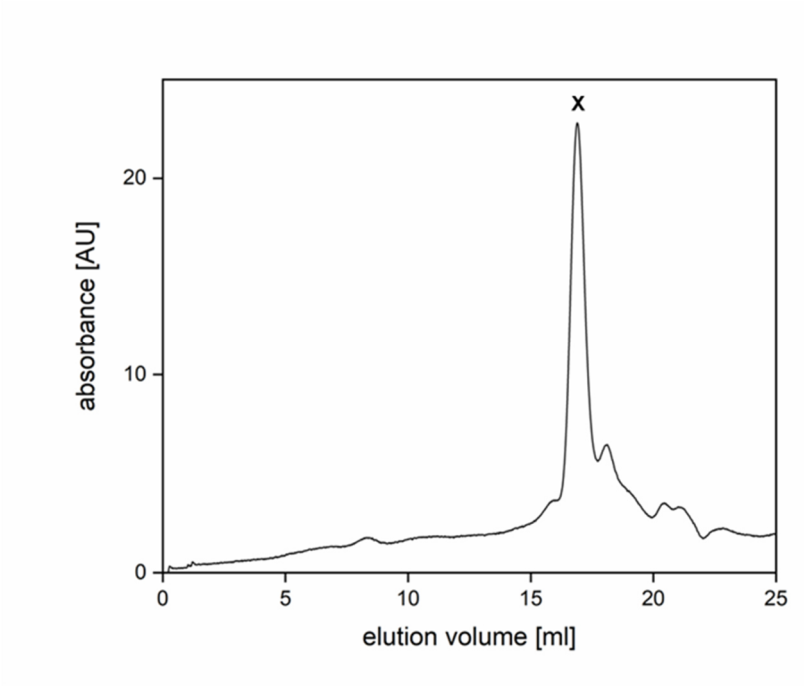

Figure 3.12. SEC profile of PK produced in *E. coli* Nissle 1917 with heme. Elution profile of purified PK via size exclusion chromatography produced in *E. coli* Nissle 1917 with heme. The protein was separated via a Superose™ 6 10/300 GL column (GE Healthcare) and equilibrated with $NaHPO_4$ buffer pH 7.0. Absorbance of the eluted protein (marked with a X) was monitored at a wavelength of 280 nm.

3.1.4.3 Autophosphorylation activity of the histidine hybrid kinase MA4377 is not redox-dependent

As *M. acetivorans* is an anaerobic living organism where the heme cofactor of MA4377 could serve as redox-sensing cofactor and therefore affecting the kinase activity. To investigate the redox dependency of MA4377, kinase assays were performed under oxidizing and reducing conditions. The truncated version PK containing the heme cofactor was employed under both conditions and the activity monitored over time (Figure 3.13).

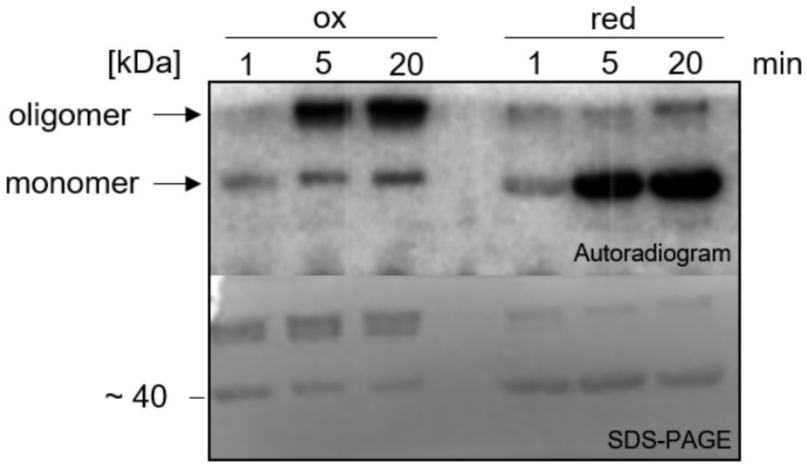

Figure 3.13. Autophosphorylation assay of the truncated version PK from *E. coli* Nissle 1917 with the addition of heme. 10 µM of purified PK was phosphorylated with [γ-^{32}P]-ATP. Samples under oxidized (ox) conditions were stopped after certain time points with 4x SDS sample buffer lacking β-mercaptoethanol. Samples under reduced (red) conditions contained DTH and were flushed with N_2. Samples were taken after different time points and the reaction was stopped with 4x SDS sample buffer containing β-mercaptoethanol. All samples (10 µl) were resolved on SDS-PAGE and subjected to autoradiography and subsequently, Coomassie stained to show protein amount.

The kinase assay revealed autophosphorylation activity under oxidizing and reducing conditions but showed a difference in its oligomerization state. Under reducing conditions, using a 4x SDS sample buffer containing β-mercaptoethanol, PK was mainly active as a monomer. Whereas under oxidizing conditions, the ratio shifted to a primarily phosphorylated oligomeric form of PK.

3.1.4.4 Heme cofactor of the histidine hybrid kinase is not covalently bound

To investigate if the cofactor is covalently bound, as is the case for MsmS and RdmS, an acidified butanone extraction was performed with the truncated version PKR1R2. PKR1R2, containing the C-terminal fused receiver domains (Figure 3.2.B), was used for determination due to its highest similarity to the full-length protein MA4377. UV/vis spectra analysis revealed the same results as for the truncated version PK (Figure 3.12). The purified protein showed a brownish color that proofed the presence of the heme cofactor, as hemin was added after inducing protein production in *E. coli* Nissle 1917. By incubating the protein with 2-butanol, the cofactor stays in the aqueous phase like in the case of cytochrome C if it is covalently bound. In the case of a non-covalently bound cofactor, it can get extracted to the organic upper phase, for instance for hemoglobin (Teale, 1959). The version PKR1R2 revealed a brownish color in the upper organic phase, which concluded that the heme cofactor is not covalently bound to the truncated version of MA4377 (Figure 3.14).

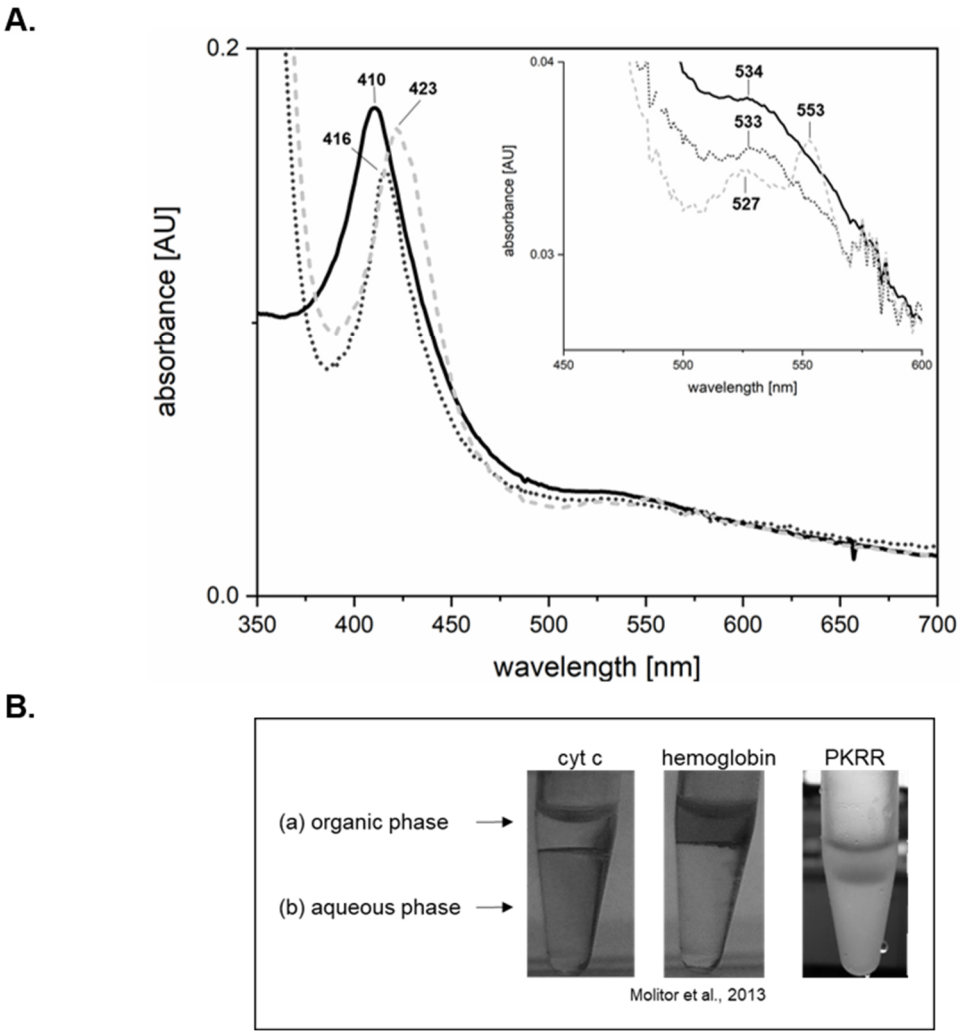

Figure 3.14. UV/vis spectra of PKR1R2 produced in *E. coli* Nissle 1917 with heme and acidified butanone extraction of PKR1R2. A. UV/vis spectra of PKR1R2 shown as Fe(III) (black line), Fe(II) (light grey dashed line), Fe-CO (grey dotted line). The box in the right corner shows Q-bands by enlargement of absorbance [AU]. **B.1** Acidified butanone extraction of cyt c with covalently bound heme cofactor in the aqueous phase and **B.2** shows hemoglobin with extracted heme cofactor in the organic phase. Acidified butanone extraction of PKR1R2 reveals extracted heme cofactor in the organic phase.

To verify the results of the butanone extraction a different method, the pyridine hemochromogen assay, was conducted. Pyridine serves as a ligand for heme in the reduced state that results in a specific pyridine-hemochromogen peak. Comparing the pyridine-hemochromogen peak of PKR1R2 at 554 nm to references with a covalently bound heme cofactor and non-covalently bound heme cofactor gave insights into binding characteristics.

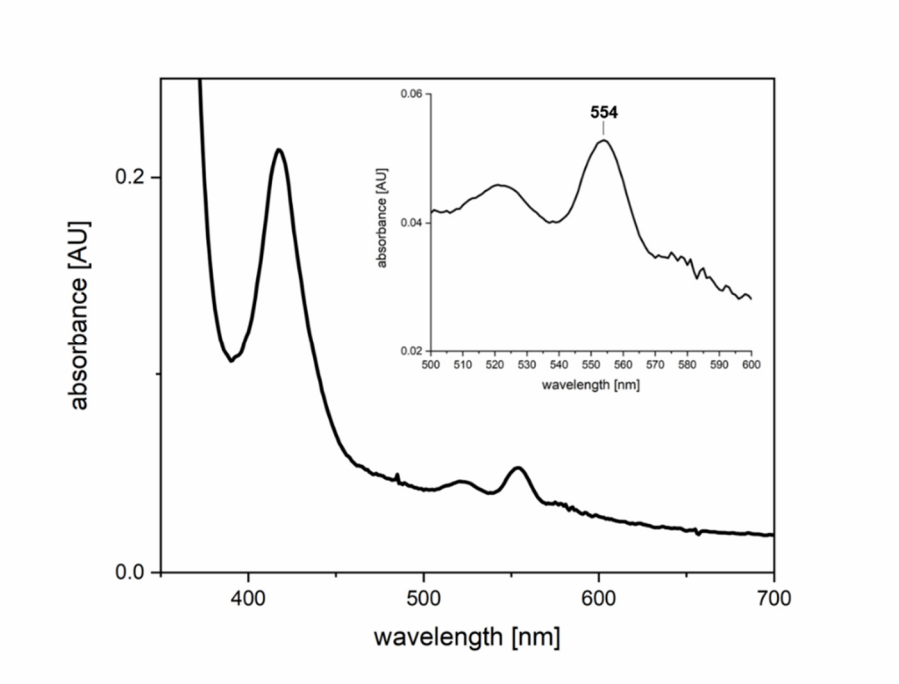

Figure 3.15. Pyridine hemochromogen assay of truncated version PKR1R2 of MA4377. UV/vis spectroscopy of PKR1R2 produced in *E. coli* Nissle 1917 with addition of heme. Black line shows heme Soret band in its reduced state with pyridine as ligand. The Q-bands are extended in the upper box.

For heme c the two-times covalently bound heme cofactor absorbs at 550 nm. Absorption at 553 nm results in a one-time covalently bound cofactor and absorption at 556 nm, like for heme b, indicates a non-covalent binding. Comparing these absorption spectra with PKR1R2 leads to the conclusion of a non-covalently bound heme cofactor (Figure 3.15).

3.1.4.5 Investigations of a native incorporation of the heme cofactor

According to the heme biosynthesis of *E. coli,* the heme cofactor should be natively incorporated into the apo-protein and therefore a heme Soret band should be detectable via UV/vis spectra. To determine the native incorporation of heme in MA4377, PK was purified from *E. coli* BL21 (DE3) (Figure 3.16.A.1) and *E. coli* Nissle 1917 without adding hemin (Figure 3.16.B.1) to the growing culture. Purified proteins from both expression systems showed the same estimated molecular weight on SDS-gel. Also, the SEC profile revealed a similar oligomerization behavior of ~115 kDa from PK from *E. coli* BL21 (DE3) (Figure 3.16.B.1) which was comparable with ~109 kDa from PK produced with heme in *E. coli* Nissle 1917 (Figure 3.16.B2).

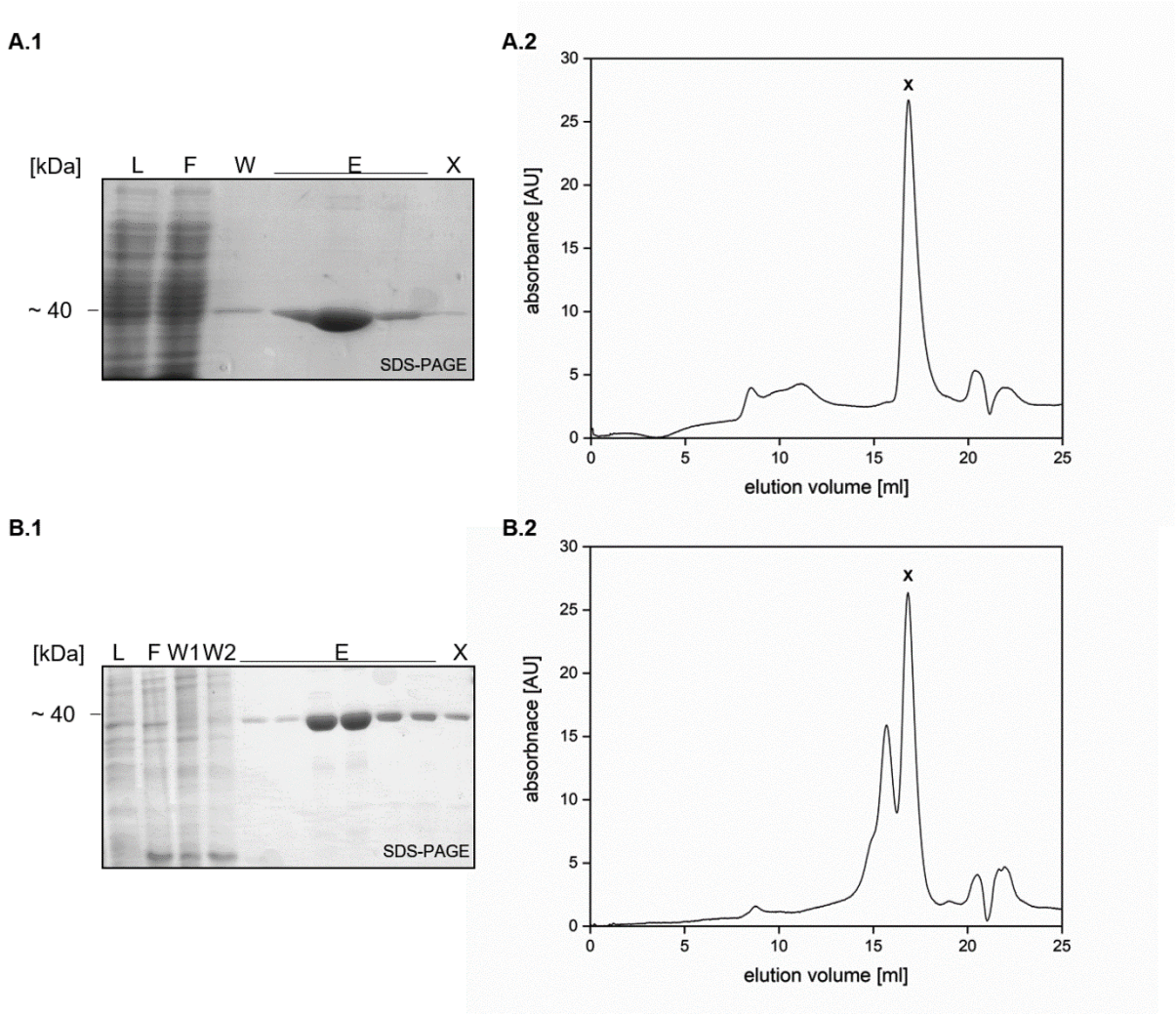

Figure 3.16. SDS-PAGE and SEC of PK from *E. coli* Nissle 1917 w/o heme and BL21 (DE3).
A.1. SDS-PAGE of purified PK from *E. coli* BL21(DE3) without heme via affinity chromatography. L= lysate; F= flow-through fraction; W= washing fraction; E= elution fractions of PK (MW=~40 kDa) from 2 l culture volume. X= marks the eluted protein from the SEC profile of PK. **A.2.** Elution profile of purified PK via size exclusion chromatography produced in *E. coli*. BL21(DE3). The protein was separated via a Superose™ 6 10/300 GL column (GE Healthcare) and equilibrated with $NaPOH_4$ buffer pH 7.0. Absorbance of the eluted protein (marked with a X) was monitored at a wavelength of 280 nm. **B.1.** SDS-PAGE of purified PK from *E. coli* Nissle 1917 without heme via affinity chromatography. L= lysate; F= flow-through fraction; W1= washing fraction; W2= washing fraction; E= elution fractions of PK (MW=~40 kDa) from 2 l culture volume. X= marks the eluted protein from the SEC profile of PK. **B.2.** Elution profile of purified PK via size exclusion chromatography produced in *E. coli* Nissle 1917 without heme. The protein was separated via a Superose™ 6 10/300 GL column (GE Healthcare) and equilibrated with $NaPOH_4$ buffer pH 7.0. Absorbance of the eluted protein (marked with a X) was monitored at a wavelength of 280 nm.

Purified proteins were concentrated and obtained by UV/vis spectra. From PK produced in *E. coli* BL21 (DE3) and *E. coli* Nissle 1917 without additional heme, no heme Soret band could be observed in the UV/vis spectra. Except for the production of PK in *E. coli* Nissle 1917 with additional heme (Figure 3.17) which led to the conclusion that heme is not naturally incorporated in PK of MA4377.

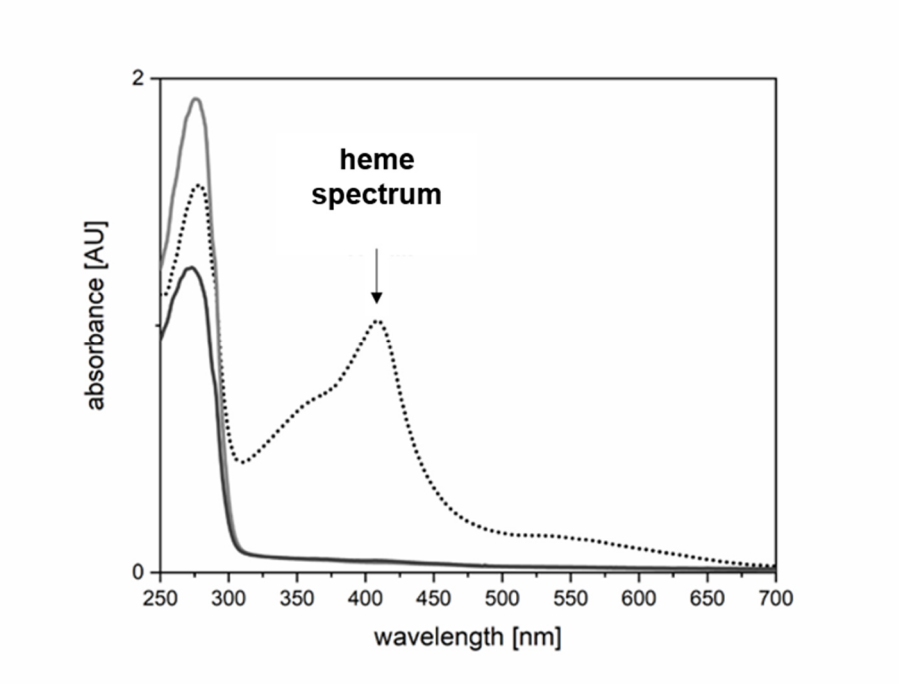

Figure 3.17. UV/vis spectra of heme Soret band of purified PK from *E. coli* BL21 (DE3), *E. coli* Nissle 1917 w/o heme and *E. coli* Nissle 1917 with hemin. Black line shows absorbance spectra of PK which was produced in *E. coli* Nissle 1917 w/o heme. Black dotted line shows absorbance spectra of PK produced in *E. coli* Nissle 1917 with additional heme. The arrow marks the Soret band of the heme spectrum. Dark grey line shows absorbance spectra of PK produced in *E. coli* BL21(DE3) w/o heme.

3.1.4.6 Autophosphorylation activity of the histidine hybrid kinase MA4377 is not dependent on the heme cofactor

To determine the requirement of the heme cofactor for kinase activity, autophosphorylation assays were performed with PK produced in *E. coli* BL21 (DE3), used as reference and *E. coli* RP523, a strain that can not take up heme due to gene loss. *E. coli* BL21 is metabolizing glutamate to aminolevulinic acid (ALA) and is synthesizing hemin as an end product, without adding additional hemin to the media (Zhang et al., 2015). If MA4377 possesses a hemecofactor concentrated PK should show the natural incorporation. Whereas the strain *E. coli* RP523 is not able to synthesize heme due to the loss of the porphobilinogen synthase (*hemB*) (Woodward et al., 2007; Li et al., 1988) and requires heme to grow under aerobic conditions. By adding fermentable carbohydrates, *E. coli* RP523 can grow under anaerobic conditions without heme and ensures the production of the desired apoprotein. SEC Data from PK from *E. coli* RP523 revealed an oligomerization state of ~112 kDa (Figure 3.18) and showed the same elution profile of PK from *E. coli* BL21 (DE3) without adding extra hemin.

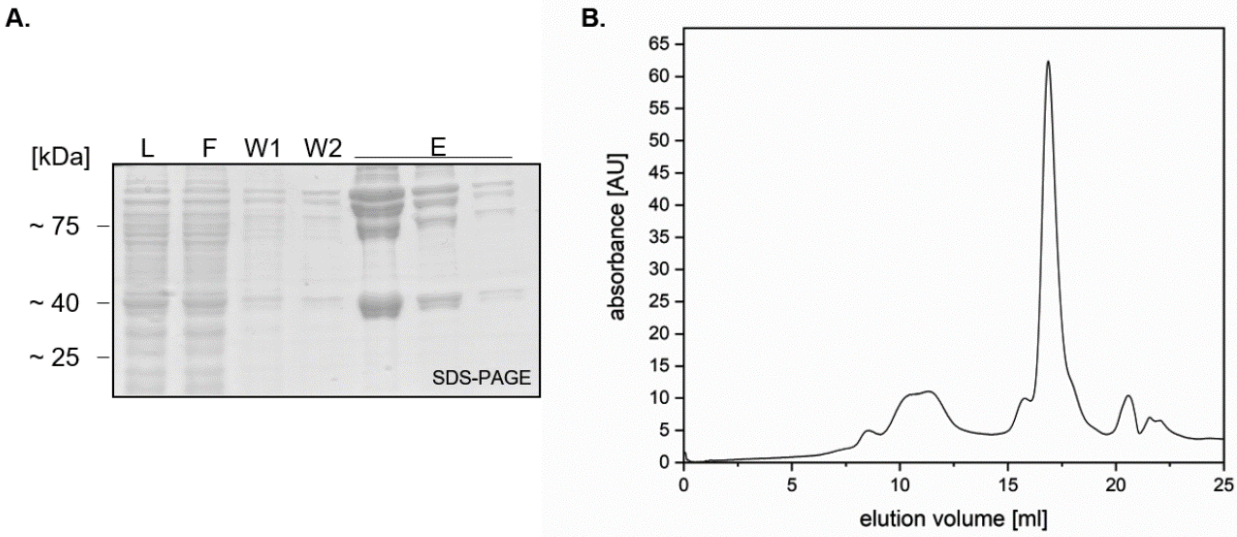

Figure 3.18. SDS-PAGE and SEC of PK from *E. coli* RP523. A. SDS-PAGE of purified PK via affinity chromatography. L= lysate; F= flow-through fraction; W1= washing fraction 1; W2= washing fraction 2; E= elution fractions of PK (MW=~40 kDa) from 2 l culture volume. X= marks the SEC fraction of PK. **B.** Elution profile purified PK via size exclusion chromatography of produced in *E. coli* RP523. The protein was separated via a Superose™ 6 10/300 GL column (GE Healthcare) and equilibrated with $NaPOH_4$ buffer pH 7.0. Absorbance of the eluted protein (marked with a X) was monitored at a wavelength of 280 nm.

Autophosphorylation assays showed kinase activity under oxidizing and reducing conditions. PK revealed kinase activity only as monomer under reducing conditions, as no disulfide bonds can be formed du to the addition of DTT in the kinase buffer. Repeated kinase assays revealed that PK showed sometimes oligomer formation under reduced conditions due to old protein or the sensitivity of the assay (Data not shown). Therefore it cannot be said that a missing heme cofactor did affect the activity of MA4377 (Figure 3.19).

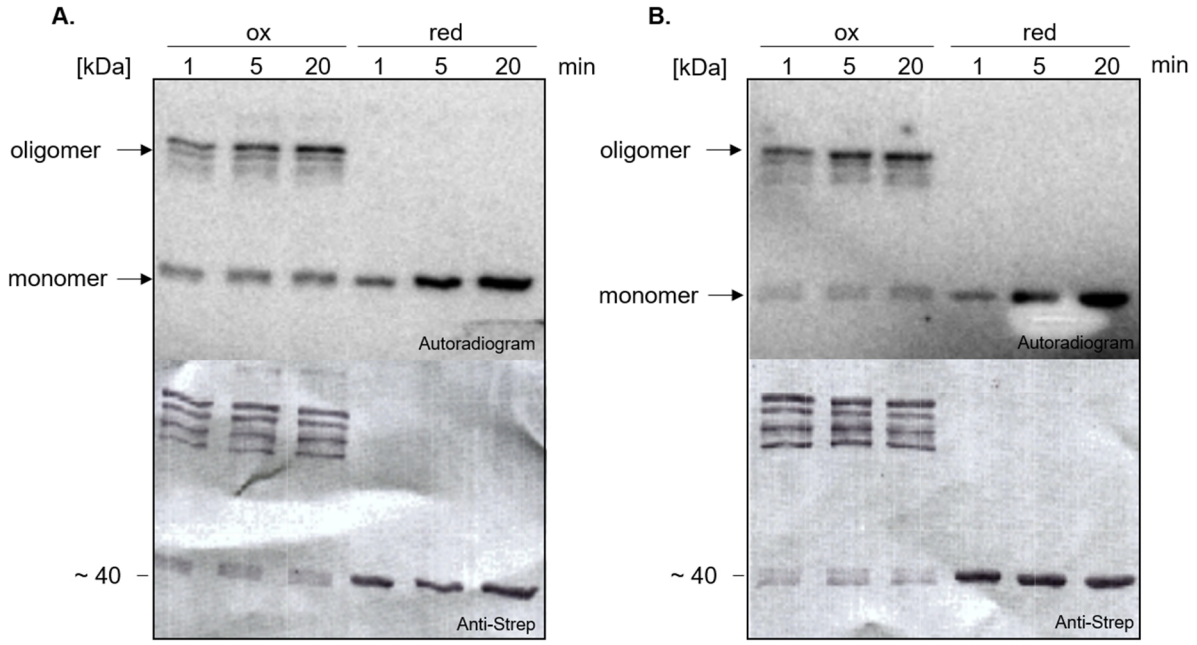

Figure 3.19. Influence of lacking heme cofactor on autophosphorylation assay of PK from *E. coli* BL21 (DE3) and *E. coli* RP523. 10 µM of purified PK from **A.** *E. coli* BL21 (DE3) and **B.** *E. coli* RP523 were phosphorylated with [γ-^{32}P]-ATP and samples were taken after 1, 5 and 20 min. Oxidized (ox) conditions contain 4x SDS sample buffer lacking β-mercaptoethanol. Samples under reduced (red) conditions contained DTH, were flushed with N_2 and stopped with buffer containing β-mercaptoethanol. All samples (10 µl) were resolved on SDS-PAGE and subjected to autoradiography. Protein samples were transferred to PVDF membrane and detected by anti-Strep-Tactin®-AP-conjugate.

In conclusion, the investigations of the heme cofactor in MA4377 revealed, that the heme as a cofactor is not covalently bound in PK and is not involved in activation of the hybrid kinase MA4377.

3.1.4.7 The histidine hybrid kinase MA4377 possesses no flavin as cofactor

Since, the data concerning the binding of a heme cofactor to the PAS domain are not conclusive at this point, other cofactor known to bind to PAS domains were tested. Therefore, it was investigated whether PK is able to bind a flavin cofactor, as MA4377 showed similarity to light-sensing kinases (hhpred database) (Figure 4.3), PK was produced in *E. coli* BL21 (DE3) by adding riboflavin to the media. Investigations on the oligomerization state of PK via SEC revealed no difference compared to purification from other heterologous expression systems (Figure 3.20).

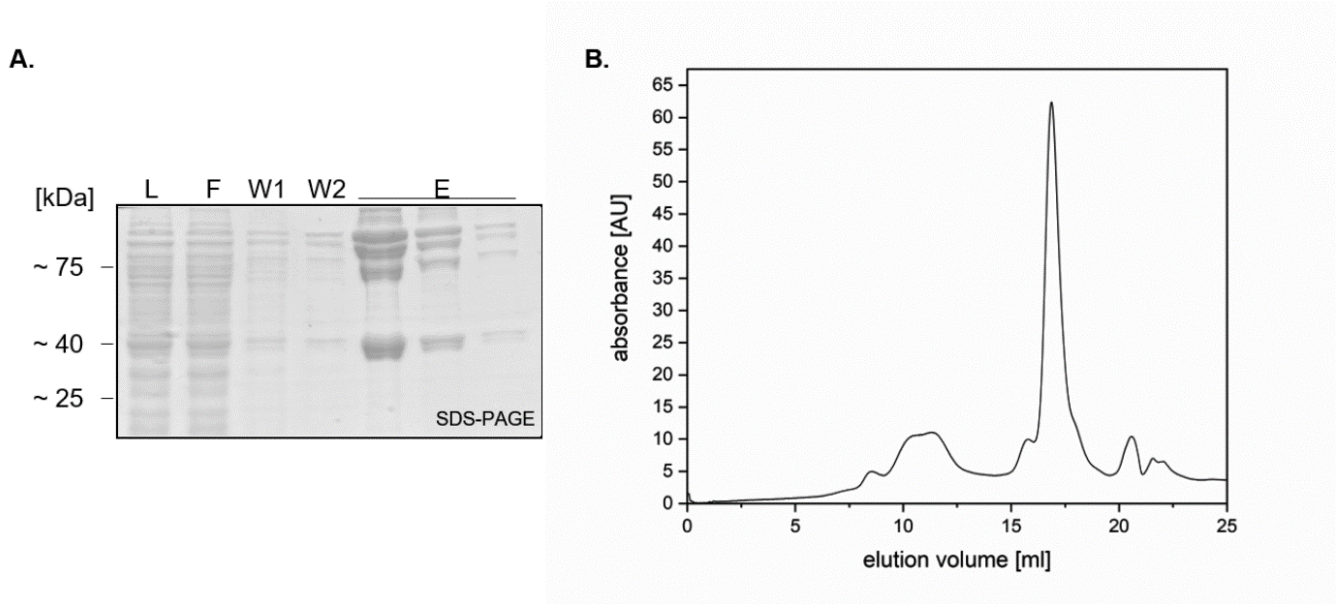

Figure 3.20. SDS-PAGE and SEC of PK from *E. coli* BL21 (DE3) with riboflavin. A. Elution profile of purified PK via affinity chromatography. L= lysate; F=flow-through fraction; W1= washing fraction 1; W2= washing fraction 2; E= elution fractions of PK (MW=~40 kDa) from 2 l culture volume. X= marks the SEC fraction of PK. **B.** elution profile of purified PK via size exclusion chromatography produced in *E. coli* BL21 (DE3). The protein was separated via a Superose™ 6 10/300 GL column (GE Healthcare) and equilibrated with $NaPOH_4$ buffer pH 7.0. Absorbance of the eluted protein (marked with a X) was monitored at a wavelength of 280 nm.

The Soret band of riboflavin that absorbs at 440 nm (Koziol, 1965) was determined by UV/vis spectra but no flavin peak could be detected (Figure 3.21).

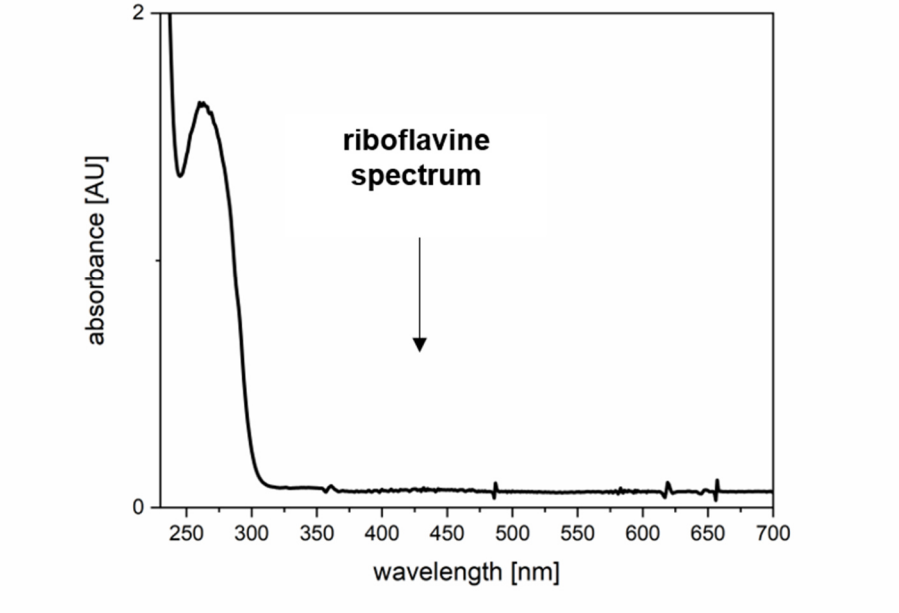

Figure 3.21. UV/vis spectra of flavin Soret band of purified PK from *E. coli* BL21 (DE3). Black line shows absorbance spectra of concentrated PK from *E. coli* BL21(DE3).

These experiments reveal that the PAS domain of the hybrid kinase MA4377 possesses no covalently bound heme cofactor nor riboflavin as a cofactor. An explanation could be the lack of cysteine residues in the PAS domain of MA4377.

3.1.5 PAS domain of the histidine kinase MA4377 influences kinase activity

The third sensor domain of MA4377, the PAS domain, is known to influence the kinase activity by sensing signals with the help of a cofactor or entering protein-protein interaction (Taylor and Zhulin, 1999). As it could be shown that the PAS domain is not possessing a covalently bound heme cofactor and missing a riboflavin, the function was determined with the truncated version K, only containing the kinase catalytic core (Figure 3.2.E) which was recombinantly produced in *E. coli* BL21 (DE3) and revealed a a protein of ~ 26 kDa (Figure 3.22.B1). Oligomerization state verified by SEC corresponded to a molecular mass of about 59 kDa and resembled therefore in a dimer and not in a long stretched dimer like for PK (Figure 3.22.B2). Autophosphorylation assays revealed only activity under oxidizing conditions (Figure 3.22.B3) which differed from the kinase activity under oxidizing and reducing conditions of PK (Figure 3.22.A3) and PKR1R2. As kinase buffer and 4xSDS sample buffer used for assays under oxidizing conditions contained no DTT and β-mercaptoethanol, autohphosphorylation activity might therefore be an artifact. However no kinase activity under reducing conditions was determined which might reveal an important role of the PAS domain regarding the kinase activity by sensing a possible signal or forming protein-protein interactions that are required for the kinase activity.

To implement autophosphorylation, kinases from dimers to phosphorylate the DHp domain of the adjacent kinase. Cysteine residues of the kinase catalytic core could be in charge of this dimerization by forming disulfide bonds. Therefore, all cysteine residues of the truncated version K were substituted with serine by site-directed mutagenesis. The construct K with $C_{486,631,673}S$ variant was employed for kinase assay but showed no autophosphorylation activity under reducing nor under oxidizing conditions compared to K (Figure 3.22.C.3).

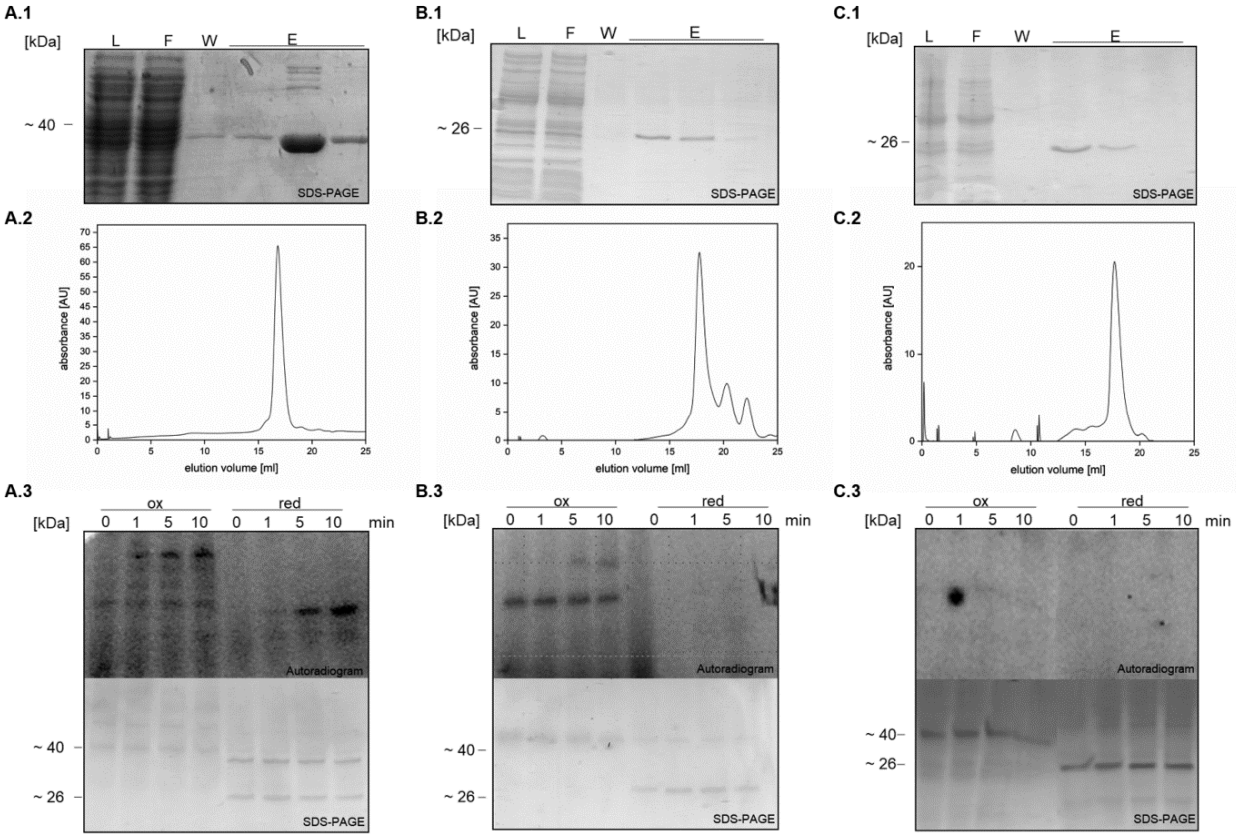

Figure 3.22. SDS-PAGE and SEC of PK, K, and KC$_{486,631,673}$S from *E. coli* BL21(DE3) under oxidized and reduced conditions. A.1 SDS-PAGE of purified PK via affinity chromatography. L= lysate; F= flow-through fraction; W= washing fraction; E= elution fractions of PK (MW=~40 kDa) from 2 l culture volume. **B.1** SDS-PAGE of purified K via affinity chromatography. L= lysate; F= flow-through fraction; W= washing fraction; E= elution fractions of K (MW=~26 kDa) from 2 l culture volume.
C.1 SDS-PAGE of purified KC$_{486,631,673}$S via affinity chromatography. L= lysate; F= flow-through fraction; W= washing fraction; E= elution fractions of K (MW=~26 kDa) from 2 l culture volume. Elution profile of all purified proteins **A.2** PK, **B.2** K, and **C.2** KC$_{486,631,673}$S via size exclusion chromatography. The proteins were separated via Superose™ 6 10/300 GL column (GE Healthcare) and equilibrated with Tris buffer pH 8.0. Absorbance of the eluted protein was monitored at a wavelength of 280 nm. 10 µM of purified **A.3** PK, **B.3** K, **C.3** KC$_{486,631,673}$S were phosphorylated with [γ-^{32}P]-ATP, and samples were taken after several time points. Oxidized (ox) conditions contain 4x SDS sample buffer lacking β-mercaptoethanol. Samples under reduced (red) conditions contained DTT (2 mM), were flushed with N_2 and stopped with buffer containing β-mercaptoethanol. All samples (10 µl) were resolved on SDS-PAGE, subjected to autoradiography and Coomassie blue staining to show protein amount.

Concluding that the PAS domain has an important function for the kinase activity, the kinase catalytic core is not active with a missing PAS domain under reducing conditions. Whereas autophosphorylation activity under oxidizing conditions could be an artifact, as DTT was missing in the kinase buffer as well as β-mercaptoethanol in the 4xSDS sample buffer, resulting in dimerization of the truncated version K. However, the formed oligomer due to disulfide bonds is showing a radioactive signal whereby it is not a signal of autophosphorylation activity of K. If the truncated version K was due to cysteine variants (Figure 3.22.C3) not able anymore to form oligomers, a radioactive signal under oxidizing conditions was missing. This might show that disulfide bonds are somehow interacting with radiolabeled ATP which results in a radioactive signal.

The artifact of an appearing radioactive signal of the kinase without reducing agents in kinase or sample buffer is explained more in detail in the Supplementary data 5.3.
Fact is that all SEC profile of truncated MA4377 versions under reducing and oxidizing conditions reveal dimer formation of the kinase which is important for autophosphorylation activity and after SDS-PAGE visible as monomer on the SDS gel. As long as H_{497} and the PAS domain are available the kinase is active under reducing conditions and the three cysteine residues in the kinase catalytic core might be important for dimerization.

3.2 Investigation of phosphorelay of the histidine hybrid kinase MA4377

As MA4377 is annotated as histidine hybrid kinase (Ashby, 2006), it was of high interest to unveil the MCS of MA4377. Upon autophosphorylation, the phosphoryl group of the kinase gets transferred to the cognate RR that transforms the signal into a specific cellular response. In the case of hybrid kinases, the phosphoryl group gets transferred to two phosphointermediates before the output domain containing receiver is phosphorylated (Stock et al., 2000). To identify the next phosphate acceptor in the phosphorelay of MA4377 a closer look at the genomic localization of the kinase implied many opportunities for signal transfer. Overlapping with 29 nt a single receiver MA4376 (R) localized downstream of MA4377 and adjacent to R a transcription factor MA4375 (TF) of the Msr protein family is positioned (Galagan et al., 2002), indicating possible candidates for phosphotransfer (Figure 3.24).

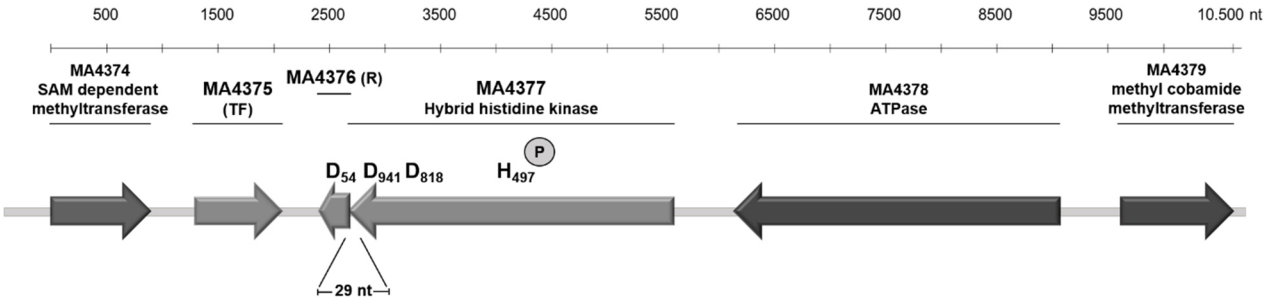

Figure 3.23. Genetic localization of MA4377 with hypothetical phosphorylation sites. Schematic figure of MA4377, receiver MA4376, and transcription factor MA4375 (light grey arrows) arrangement in the genome of *M. acetivorans* drawn to scale. Phosphorylation sites H_{497}, D_{818}, D_{941} of MA4377, and D_{54} of MA4376 are outpointed (Galagan et al., 2002).

The archaeal kinase RdmS is interacting with TFs of the Msr protein family that are regulating methyltransferases on a transcriptional level (Fiege and Frankenberg-Dinkel, 2019). Interestingly MA4375 has the same structure as the above-mentioned TFs, consisting of a helix-turn-helix (HTH) domain and a domain of unknown function 1724 (DUF) (Bose et al., 2006; Bose and Metcalf, 2008). A possible phosphate acceptor is also one of the C-terminal fused receiver domains R1 and R2 of MA4377, as fused receiver domains are described for many hybrid kinases to be the second component of the MCS (Appleby et al., 1996) (Figure 3.23).

BLASTp analysis (NCBI) of the receiver domains R1 and R2 and MA4376 revealed a sequence identity of ~ 30% with the well-characterized single receiver CheY of *E. coli* including the conserved aspartate residue D_{57} (Sanders et al., 1989). As in TCS and phosphorelay of hybrid kinases, the phosphate gets transferred from a histidine (His1) to an aspartate residue (Asp1), initiating an output reaction. Therefore, the conserved aspartate residue of R1, R2, and MA4376 could be a possible phosphate acceptor (Asp1) of MA4377 (His1) (Figure 3.24) (Zhang and Shi, 2005; Appleby et al., 1996).

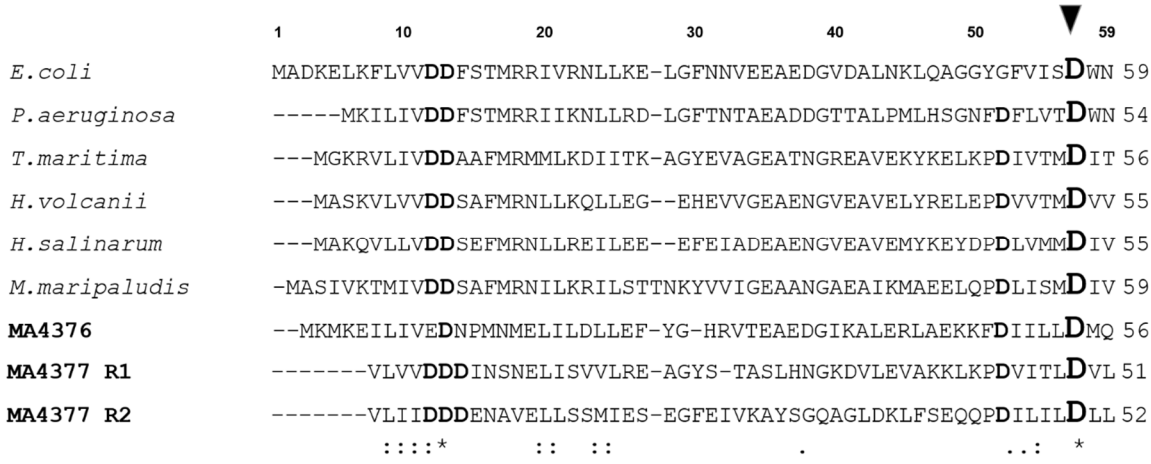

Figure 3.24. Amino acid sequence alignment of receiver CheY from different organisms. Aligned CheY receiver sequences (NCBI database) with MA4376, R1 and R2 from MA4377 with Clustal Omega Referring to the aspartate at position 57 from CheY of *E. coli*, variants of R1 and MA4376 containing aspartates at this position were substituted with an asparagine ($R1D_{818}N$) (MA4376 $D_{54}N$).

3.2.1 Investigation of intra-phosphotransfer of the histidine hybrid kinase MA4377

Verifying the phosphotransfer inside the kinase, radioactive assays were performed. To distinguish which receiver domain of the hybrid kinase accepts the phosphoryl group, two truncated versions $PKH_{497}QR1$ and $PKH_{497}QR1D_{818}NR2$ both lacking the autophosphorylation site, His_{497}, were generated (Fig. 3.25). To track the potential phosphotransfer to R1, the construct $PKH_{497}QR1$, in combination with PK, was employed and the phosphotransfer to the R2 of MA4377 was investigated using the construct $PKH_{497}QR1D_{818}NR2$. The latter was missing the potential phosphorylation site D_{818} within receiver domain 1.

The purified truncated variant PK was radiolabeled and excess [γ-^{32}P]-ATP removed by illustra™ MicroSpin™ G-50 columns (VWR), before PKR1 and $PKH_{497}QR1$ (Figure 3.26.A) or PKR1R2 and $PKH_{497}QR1D_{818}NR2$ (Figure 3.25.B) were added. Both unmodified variants, PKR1 and PKR1R2 were used as reference and showed autophosphorylation activity due to excessive and therefore available [γ-^{32}P]-ATP

(Supplementary data Figure 5.4). Performing the same experiment with the variants $PKH_{497}QR1$ and $PKH_{497}QR1D_{818}NR2$ resulted in no intramolecular phosphotransfer from the kinase PK to one of the fused receiver domains (Figure 3.25 A+B).

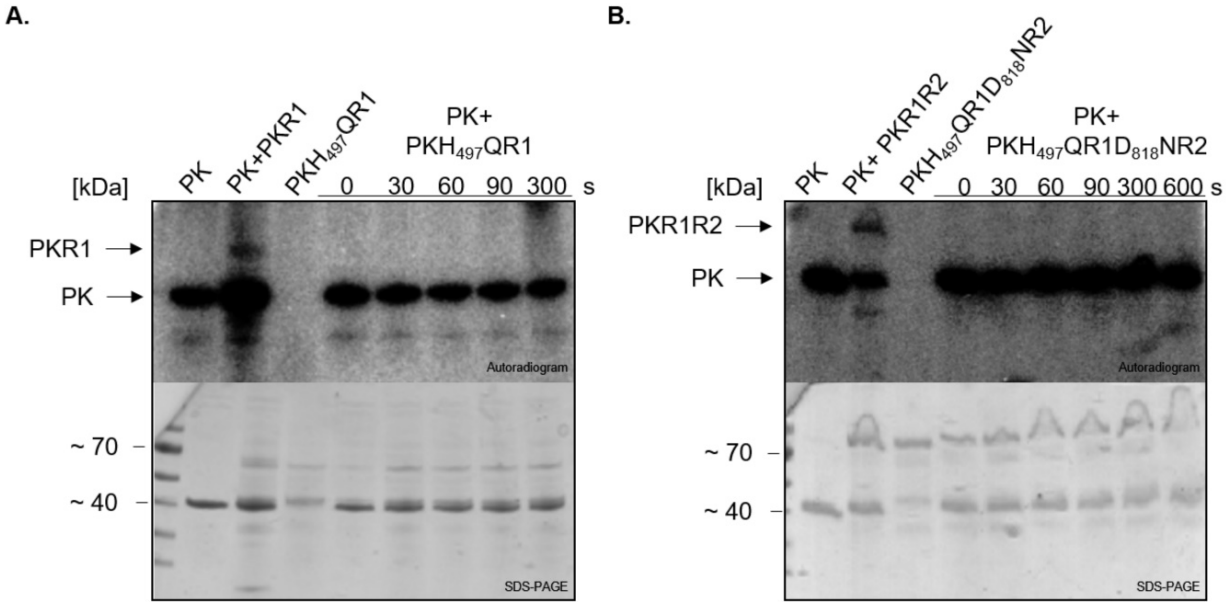

Figure 3.25. Autophosphorylation assay of Intra-molecular phosphotransfer assay of MA4377.
A. Incubation of [γ-^{32}P]-ATP phosphorylated truncated version PK with non-radiolabeled variant $PKH_{497}QR1$. PK, PKR1, and $PKH_{497}QR1$ applied as references. **B.** Incubation of [γ-^{32}P]-ATP radiolabeled truncated version PK with non-radiolabeled variant $PKH_{497}QR1D_{818}NR2$. PK, PKR1R2, and $PKH_{497}QR1D_{818}NR2$ applied as references. Samples contained DTT (2 mM), were flushed with N_2 and stopped with buffer containing β-mercaptoethanol. The reaction was stopped after different time points and resolved (10 µl) on SDS-PAGE, subjected to autoradiography and Coomassie blue staining to show protein amount.

The rather unexpected observation of the lack of intramolecular transphosphorylation prompted the search for a potential phosphate acceptor. While these results do not exclude a potential function of the intrinsic receiver domains, the study here focused on the identification of the succeeding receiver.

3.2.2 MA4377 transphosphorylates the downstream encoded single receiver MA4376

As the signal is not transferred from His_{497} to one of the fused receiver domains another candidate as phosphate acceptor is the single receiver MA4376 regarding its overlapping genomic localization with the kinase. Therefore, the His-tagged receiver was purified via affinity chromatography using ÄKTAprime and revealed a protein of ~14 kDa determined by SDS-PAGE and a globular dimer of ~27 kDa which was predicted by SEC profile (Figure 3.26).

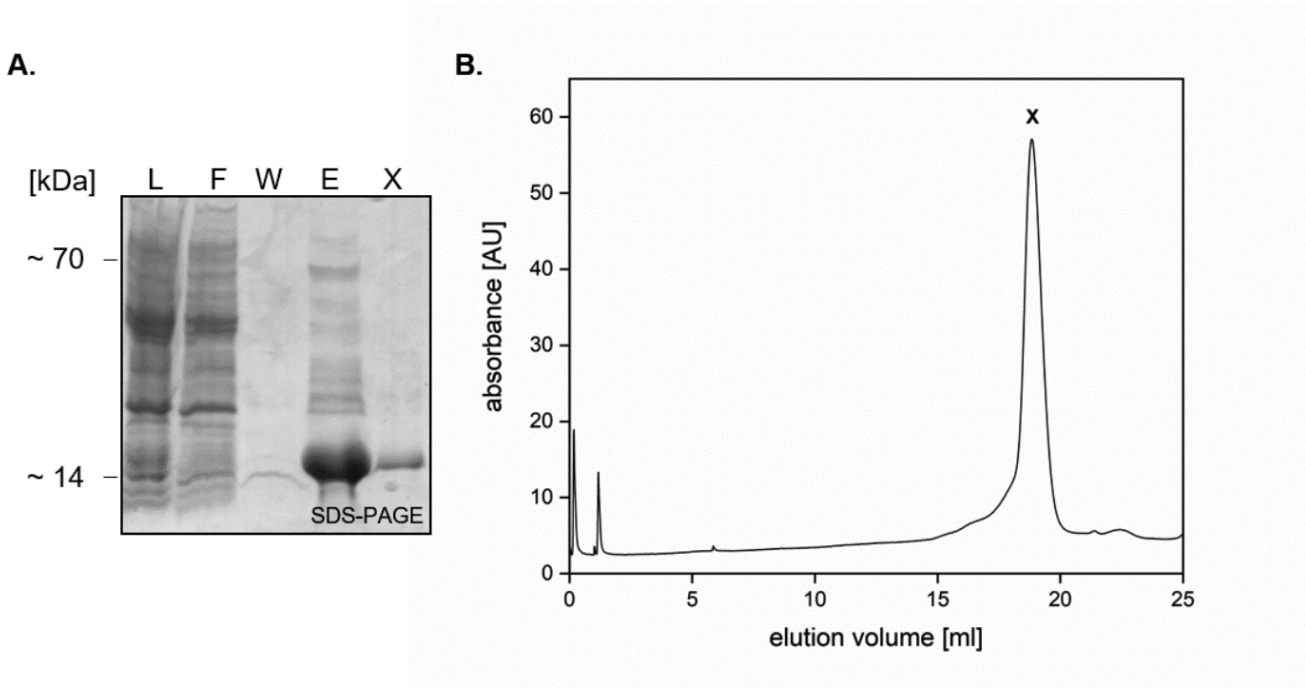

Figure 3.26. SDS-PAGE and SEC of MA4376 from *E. coli* BL21 (DE3). A. SDS-PAGE of purified MA4376 via affinity chromatography with ÄKTAprime plus (GE Healthcare). L= lysate; F= flow-through fraction; W= washing fraction; E= elution fractions of His-tagged MA4376 (MW=~14 kDa) from 2 l culture volume. X= marks the SEC fraction of PK. **B.** Elution profile of PK via size exclusion chromatography produced in *E. coli* BL21 (DE3). The protein was separated via a Superose™ 6 10/300 GL column (GE Healthcare) and equilibrated with Tris buffer pH 8.0. Absorbance of the eluted protein at 18,849 ml (marked with a X) was monitored at a wavelength of 280 nm.

To examine the intermolecular phosphotransfer of MA4377 to MA4376, the purified recombinant receiver was added to the autophosphorylated kinase without excessive [γ-^{32}P]-ATP. Immediately after incubation, a transfer of the radioactive signal to the receiver was observed, while the receiver itself showed no autophosphorylation activity (Figure 3.27).

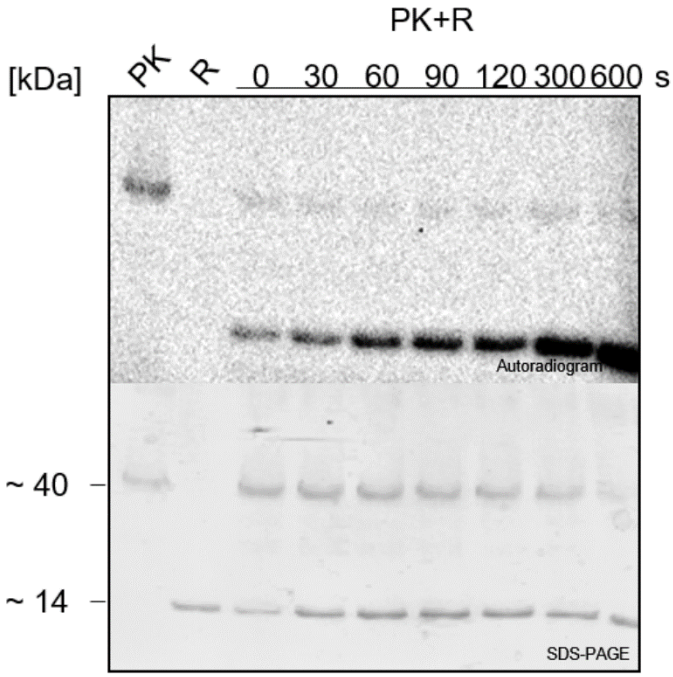

Figure 3.27. Transphosphorylation assay from MA4377 to MA4376 (R). Phosphotransfer was assayed by addition of His-tagged R (30 µM) to the autophosphorylated truncated kinase PK (10 µM). Reaction was stopped after different time points (30-600 s). As reference PK and R were autophosphorylated alone (10 min). Reaction contained DTT (2 mM), were flushed with N_2 and stopped with buffer containing β-mercaptoethanol. Samples (10 µl) were resolved on SDS-PAGE, subjected to autoradiography and Coomassie blue staining to show protein amount.

To verify the His1-Asp1 phosphorelay of MA4377 to MA4376 and to prove that the phosphoryl group is transferred to an aspartate residue within the receiver. The variant MA4376D_{54}N (RD_{54}N) was generated due to a sequence alignment with CheY from *E. coli* (Figure 3.24). The RD_{54}N variant was purified via affinity chromatography, and SEC analysis was performed. The receiver variant showed the same performance due to the estimated molecular weight and oligomerization state as the wildtype (Figure 3.28).

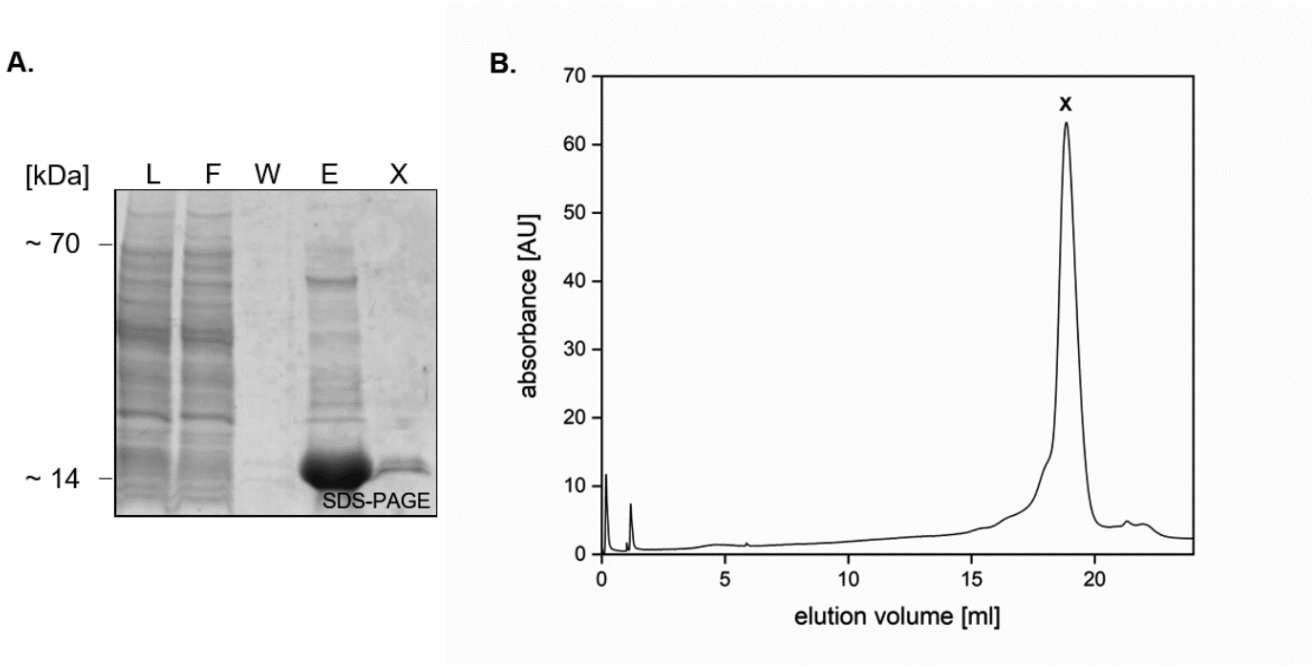

Figure 3.28. SDS-PAGE and SEC of MA4376D$_{54}$N from *E. coli* BL21 (DE3). A. SDS-PAGE of purified MA4376D$_{54}$N via affinity chromatography with ÄKTAprime plus (GE Healthcare). L= lysate; F= flow-through fraction; W= washing fraction; E= elution fractions of His-tagged MA4376D$_{54}$N (MW=~14 kDa) from 2 l culture volume. X= marks the SEC fraction of PK. **B.** Elution profile of purified PK via size exclusion chromatography produced in *E. coli* BL21 (DE3). The protein was separated via a Superose™ 6 10/300 GL column (GE Healthcare) and equilibrated with Tris buffer pH 8.0. Absorbance of the eluted protein at 18,852 ml (marked with a X) was monitored at a wavelength of 280 nm.

Using the variant MA4376D$_{54}$N (RD$_{54}$N), transphosphorylation assays were performed. No signal of RD$_{54}$N was detected after adding the phosphorylated kinase PK which remained phosphorylated, indicating that the phosphoryl group is not accepted by the receiver variant. In addition, these data also verify Asp$_{54}$ of MA4376 as the phosphate acceptor site (Asp1) (Figure 3.29).

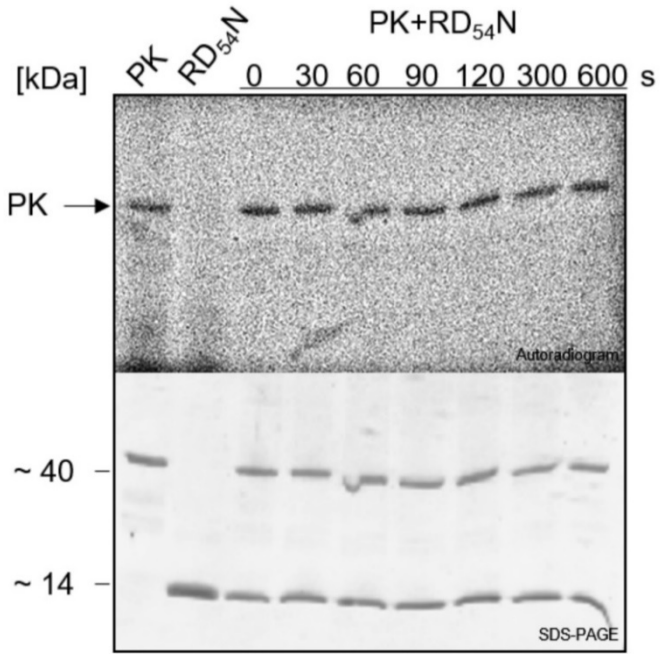

Figure 3.29. Autophosphorylation assay of Inter-molecular phosphotransfer assay from MA4377 to MA4376D$_{54}$N (RD$_{54}$N). Phosphotransfer was assayed by addition of His-tagged RD$_{54}$N (30 µM) to autophosphorylated truncated kinase PK (10 µM). Reaction was stopped after different time points (30-600 s). As reference PK and RD$_{54}$N were autophosphorylated alone (10 min). Reaction contained DTT (2 mM), were flushed with N_2 and stopped with buffer containing β-mercaptoethanol. Samples (10 µl) were resolved on SDS-PAGE, subjected to autoradiography and Coomassie blue staining to show protein amount.

In summary, these data show signal transduction from His$_{497}$ of the kinase MA4377 to Asp$_{54}$ of the receiver MA4376.

3.2.3 A transcription factor as the final phosphocomponent in the phosphorelay of MA4377?

Single receiver domains of bacteria often rely on protein-protein interaction in order to fulfill their function (Bren and Eisenbach, 1998). If fused to DNA binding domains, they are able to regulate transcription (Martínez-Hackert and Stock, 1997). Thus far, not much is known about the function of bacterial-type single receiver domains in Archaea. Yet, interaction with another protein partner is conceivable. Therefore, we had another closer look at the genomic localization of the MCS. Downstream of MA4377 and MA4376, the transcription factor (TF) MA4375 encoded (Figure 3.23). MA4375 belongs to the Msr family of archaeal transcription factors and related ones have been identified to be involved in the transcriptional activation of corrinoid-methyltransferase fusion proteins (Bose and Metcalf, 2008). MA4375 has the same structure as the above-mentioned TFs, consisting of a helix-turn-helix (HTH) domain and a domain of

unknown function 1724 (DUF1724) (Bose and Metcalf, 2008). Therefore, a possible link between the MCS of MA4377 and MA4376 and the TF MA4375, maybe through transphosphorylation, was determined (Figure 3.30).

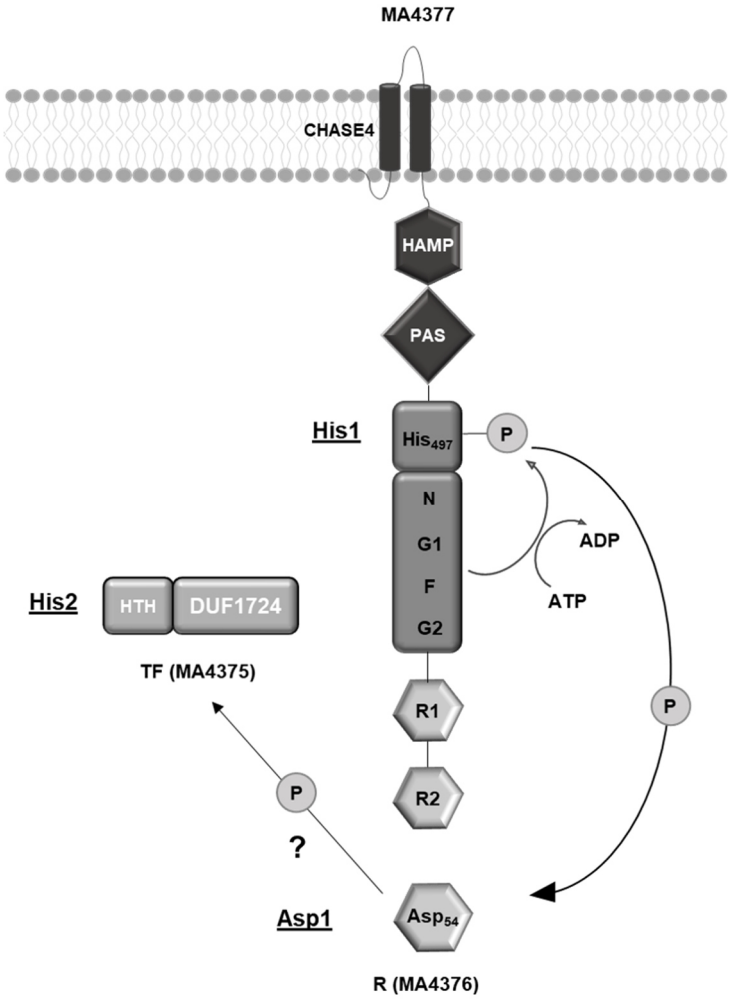

Figure 3.30. Schematic figure of the hypothetical phosphorelay of MA4377. Autophosphorylation of MA4377 at His_{497} resembles first step in the phosphorelay (His1). Γ-phosphate gets transferred to the conserved Asp_{54} of the receiver MA4376 (R) which resembles the second step in the phosphorelay (Asp1). Putative phosphotransfer to transcription factor (TF) MA4375 that might resemble the third step of the phosphorelay (His2).

To reveal the MCS of MA4377, phosphotransfer assays were performed to see a possible interaction with the transcription factor MA4375. Therefore, MA4375 was purified via affinity chromatography, and the oligomerization state was determined by SEC. The protein elutes at ~17.5 ml which resembles a dimer of ~70 kDa since the predicted molecular weight is ~24 kDa determined by SDS-PAGE (Figure 3.31).

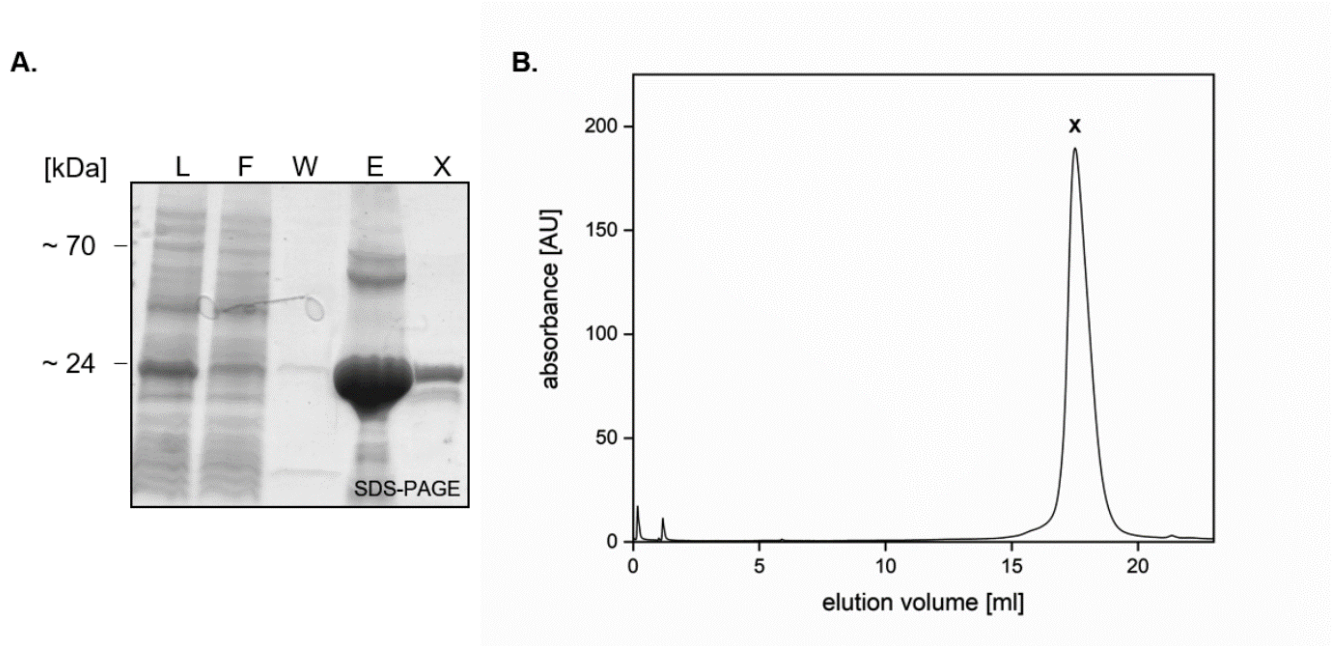

Figure 3.31. SDS-PAGE and SEC of TF from *E. coli* BL21 (DE3). A. SDS-PAGE of purified TF via affinity chromatography with ÄKTAprime plus (GE Healthcare). L= lysate; F= flow-through fraction; W= washing fraction; E= elution fractions of His-tagged TF (MW=~24 kDa) from 2 l culture volume. X= marks the SEC fraction of PK. **B.** Elution profile of purified PK via size exclusion chromatography produced in *E. coli* BL21 (DE3). The protein was separated via a Superose™ 6 10/300 GL column (GE Healthcare) and equilibrated with Tris buffer pH 8.0. Absorbance of the eluted protein at 17.506 ml (marked with a X) was monitored at a wavelength of 280 nm.

The TF itself showed no autophosphorylation activity when incubated with [γ-^{32}P]-ATP. Also, no transphosphorylation employing radiolabeled PK and the purified transcription factor was observed (Figure 3.32). Possibly, phosphorylation of the TF is achieved through the single receiver MA4376 (Figure 3.30), resembling Asp1. For that reason it was tested whether MA4376 serves as a phosphointermediate in the signal transduction cascade.

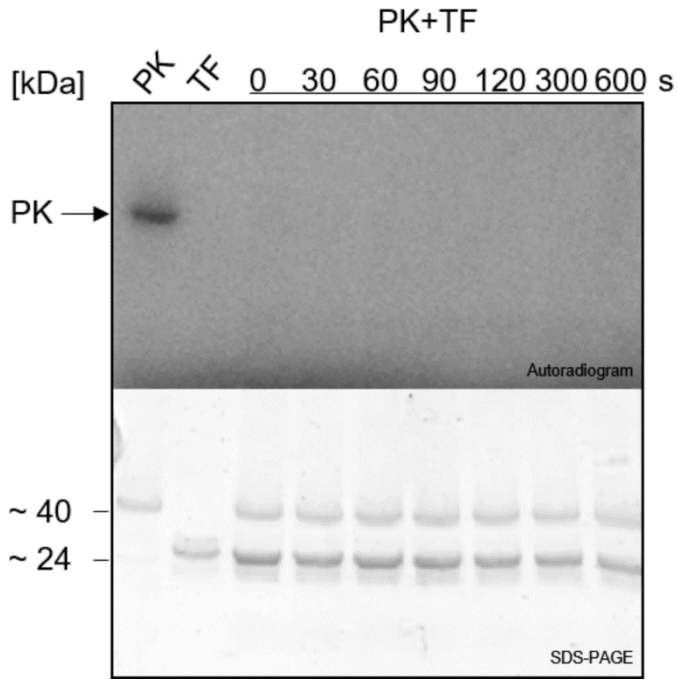

Figure 3.32. Transphosphorylation assay from MA4377 to MA4375 (TF). Phosphotransfer was assayed by addition of His-tagged MA4375 (30 µM) to autophosphorylated truncated kinase PK (10 µM). Reaction was stopped every 30 s and after 600 s as reference. Autophosphorylation sample (10 min) of PK and TF were applied as reference. Reaction contained DTT (2 mM), were flushed with N_2 and stopped with buffer containing β-mercaptoethanol. Samples (10 µl) were resolved on SDS-PAGE, subjected to autoradiography and Coomassie blue staining to show protein amount.

3.2.4 Predicted MCS of the histidine hybrid kinase MA4377

To investigate this proposed phosphorelay (His1-Asp1-His2), phosphorylated truncated kinase PK was incubated with the non-radiolabeled receiver MA4376. Subsequently, the transcription factor was added in equal molar amounts and a weak radioactive signal at the molecular mass of the TF was detected. The signal intensity of PK (His1) attenuated over time as well as the signal of the TF (His2) and the strong phosphorylated single receiver R (Asp1) (Figure 3.33.A).

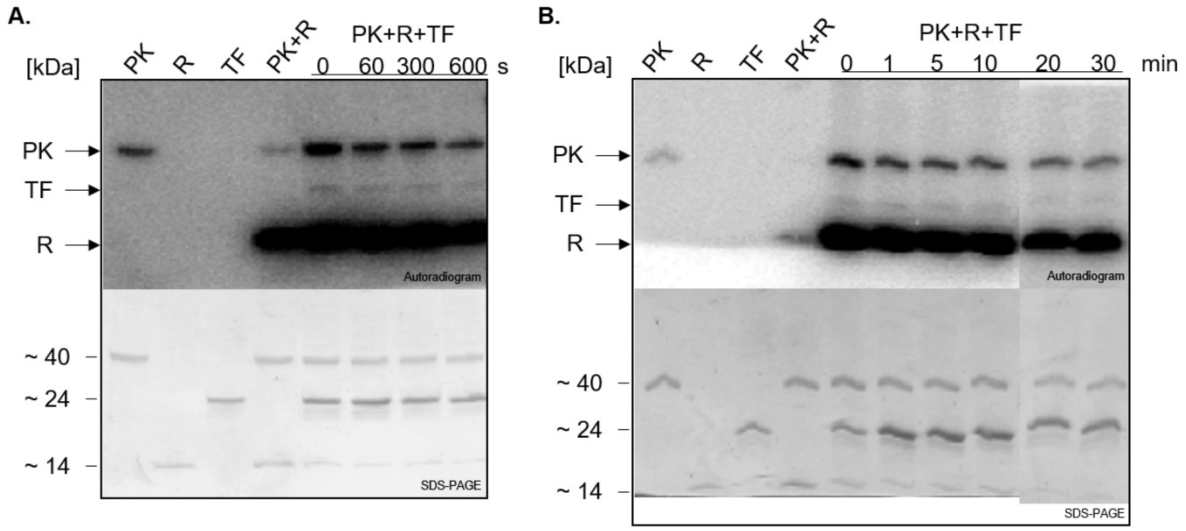

Figure 3.33. Autophosphorylation assay of Inter-molecular phosphorelay of MA4377, MA4376 (R), and MA4375 (TF). A.+ B. Phosphotransfer was assayed by addition of His-tagged R (10 µM) to autophosphorylated truncated kinase PK (10 µM) for 10 min. TF (10 µM) was added and reaction was stopped after different time points. Autophosphorylation sample (10 min) of PK, R and TF were applied as reference. Reaction contained DTT (2 mM), were flushed with N_2 and stopped with buffer containing β-mercaptoethanol. Samples (10 µl) were resolved on SDS-PAGE, subjected to autoradiography and Coomassie blue staining to show protein amount.

As reference the receiver and the transcription factor showed under reducing conditions no activity. Repeating the same experiment over 30 min revealed again an extra signal that might be the phosphorylated TF, which represents the third phosphate acceptor in the phosphorelay as His2 (Figure 3.33.B).

Due to kinase activity of MA4377 under the oxidizing condition, the MCS was determined without adding DTT and β-mercaptoethanol. Hence, autophosphorylated PK (His1) formed oligomers and phosphorylated the receiver MA4376 (Asp1). After adding the TF to the reaction mix a band below and on top of the monomeric PK band appeared (Figure 3.34). It seemed that the oligomerized TF (His2) was phosphorylated.

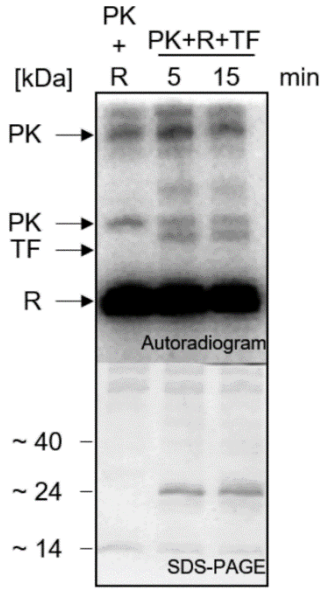

Figure 3.34. Autophosphorylation assay of Inter-molecular phosphorelay of MA4377, MA4376 (R) and MA4375 (TF) under oxidizing conditions. Phosphotransfer was assayed by addition of His-tagged R (30 µM) to autophosphorylated truncated kinase PK (10 µM) for 10 min. TF (30 µM) was added and reaction was stopped after different time points. Autophosphorylation sample (10 min) of PK, R and TF were applied as reference. Samples (10 µl) were resolved on SDS-PAGE, subjected to autoradiography and Coomassie blue staining to show protein amount.

The phosphorylation under oxidizing conditions of the TF likely is an artifact as the transcription factor showed autophosphorylation activity under these conditions (Supplementary data Figure 5.2).

3.2.5 Central role of the receiver MA4376 in the phosphorelay of the kinase MA4377

In signal transduction systems receiver and transcription factors can be involved in reverse phosphotransfer by phosphorylating the kinase (Lassak et al., 2013). To determine if MA4376 is able to phosphorylate the kinase, the radiolabeled single R (R-P) was incubated with MA4377. Therefore, R-P had to be obtained, which was implemented by a phosphotransfer from PK to R in a 1:10 ratio and subsequent purification of R-P by affinity chromatography In the elution fraction (E) not only the receiver but also the kinase was still available suggesting a tight interaction of both proteins (Figure 3.35).

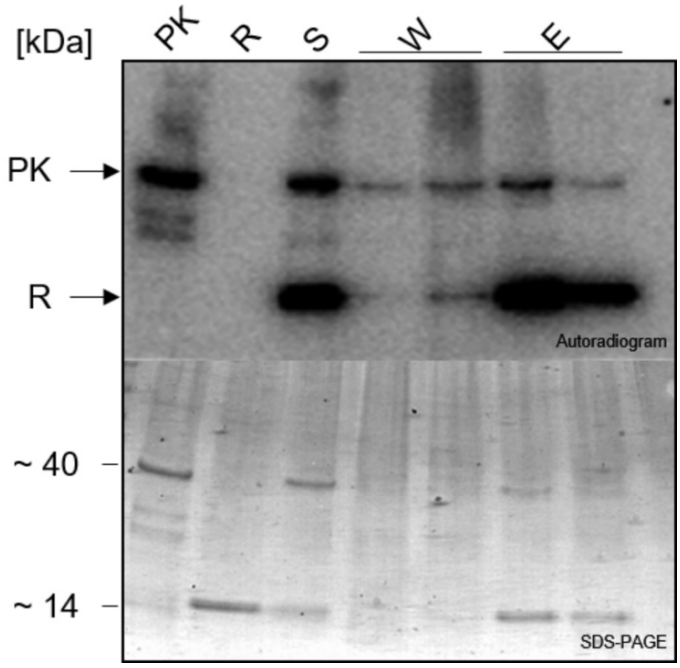

Figure 3.35. Radioactive His-tagged protein purification of the receiver (R). Incubation of [γ-^{32}P]-ATP radiolabeled PK with non-radiolabeled receiver R in a 1:10 ratio. Supernatant (S), washing (W) and elution (E) fractions of purification steps resolved (10µl) on SDS-PAGE and subjected to autoradiography and Coomassie blue staining to show protein amount.

Phosphorylated receiver was obtained as described in Material and Methods. After desalting, the sole phosphorylated R-P was available, still showing a phosphorylation signal (Figure 3.36). To investigate the reverse phosphotransfer from R-P to the kinase MA4377, R-P was incubated with the truncated versions PKR1 and PKR1R2. Interestingly, our data show a reverse phosphotransfer from R-P to the truncated versions of MA4377 (Figure 3.36). Having the phosphorylated and purified single receiver available we furthermore tested whether the receiver by itself is able to phosphorylate the TF or whether the observed phosphotransfer shown in Figure 3.33 requires the presence of the kinase. Therefore, the phosphorylated receiver (R-P) was incubated with the TF MA4375. However, no phosphorylation of the TF was observed indicating the importance of the kinase in the phosphorelay. As a reference, the histidine kinase BphP from *Pseudomonas aeruginosa* (Tasler et al., 2005) was incubated with R-P which showed no reverse phosphotransfer (Figure 3.33).

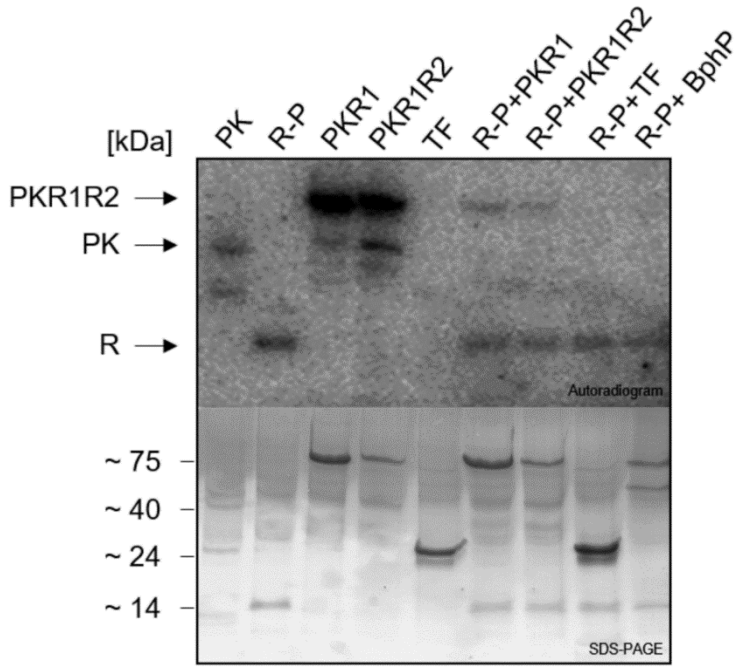

Figure 3.36. Reverse phosphotransfer of radiolabeled receiver R to histidine kinase MA4377. Via His-Tag affinity chromatography purified receiver (R-P) was incubated with non-radiolabeled truncated versions PKR1 (R-P+PKR1) and PKR1R2 (R-P+ PKR1R2) of MA4377, transcription factor (TF) (R-P+TF) and as control with histidine sensor kinase BphP (R-P+BphP). As a reference autophosphorylation activity of PK, R-P, PKR1, PKR1R2, TF is shown. Samples (10 µl) were resolved on SDS-PAGE, subjected to autoradiography and Coomassie blue staining to show protein amount.

This experiment indicated that MA4376 is not only acting as phosphointermediate in the MCS. Instead, by phosphorylating the kinase, R might be involved in the regulation of the kinase phosphorylation state and therefore in the regulation of the whole phosphorelay. Moreover, R could receive signals from other kinases and therefore evolve the complexity of the MCS (Figure 3.36).

3.2.6 Reverse phosphotransfer of the transcription factor MA4375 to the histidine hybrid kinase MA4377

Due to investigations of a reverse phosphotransfer of the TF MA4375 to MA4376 and the kinase MA4377, radioactive affinity chromatography was performed to gain and implement the single TF for further reverse phosphotransfer assays. Therefore, autophosphorylated PK was incubated with the His-tagged TF. To isolate single MA4375 the same procedure was used as for MA4376 as described above (3.2.5).

Unfortunately, purification of the phosphorylated TF was not successful and therefore also no reverse feedback regulation could be examined (Figure 3.37). Considering the samples of the fraction PK+TF and S (supernatant) containing the incubated TF with the autophosphorylated PK, revealed a phosphorylated TF. This suggested that TF

received the phosphoryl group of MA4377, but it has to be investigated whether it is specific phosphorylation or if the preceding experiments were not performed under ideal conditions.

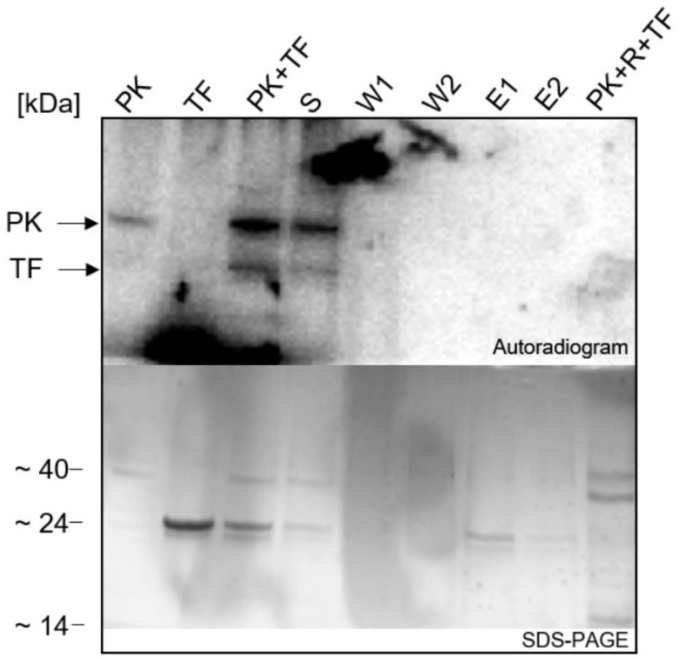

Figure 3.37. Radioactive His-tagged protein purification of transcription factor (TF). Incubation of [γ-^{32}P]-ATP radiolabeled PK with non-radiolabeled receiver TF in a 1:10 ratio. Supernatant (S), washing (W) and elution (E) fractions of purification steps resolved on SDS-PAGE and subjected to autoradiography and Coomassie blue staining to show protein amount.

4 Discussion

4.1 Proposal of an intramolecular phosphorelay of MA4377

Bacterial signal transduction, whether via a two- or multi-component system involving a phosphorelay, is a well-investigated and understood mechanism used by microorganisms in order to respond to environmental changes (Parkinson and Kofoid, 1992; Stock et al., 1989a; Stock et al., 2000; Appleby et al., 1996). However, their function in Archaea is still largely unexplored, owing in part to only a limited number of genetically accessible organisms being available (Esser et al., 2016). In screening the ever-increasing number of genomes being released, it becomes obvious that these signal transduction systems are also present in Archaea, having possibly radiated from Bacteria via horizontal gene transfer (Koretke et al., 2000). This study made progress in investigating and understanding a bacterial-type phosphorelay system in a methanogenic archaeon *M. acetivorans* (Galagan et al., 2002). Using *in vitro* phosphorylation experiments with recombinant protein, we were able to show the autokinase activity of a hybrid kinase MA4377 at the specific histidine residue at position 497, located in a conserved H-box. The histidine residue was revealed as the phosphorylation site while substitution led to a loss of activity.

Although the two fused receiver domains at the C-terminus of the MA4377 protein are not directly involved in the phosphorelay, whereas the necessity of two C-terminal fused receiver domains is so far not clear. Several hybrid kinases possess two receiver domains like DhkA of *Dictyostelium credensis* and Cre1 of *Arabidopsis thaliana* with unknown function. In the case of LuxN of *Vibrio cholerae* and BarA of *E. coli* the first receiver is degenerated (Anjard, Christophe and Loomis, William F., 2003). The three-component system in *Rhizobium meliloti* consists of the kinase CheA and two single receivers CheY1 and 2. In this system, CheY2 is the major effector that affects the motility of the soil bacterium due to chemotaxis and is responsible for reverse phosphotransfer to the kinase CheA. For the organism, rapid phosphorylation and dephosphorylation of CheY2 are important to be able to react to chemotaxis. Therefore, it is predicted that CheY1 is acting as a phosphate sink. By having a higher affinity to the phosphate, it can improve dephosphorylation of CheY2 and assure that CheY2 gets phosphorylated to a significant signal that has to overstep a certain threshold. The function of the receiver describes a new regulation of signal transduction which does not require a phosphatase (Sourjik and Schmitt, 1996, 1998).

Also, the hybrid kinase ArcS of *Shewanella oneidensis* contains two fused receiver domains (ArcSR1+ArcSR2) like MA4377. It is suggested that these receivers are playing a crucial role in a 'feedback activation loop'. ArcSR1 fine-tunes the kinase activity of ArcS by receiving a phosphate of the downstream located HPt domain and the cognate response regulator (RR) ArcA. Whereas ArcSR2 is preferrably receiving the signal of ArcA and might act as a phosphate sink (Lassak et al., 2013). As MA4376 can re-phosphorylate the kinase MA4377 (Figure 3.37) it is possible that one of the fused receivers is holding a position as a phosphate sink and influences the phosphorylation state. So far, a phosphatase activity of MA4377 could not be observed (data not shown) whereas phosphatase activity by one of the receivers acting as phosphate sink would be an improvement due to the regulatory function of the MCS.

Transphosphorylation to the vicinal encoded single receiver protein, MA4376, was observed. The overlap of 29 nt between both open reading frames might suggest that at some point in their evolution, MA4377 and MA4376 were a single ORF encoding a single hybrid kinase with three R domains. The hybrid kinase RodK of *Myxococcus xanthus* consists of three receiver domains. Only the third R domain is served by an intramolecular phosphotransfer, while the other two are proposed to function as phosphate sinks to modulate the rate of kinase activity inside RodK or to alternative RR in response to incoming signals. Although the authors did not find phosphorylation of R1 and R2 of the *M. xanthus* kinase, they provide genetic evidence for the distinct function of all three R domains within RodK, with phosphorylation by other kinases or acting as phosphate sink being one possible scenario. (Rasmussen et al., 2006). Alignment studies of MA4376 revealed a similarity of 41% with the third receiver domain of the hybrid kinase RodK which suggested MA4376 as a hypothetical third domain of MA4377 and would state an earlier intramolecular phosphotransfer of the hybrid kinase MA4377. The autonomous position of MA4376 is referring to a more complex signal transduction mechanism where MA4376 could have a more exclusive role.

4.2 The receiver MA4376 might be involved in cross-regulation

M. acetivorans contains only one receiver containing a Helix-turn-Helix motif as output domain while the majority resembles single receiver domains (Galagan et al., 2002). These receivers are predicted to be involved in protein-protein interaction (Jenal and

Galperin, 2009) as the example of CheY of *E. coli* shows to interact with FliM to regulate flagellar rotation (Bren and Eisenbach, 1998). The region where the interaction between the receiver and the protein takes place is the same α/β sheet that is involved in the interaction with the receiver and the effector domain of the RR. Therefore the protein that interacts with the receiver domain could display a substitute for the regulator's effector domain (Jenal and Galperin, 2009). Interaction like this were detected in the archaeon *Halobacterium salinarum* where CheY interacts with the adaptor protein CheF. The structural similarity of the bacterial and archaeal CheY was shown to be similar and therefore an indication for a bacterial origin of the archaeal CheY. Although the alpha 4 domain, which is important for interaction with CheF, cannot be found in the bacterial single receiver CheY (Quax et al., 2018).

As MA4376 as well as the fused receiver domains of MA4377 are highly similar to CheY of *E. coli* and contain the conserved D_{57} aspartate (Figure 3.25), a possible interaction of MA4376 with yet unknown proteins of various regulatory function is possible (Figure 4.1). The interaction with a protein involved in motility is unlikely as *M. acetivorans* is not motile although possessing a gene cluster encoding for archaellum or formarly archaeal flagella (Galagan et al., 2002). Moreover, MA4376 is involved in a reverse phosphotransfer to the hybrid histidine kinase MA4377 (Figure 3.37). Therefore, it could not only receive signals from MA4377 as a phosphointermediate but also regulate the phosphorylation state of MA4377 by accepting signals from other donors like other kinases. As single receiver MA4376 could be involved in cross-regulation like DivK of *C. cresentus* which plays a central role in regulation. The single receiver DivK is phosphorylating two kinases: PleC that switches after being phosphorylated from phosphatase to autokinase activity and DivJ that is involved in polar localization and is phosphorylating the receiver DivK (Paul et al., 2008).

The involvement of MA4376 in cross-regulation gets supported by the kinase: receiver ratio in *M. acetivorans* (Galagan et al., 2002) as well as from prediction tools (MOTIF search) and RNA-Seq analysis (Lopez Munoz, 2017) that suggested an interaction between RdmS and R. Concerning the receiver’s reverse phosphotransfer to MA4377 a similar regulating function could be the case for RdmS (Figure 4.1.D).

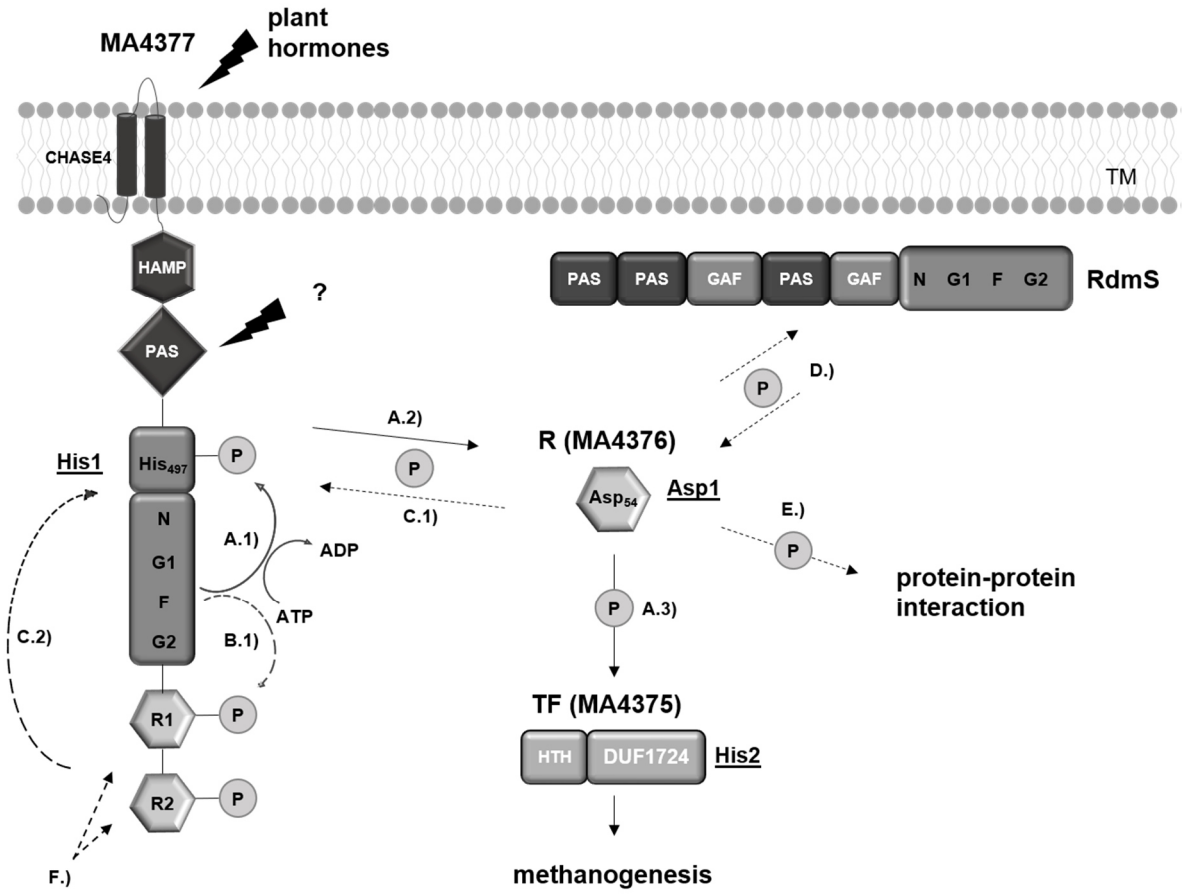

Figure 4.1. Schematic figure of a putative function of R (MA4376) in the phosphorelay. R is demonstrated in the central role of the phosphorelay with outpointed phosphotransfer pathways. **A.1)** Shows autophosphorylation of MA4377 induced by signal sensing, where the γ-phosphate of ATP gets transferred to the conserved histidine residue (His_{497}) that is the first step in the phosphorelay (His1). **A.2)** The phosphoryl group gets transferred to the single receiver (R) MA4376, which is the second step in the phosphorelay (Asp1). **A.3)** The signal gets transferred to the transcription factor (TF) MA4375, which is the third step in the phosphorelay (His2) and might be involved in methanogenesis. **B.1)** Possible function of receiver domains (R1+R2) as phosphate sink during autophosphorylation of the kinase MA4377. **C.1)** Reverse phosphotransfer of R to R1 or R2 of MA4377. **C.2)** Phosphorylated R1 or R2 might affect phosphorylation state of the kinase MA4377. **D.)** Possible cross-regulation of R with RdmS or other kinases. **E.)** Phosphorylated R might interact with other proteins. **F.)** R1 and R2 of MA4377 could be involved in cross-regulation. Continuous lines resemble proved interactions. Dashed lines resemble hypothetical interactions.

4.3 Engagement of the investigated multi-component system of MA4377 in methanogenesis

As all results obtained in this study were from *in vitro* experiments in the absence of most signal input domains (PAS domain still present in employed PK construct), it is necessary to include the membrane-bound signaling domains in future studies to confirm the function of MA4377 *in vivo*. The major signal input domain in MA4377 is likely to be the membrane-bound CHASE domain (Heyl et al., 2007). Although it is widespread in prokaryotes, lower eukaryotes and plants, not much is known about its function. It is predicted to bind various low molecular weight ligands. In the case of MA4377, the CHASE domain might be involved in sensing methylated compounds as

alternative substrates for methanogenesis. Data from the Metcalf group support such an assumption (Lopez Munoz, 2017). This group demonstrated that deletion of the kinase MA4377 and the TF MA4375 in *M. acetivorans* had a significant impact on the transcription of the corrionoid-methyltransferase gene *mtsF* (MA4384), with transcription being upregulated when cells were grown on the alternative substrate trimethylamine (TMA). The synthesis of MtsF was furthermore influenced by the redox-responsive kinase, MsmS (Molitor et al., 2013), indicating that MA4377-MA4376-MA4375 and MsmS might belong to one large signal transduction network (Figure 4.2). This system furthermore also includes RdmS as a signal input kinase in *M. acetivorans*, as its deletion had an impact on the transcription of *mtsD* when cells are grown in methanol (Fiege and Frankenberg-Dinkel, 2019; Lopez Munoz, 2017). Interestingly, the kinases MsmS and RdmS are not bacterial-type histidine-kinases and their downstream signal transduction sequence is still not yet fully understood (Fiege and Frankenberg-Dinkel, 2019).

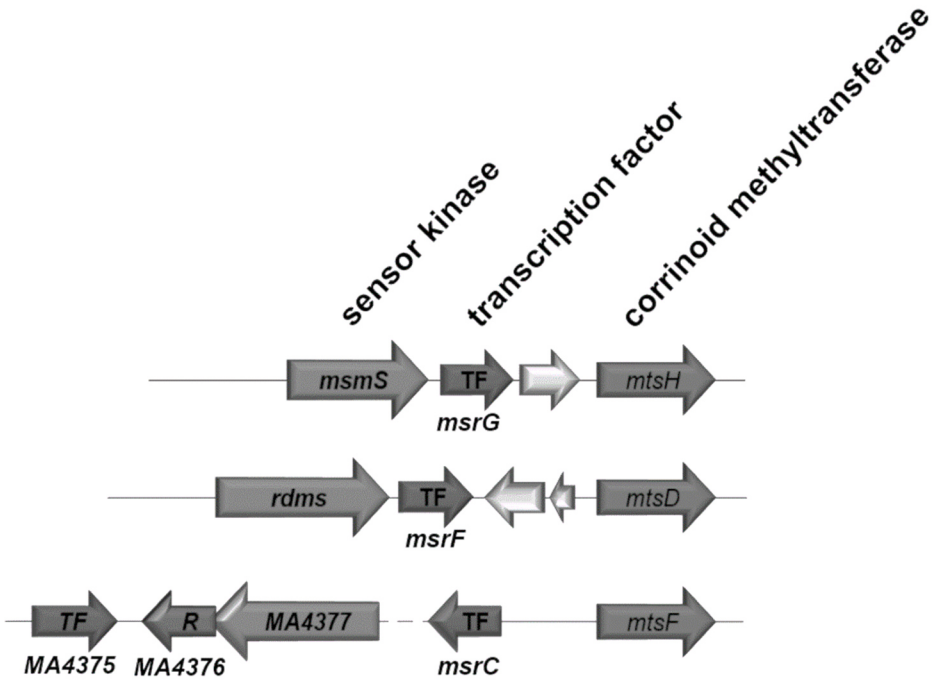

Figure 4.2. Schematic overview of the methanogenesis related signal transduction system mentioned in the discussion. The genetic organization of kinases, TF and corrinoid methyltransferases are shown as arrows indicating the direction of transcription.

More experiments are needed to clarify whether the receiver MA4376 serves as a central hub in connecting the kinases MsmS, RdmS and MA4377 with the respective TF MA4375, MsrC, MsrF and MsrG, thereby regulating methylotrophic

methanogenesis. Whether this interaction involves functional phosphotransfer remains to be determined.

4.4 The histidine hybrid kinase MA4377 is of bacterial origin

In screening the ever increasing number of genomes being released, it becomes obvious that signal transduction systems are also present in Archaea, having possibly radiated from Bacteria via horizontal gene transfer (Koretke et al., 2000). The major question arises as to how these systems have adapted to work together with the archaeal transcription machinery, which differs significantly from that found in Bacteria. In fact, the archaeal RNA polymerase rather resembles eukaryotic RNA polymerase II (Bell and Jackson, 1998; Soppa, 1999).

Horizontal gene transfer is an important event in evolution to evolve new species (Cadillo-Quiroz et al., 2012) and for adapting to new niches (Wagner et al., 2017). Archaea utilize this lateral gene transfer by taking up genes from distantly related organisms like bacteria (Nelson-Sathi et al., 2015). It was shown that this event occurs from Bacteria to Archaea five times more often than the other way around (Nelson-Sathi et al., 2015). A reason for this circumstance might be the higher abundance of bacteria as well as the beneficial effect for Archaea to gain new genes to improve the development of the organism. Mostly known for taking up foreign genes are methanogens that evolved into different species and adapted to new environments (Nelson-Sathi et al., 2015). Integrating genes involved in metabolism and membrane biogenesis (Deschamps et al., 2014) led to the colonization of mesophilic environments (López-García et al., 2015). Sequence analysis revealed that the majority of regulatory function in archaea is executed by bacterial-like regulators (Bell and Jackson, 2001). In the archaeon *Sulfolobus solfataricus* the bacterial leucine-responsive regulatory protein (Lrp) Lrs14 and Sa-Lrp are acting in a negative autoregulatory way by binding to its promoter (Napoli et al., 1999). Regulators from the Lrp family contain an HTH domain as well as many other transcriptional regulators as it is the most common DNA binding motif (Sauer et al., 1982). It is supposed that the HTH domain evolved before Bacteria and Archaea diverged (Pérez-Rueda and Collado-Vides, 2001; Bell and Jackson, 2001). Originating from a common ancestor it is suggested that they have a common interaction mechanism regardless of their

presence in bacteria or archaea. In the RNA polymerase of the genus *Sulfolobus*, a subunit Rpo13 was identified, which might be involved in mRNA elongation. Rpo13 has structural similarity to insertion of the bacterial subunit of *Thermus aquaticus* (Korkhin et al., 2009). The similar structure of archaeal RNA polymerases to bacterial subunits and similarities in function concludes archaeal transcription as a eukaryotic and bacterial composition and therefore a conserved basic function of RNA-polymerases (A Darst, 2001; Hirata and Murakami, 2009).

There are many ways for exchanging genes like by transformation shown in members of Euryarchaeota (Gaudin et al., 2013), by producing membrane vesicles that contain chromosomal or plasmid DNA in Thermococcales (Soler et al., 2008), by virus-like vesicles and extracellular DNA produced by hyperthermophilic archaea, by cell budding shown in Haloarchaea (Mevarech and Werczberger, 1985) and by transduction (Held et al., 2010).

As the origin of histidine kinases is supposed to be from Bacteria it is suggested to be radiated by one of those mechanisms to archaea (Koretke et al., 2000). *M. acetivorans* possesses 64 histidine kinases (Zhang and Shi, 2005) and five hybrid histidine kinases where MA4377 belongs to. This low abundance of hybrid kinases in the organism underlines the suggestion to be integrated by HGT as it is a cluster that rarely occurs relating to the genome size of 5.75 Mbp (Tatusov et al., 2000). Kim and Forst classified histidine kinases due to the sequence of their H-box and N, G1, F, G2 motif in the CA domain (Kim and Forst, 2001). Additionally, they distinguished in their studies between orthodox and unorthodox kinases due to the distance of the conserved histidine to the first asparagine of the N motif located in the CA domain. MA4377 contains a highly conserved H-box (NMS**H**ELRTPL) and CA-domain motifs and can therefore be counted to type class Ia and because of the distance between H and N of 117 aa it is grouped to the orthodox kinases (Kim and Forst, 2001). Three other hybrid histidine kinases of *M. acetivorans* (Ashby, 2006) share the same conserved motifs. Mostly bacterial kinases belong to this class I and are orthodox why this analysis relates to the suggestion of MA4377 to be of bacterial origin.

Another way to trace the bacterial origin of proteins is the difference in codon usage between species. Comparison of the codon usage of MA4377 with the archaeal kinase MsmS showed no significant difference. Even investigations of the promoter region of

MA4377 showed no bacterial -10 and -35 region, instead, a conserved archaeal promoter region containing a TATA like element and a BRE-element were observed.

Furthermore, to investigate the possibility that MA4377 was integrated through transfection the tool PHASTER was used which searches on inserted virus genes. The whole cluster from MA4374 until MA4379 showed no virus insertion. Investigations on sequence similarity with Phyre2, BLASTp (NCBI), and hhpred (MPI Bioinformatics Toolkit) of MA4377 were performed with defined searches. The predictions with a high likelihood were aligned by Clustal Omega. For a better understanding of the relation between the predicted kinases to MA4377, a phylogenetic tree was compiled by Clustal Omega (Figure 4.3). As a reference for archaeal kinases MsmS and RdmS were added.

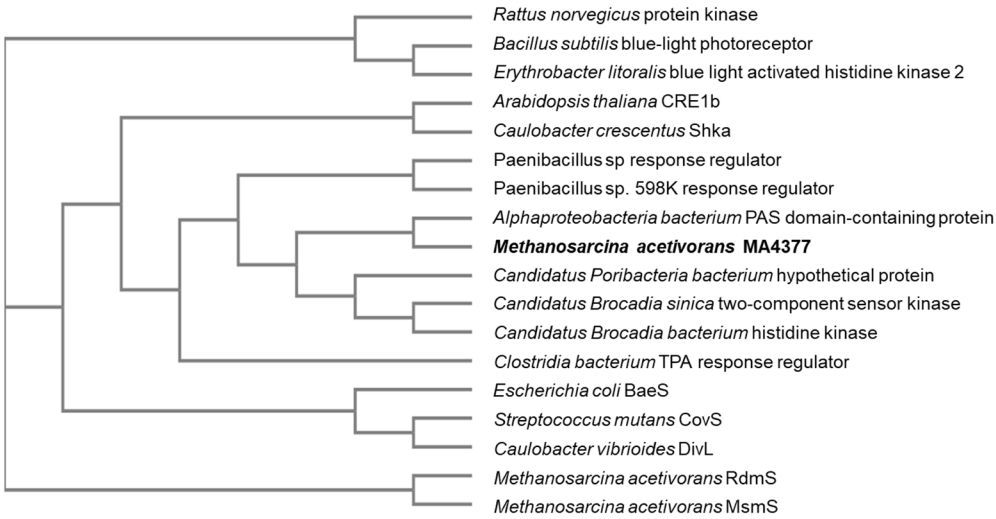

Figure 4.3. Phylogenetic tree of MA4377. Blast analysis with BLAST (NCBI), hhpred, Phyre2, was performed. The phylogenetic tree was generated with the omega clustle tool.

MA4377 is closely related to a kinase of Alphaproteobacteria and kinases from the unapproached *Candidatus* species belonging to the Planctomycetes. Striking of the sequence analysis is the appearance of photoreceptor kinases which could be interesting for further investigation. In general, the abundance of bacterial kinases in a phylogenetic relation shows evidence of MA4377 being related to histidine kinase of bacteria.

4.5 Role of MA4377 as cytokinin sensing hybrid kinase

Histidine hybrid kinases resembling the same structure as MA4377, including a CHASE domain as the first input domain, and two C-terminal fused receiver domains that can also be found in plants (Daudu et al., 2017). CHASE domains are known to be included in phytohormone sensing like the sensor kinase Etr1 binding ethylene or Cre1b sensing cytokinin of *A. thaliana* (Schaller and Bleecker, 1995; Inoue et al., 2001). Cytokinin signaling in plants is involved in a wide range of physiological processes like cell division and light response (Sakakibara, 2006; Zürcher and Müller, 2016) but also in the regulation of osmotic and cold stress (Jeon et al., 2016). The apple tree *Malus domestica* contains a CHASE histidine kinase with two C-terminal fused receiver domains containing both conserved aspartate residues, suggested to improve the complexity of the involved phosphorelay (Daudu et al., 2017). Due to the structural similarity of MA4377 an interaction of *M. acetivorans* with plants could be possible. For complete development of a plant, a symbiotic microbiome is necessary where also *M. acetivorans* belongs to. It could be shown that *M. acetivorans* grows in rice fields where it gains energy by methanogenesis when the fields get flooded and anaerobic conditions prevail (Lueders and Friedrich, 2000). Somehow there is a beneficial effect by interaction with plants which might be the access of compounds for metabolic processes (Moissl-Eichinger et al., 2018). In that case, the hybrid kinase would sense plant vicinity by its transmembrane CHASE domain that is binding a phytohormone. Sensing the possible signal could lead to an activation of the MA4377 phosphorelay that might stimulate metabolism by affecting methanogenesis. There is evidence that bacteria like *Mycobacterium tuberculosis* synthesizing the hormone which influences gene expression (Samanovic et al., 2018) which could also be the case for *M. acetivorans*.

The third domain of MA4377, the PAS domain, was revealed to be the sensor domain, that affects the kinase activity (3.1.5). The kinase showed no activity when the PAS domain was not present. Therefore, it can be concluded that MA4377 is either detecting signals via the PAS domain or gets engaged in protein-protein interaction with help of the PAS domain after sensing a signal via the CHASE domain.

To draw a conclusion, a putative function of MA4377 could be the sensing of a plant hormone by the CHASE domain which gives the organism the information of plant proximity. This signal activates the phosphorelay system including MA4377, R, and

TF, and is affecting methanogenesis by regulating methyltransferases depending on the available substrate. As the hybrid kinase has three sensor domains, it can also sense cytoplasmic signals by the PAS domain that lead to an activation of MA4377 and its MCS. Moreover, this sensitive system gets tightly regulated by R which has various regulatory functions of the kinase phosphorylation state by acting as phosphate sink, phosphatase, and as phosphate donor. Additionally, R is suggested to be involved in cross-regulation with other kinases like RdmS and therefore enhancing the complexity of the MCS of MA4377 (Figure 4.1).

As all results obtained in this study were from *in vitro* experiments in the absence of most signal input domains (PAS domain still present in employed PK construct), it is necessary to include the membrane-bound signaling domains in future studies to confirm the function of MA4377 *in vivo*.

5 Summary

Signal transduction systems are of great importance for the adaptation of organisms to new conditions. These systems occur most frequently in bacteria and are well-understood thanks to research. It was not until 10 years after the discovery of two-component systems in bacteria that such a system was reported in archaea. This work provides new insights into signal transduction in archaea, through the characterization of a histidine kinase MA4377 and its multi-component system in the methanogenic archaeon *Methanosarcina acetivorans*. MA4377 is a hybrid kinase of bacterial origin and was probably integrated into *M. acetivorans* via horizontal gene transfer. Based on the fused receiver domains, MA4377 is classified as a hybrid kinase that regulates a cell response upon the perception of a signal through a multi-component system. These systems consist of four components, the first of which is the kinase. MA4377 has autophosphorylation activity and is phosphorylated at a conserved histidine residue (His_{497}). While the kinase activity is independent of the redox state of the protein, the PAS domain is mandatory for autokinase activity. Using different protein variants, it could be shown that the two fused receiver domains are not involved in the phosphorelay. Rather, the single receiver domain MA4376 serves as the second component of the system. The signal is ultimately transmitted to a transcription factor (MA4375) of the Msr family. Factors of this family are involved in the regulation of methanogenesis, among other things. MA4377 could thus be involved in a multi-component system regulating methanogenesis. The receiver MA4376 plays a central role here since feedback regulation on the kinase was observed. Further investigations will show to what extent cross-regulation with other kinases takes place and in what way the receiver MA4376 plays a key role in this multi-component system.

6 Zusammenfassung

Signaltransduktionssysteme sind für die Anpassung von Organismen an neue Bedingungen von großer Bedeutung. Am häufigsten treten diese Systeme in Bakterien auf und sind dank der Forschung gut verstanden. Erst 10 Jahre nach der Entdeckung von Zwei-Komponenten Systemen in Bakterien wurde über ein solches System in Archaea berichtet. Diese Arbeit liefert neue Erkenntnisse über die Signalübertragung in Archaea, durch die Charakterisierung einer Histidinkinase MA4377 und deren Multi-Komponenten-System in dem methanogenen Archaeon *Methanosarcina acetivorans*. MA4377 ist eine Hybridkinase bakteriellen Ursprungs und wurde vermutlich über horizontalen Gentransfer in *M. acetivorans* integriert. Aufgrund der fusionierten Receiverdomänen wird MA4377 als Hybridkinase klassifiziert, die durch ein Multi-Komponenten-System eine Zellantwort nach Wahrnehmung eines Signals reguliert. Diese Systeme bestehen aus vier Komponenten, wovon die Erste die Kinase darstellt. MA4377 weist Autophosphorylierungsaktivität auf und wird an einem konservierten Histidinrest (His_{497}) phosphoryliert. Während die Kinaseaktivität unabhängig vom Redoxzustand des Proteins ist, wird die PAS- Domäne zwingend für die Autokinase Aktivität benötigt. Mittels verschiedener Proteinvarianten konnte gezeigt werden, dass die beiden fusionierten Receiverdomänen nicht am Phosphorelay beteiligt sind. Vielmehr dient die alleinstehende Receiverdomäne MA4376 als zweite Komponente des Systems. Das Signal wird letztendlich auf einen Transkriptionsfaktor (MA4375) der Msr-Familie übertragen. Faktoren dieser Familie sind u.a. an der Regulation der Methanogenese beteiligt. MA4377 könnte somit in ein die Methanogenese regulierendes Multi-Komponenten-System eingebunden sein. Der Receiver MA4376 nimmt hierbei eine zentrale Rolle ein, da eine Feedbackregulation auf die Kinase beobachtet wurde. Weitere Untersuchungen werden zeigen, inwieweit eine Kreuzregulation zu anderen Kinasen stattfindet und dem Receiver MA4376 somit eine Schlüsselrolle in diesem Multikomponentensystem zukommt

7 References

A Darst, S. (2001). Bacterial RNA polymerase. Current Opinion in Structural Biology **11** (2): 155–162.

Albers, S.-V., and Meyer, B.H. (2011). The archaeal cell envelope. Nat Rev Microbiol **9** (6): 414–426.

Anantharaman, V., and Aravind, L. (2000). Cache – a signaling domain common to animal Ca2+-channel subunits and a class of prokaryotic chemotaxis receptors. Trends in Biochemical Sciences **25** (11): 535–537.

Anjard, Christophe and Loomis, William F. (2003). Histdine Kinases in Signal Transduction: Histidine Kinases of *Dictyostelium*. Elsevier Science: 421–436.

Appleby, J.L., Parkinson, J.S., and Bourret, R.B. (1996). Signal Transduction via the Multi-Step Phosphorelay: Not Necessarily a Road Less Traveled. Cell **86** (6): 845–848.

Aravind, L. and Ponting, C. P. (1997). The GAF domain: an evolutionary link between diverse phototransducing proteins. Elsevier Science (97).

Ashby, M.K. (2006). Distribution, structure and diversity of "bacterial" genes encoding two-component proteins in the Euryarchaeota. Archaea **2** (1): 11–30.

Bell, S.D., and Jackson, S.P. (1998). Transcription and translation in Archaea: a mosaic of eukaryal and bacterial features. Trends in Microbiology **6** (6): 222–228.

Bell, S.D., and Jackson, S.P. (2001). Mechanism and regulation of transcription in archaea. Curr Opin Microbiol **4** (2): 208–213.

Bhate, M.P., Molnar, K.S., Goulian, M., and DeGrado, W.F. (2015). Signal transduction in histidine kinases: insights from new structures. Structure **23** (6): 981–994.

Boccazzi, P., Zhang, J.K., and Metcalf, W.W. (2000). Generation of dominant selectable markers for resistance to pseudomonic acid by cloning and mutagenesis of the ileS gene from the archaeon *Methanosarcina barkeri* fusaro. J Bacteriol **182** (9): 2611–2618.

Bose, A., Kulkarni, G., and Metcalf, W.W. (2009). Regulation of putative methyl-sulphide methyltransferases in *Methanosarcina* acetivorans C2A. Mol Microbiol **74** (1): 227–238.

Bose, A., and Metcalf, W.W. (2008). Distinct regulators control the expression of methanol methyltransferase isozymes in *Methanosarcina acetivorans* C2A. Mol Microbiol **67** (3): 649–661.

Bose, A., Pritchett, M.A., Rother, M., and Metcalf, W.W. (2006). Differential regulation of the three methanol methyltransferase isozymes in *Methanosarcina acetivorans* C2A. J Bacteriol **188** (20): 7274–7283.

Bren, A., and Eisenbach, M. (1998). The N terminus of the flagellar switch protein, FliM, is the binding domain for the chemotactic response regulator, CheY. J Mol Biol **278** (3): 507–514.

Burbulys, D., Trach, K.A., and Hoch, J.A. (1991). Initiation of sporulation in B. subtilis is controlled by a multicomponent phosphorelay. Cell **64** (3): 545–552.

Cadillo-Quiroz, H., Didelot, X., Held, N.L., Herrera, A., Darling, A., Reno, M.L., Krause, D.J., and Whitaker, R.J. (2012). Patterns of gene flow define species of thermophilic Archaea. PLoS Biol **10** (2): e1001265.

Capra, E.J., and Laub, M.T. (2012). Evolution of two-component signal transduction systems. Annu Rev Microbiol **66**: 325–347.

Chang, C., Kwok, S.F., Bleecker, A.B., and Meyerowitz, E.M. (1993). Arabidopsis ethylene-response gene ETR1: similarity of product to two-component regulators. Science **262** (5133): 539–544.

Cheung, J., and Hendrickson, W.A. (2009). Structural analysis of ligand stimulation of the histidine kinase NarX. Structure **17** (2): 190–201.

Cho, U.S., Bader, M.W., Amaya, M.F., Daley, M.E., Klevit, R.E., Miller, S.I., and Xu, W. (2006). Metal bridges between the PhoQ sensor domain and the membrane regulate transmembrane signaling. J Mol Biol **356** (5): 1193–1206.

Cock, P.J.A., and Whitworth, D.E. (2007). Evolution of prokaryotic two-component system signaling pathways: gene fusions and fissions. Molecular biology and evolution **24** (11): 2355–2357.

Conway de Macario, E., Guerrini, M., Dugan, C.B., and Macario, A.J. (1996). Integration of foreign DNA in an intergenic region of the archaeon Methanosarcina mazei without effect on transcription of adjacent genes. J Mol Biol **262** (1): 12–20.

Daudu, D., Allion, E., Liesecke, F., Papon, N., Courdavault, V., Dugé de Bernonville, T., Mélin, C., Oudin, A., Clastre, M., Lanoue, A., Courtois, M., Pichon, O., Giron, D., Carpin, S., Giglioli-Guivarc'h, N., Crèche, J., Besseau, S., and Glévarec, G. (2017). CHASE-Containing Histidine Kinase Receptors in Apple Tree: From a Common Receptor Structure to Divergent Cytokinin Binding Properties and Specific Functions. Front Plant Sci **8**: 1614.

Deppenmeier, U., Lienard, T., and Gottschalk, G. (1999). Novel reactions involved in energy conservation by methanogenic archaea. FEBS Letters **457** (3): 291–297.

Deschamps, P., Zivanovic, Y., Moreira, D., Rodriguez-Valera, F., and López-García, P. (2014). Pangenome evidence for extensive interdomain horizontal transfer affecting lineage core and shell genes in uncultured planktonic thaumarchaeota and euryarchaeota. Genome biology and evolution **6** (7): 1549–1563.

Duclos, B., Marcandier, S., and Cozzone, A.J. (1991). [2] Chemical properties and separation of phosphoamino acids by thin-layer chromatography and/or electrophoresis. In Protein Phosphorylation Part B: Analysis of Protein Phosphorylation, Protein Kinase Inhibitors, and Protein Phosphatases (Elsevier), pp. 10–21.

Esser, D., Hoffmann, L., Pham, T.K., Bräsen, C., Qiu, W., Wright, P.C., Albers, S.-V., and Siebers, B. (2016). Protein phosphorylation and its role in archaeal signal transduction. FEMS Microbiol Rev **40** (5): 625–647.

Fiege, K., and Frankenberg-Dinkel, N. (2019). Thiol-based redox sensing in the methyltransferase associated sensor kinase RdmS in *Methanosarcina acetivorans*. Environmental microbiology **21** (5): 1597–1610.

Fiege, K., Querebillo, C.J., Hildebrandt, P., and Frankenberg-Dinkel, N. (2018). Improved Method for the Incorporation of Heme Cofactors into

Recombinant Proteins Using *Escherichia coli* Nissle 1917. Biochemistry **57** (19): 2747–2755.

Freeman, J.A., Lilley, B.N., and Bassler, B.L. (2000). A genetic analysis of the functions of LuxN: a two-component hybrid sensor kinase that regulates quorum sensing in *Vibrio harveyi*. Mol Microbiol **35** (1): 139–149.

Galagan, J.E., Nusbaum, C., Roy, A., Endrizzi, M.G., Macdonald, P., FitzHugh, W., Calvo, S., Engels, R., Smirnov, S., Atnoor, D., Brown, A., Allen, N., Naylor, J., Stange-Thomann, N., DeArellano, K., Johnson, R., Linton, L., McEwan, P., McKernan, K., Talamas, J., Tirrell, A., Ye, W., Zimmer, A., Barber, R.D., Cann, I., Graham, D.E., Grahame, D.A., Guss, A.M., Hedderich, R., Ingram-Smith, C., Kuettner, H.C., Krzycki, J.A., Leigh, J.A., Li, W., Liu, J., Mukhopadhyay, B., Reeve, J.N., Smith, K., Springer, T.A., Umayam, L.A., White, O., White, R.H., Conway de Macario, E., Ferry, J.G., Jarrell, K.F., Jing, H., Macario, A.J.L., Paulsen, I., Pritchett, M., Sowers, K.R., Swanson, R.V., Zinder, S.H., Lander, E., Metcalf, W.W., and Birren, B. (2002). The genome of M. acetivorans reveals extensive metabolic and physiological diversity. Genome Res **12** (4): 532–542.

Galperin, M.Y., Makarova, K.S., Wolf, Y.I., and Koonin, E.V. (2018). Phyletic Distribution and Lineage-Specific Domain Architectures of Archaeal Two-Component Signal Transduction Systems. J Bacteriol **200** (7).

Gao, R., and Stock, A.M. (2009). Biological insights from structures of two-component proteins. Annu Rev Microbiol **63**: 133–154.

Gardina, P.J., Bormans, A.F., and Manson, M.D. (1998). A mechanism for simultaneous sensing of aspartate and maltose by the Tar chemoreceptor of Escherichia coli. Mol Microbiol **29** (5): 1147–1154.

Gaudin, M., Gauliard, E., Schouten, S., Houel-Renault, L., Lenormand, P., Marguet, E., and Forterre, P. (2013). Hyperthermophilic archaea produce membrane vesicles that can transfer DNA. Environ Microbiol Rep **5** (1): 109–116.

Gilles-Gonzalez, M.-A., and Gonzalez, G. (2004). Signal transduction by heme-containing PAS-domain proteins. Journal of applied physiology (Bethesda, Md. 1985) **96** (2): 774–783.

Grant, S.G., Jessee, J., Bloom, F.R., and Hanahan, D. (1990). Differential plasmid rescue from transgenic mouse DNAs into Escherichia coli methylation-restriction mutants. Proceedings of the National Academy of Sciences of the United States of America **87** (12): 4645–4649.

Grozdanov, L., Raasch, C., Schulze, J., Sonnenborn, U., Gottschalk, G., Hacker, J., and Dobrindt, U. (2004). Analysis of the genome structure of the nonpathogenic probiotic Escherichia coli strain Nissle 1917. J Bacteriol **186** (16): 5432–5441.

Held, N.L., Herrera, A., Cadillo-Quiroz, H., and Whitaker, R.J. (2010). CRISPR associated diversity within a population of *Sulfolobus islandicus*. PLoS ONE **5** (9).

Heyl, A., Wulfetange, K., Pils, B., Nielsen, N., Romanov, G.A., and Schmülling, T. (2007). Evolutionary proteomics identifies amino acids essential for ligand-binding of the cytokinin receptor CHASE domain. BMC evolutionary biology **7**: 62.

Hirata, A., and Murakami, K.S. (2009). Archaeal RNA polymerase. Current Opinion in Structural Biology **19** (6): 724–731.

Hong, E., Lee, H.M., Ko, H., Kim, D.-U., Jeon, B.-Y., Jung, J., Shin, J., Lee, S.-A., Kim, Y., Jeon, Y.H., Cheong, C., Cho, H.-S., and Lee, W. (2007). Structure of an atypical orphan response regulator protein supports a new phosphorylation-independent regulatory mechanism. J Biol Chem **282** (28): 20667–20675.

Inoue, T., Higuchi, M., Hashimoto, Y., Seki, M., Kobayashi, M., Kato, T., Tabata, S., Shinozaki, K., and Kakimoto, T. (2001). Identification of CRE1 as a cytokinin receptor from *Arabidopsis*. Nature **409** (6823): 1060–1063.

Iuchi, S. (1993). Phosphorylation/dephosphorylation of the receiver module at the conserved aspartate residue controls transphosphorylation activity of histidine kinase in sensor protein ArcB of *Escherichia coli*. J Biol Chem (268): 23972–23980.

Jenal, U., and Galperin, M.Y. (2009). Single domain response regulators: molecular switches with emerging roles in cell organization and dynamics. Curr Opin Microbiol **12** (2): 152–160.

Jeon, J., Cho, C., Lee, M.R., van Binh, N., and Kim, J. (2016). CYTOKININ RESPONSE FACTOR2 (CRF2) and CRF3 Regulate Lateral Root Development in Response to Cold Stress in *Arabidopsis*. The Plant Cell **28** (8): 1828–1843.

Jung, K., Fried, L., Behr, S., and Heermann, R. (2012). Histidine kinases and response regulators in networks. Curr Opin Microbiol **15** (2): 118–124.

Kato, M., Mizuno, T., Shimizu, T., and Hakoshima, T. (1997). Insights into Multistep Phosphorelay from the Crystal Structure of the C-Terminal HPt Domain of ArcB. Cell **88** (5): 717–723.

Kennelly, P.J. (2003). Archaeal protein kinases and protein phosphatases: insights from genomics and biochemistry. The Biochemical journal **370** (Pt 2): 373–389.

Kim, D.-J., and Forst, S. (2001). Genomic analysis of the histidine kinase family in bacteria and archaea. Microbiology (Reading) **147** (Pt 5): 1197–1212.

Koretke, K.K., Lupas, A.N., Warren, P.V., Rosenberg, M., and Brown, J.R. (2000). Evolution of two-component signal transduction. Molecular biology and evolution **17** (12): 1956–1970.

Korkhin, Y., Unligil, U.M., Littlefield, O., Nelson, P.J., Stuart, D.I., Sigler, P.B., Bell, S.D., and Abrescia, N.G.A. (2009). Evolution of complex RNA polymerases: the complete archaeal RNA polymerase structure. PLoS Biol: e1000102.

Koziol, J. (1965). Absorption spectra of riboflavin, lumiflavin, and lumichrome in organic solvents. Experientia **21** (4): 189–190.

Krell, T. (2018). Exploring the (Almost) Unknown: Archaeal Two-Component Systems. J Bacteriol **200** (7).

Lassak, J., Bubendorfer, S., and Thormann, K.M. (2013). Domain analysis of ArcS, the hybrid sensor kinase of the *Shewanella oneidensis* MR-1 Arc two-component system, reveals functional differentiation of its two receiver domains. J Bacteriol **195** (3): 482–492.

Lee, J., Tomchick, D.R., Brautigam, C.A., Machius, M., Kort, R., Hellingwerf, K.J., and Gardner, K.H. (2008). Changes at the KinA PAS-A

dimerization interface influence histidine kinase function. Biochemistry **47** (13): 4051–4064.

Leonard, C.J., Aravind, L., and Koonin, E.V. (1998). Novel families of putative protein kinases in bacteria and archaea: evolution of the "eukaryotic" protein kinase superfamily. Genome Res **8** (10): 1038–1047.

Li, J., Zheng, X., Guo, X., Qi, L., and Dong, X. (2014). Characterization of an archaeal two-component system that regulates methanogenesis in *Methanosaeta harundinacea*. PLoS ONE **9** (4): e95502.

Li, J.M., Umanoff, H., Proenca, R., Russell, C.S., and Cosloy, S.D. (1988). Cloning of the *Escherichia coli* K-12 hemB gene. J Bacteriol **170** (2): 1021–1025.

Lopez Munoz, M. (2017). Insights into substrate utilization and transcriprional regulation in *Methanosarcina*. Illinois at Urbana-Champaign. Dissertation.

López-García, P., Zivanovic, Y., Deschamps, P., and Moreira, D. (2015). Bacterial gene import and mesophilic adaptation in archaea. Nat Rev Microbiol **13** (7): 447–456.

Lueders, T., and Friedrich, M. (2000). Archaeal population dynamics during sequential reduction processes in rice field soil. Appl Environ Microbiol **66** (7): 2732–2742.

Martínez-Hackert, E., and Stock, A.M. (1997). The DNA-binding domain of OmpR: crystal structures of a winged helix transcription factor. Structure **5** (1): 109–124.

Metcalf, W.W., Zhang, J.K., Apolinario, E., Sowers, K.R., and Wolfe, R.S. (1997). A genetic system for Archaea of the genus Methanosarcina: liposome-mediated transformation and construction of shuttle vectors. Proceedings of the National Academy of Sciences of the United States of America **94** (6): 2626–2631.

Metcalf, W.W., Zhang, J.K., and Wolfe, R.S. (1998). An anaerobic, intrachamber incubator for growth of *Methanosarcina* spp. on methanol-containing solid media. Appl Environ Microbiol **64** (2): 768–770.

Mevarech, M., and Werczberger, R. (1985). Genetic transfer in *Halobacterium volcanii*. J Bacteriol **162** (1): 461–462.

Miroux, B., and Walker, J.E. (1996). Over-production of proteins in *Escherichia coli*: mutant hosts that allow synthesis of some membrane proteins and globular proteins at high levels. J Mol Biol **260** (3): 289–298.

Mizuno, T. (1997). Compilation of all genes encoding two-component phosphotransfer signal transducers in the genome of *Escherichia coli*. DNA Res **4** (2): 161–168.

Möglich, A., Ayers, R.A., and Moffat, K. (2009). Structure and signaling mechanism of Per-ARNT-Sim domains. Structure **17** (10): 1282–1294.

Moissl-Eichinger, C., Pausan, M., Taffner, J., Berg, G., Bang, C., and Schmitz, R.A. (2018). Archaea Are Interactive Components of Complex Microbiomes. Trends in Microbiology **26** (1): 70–85.

Molitor, B., Stassen, M., Modi, A., El-Mashtoly, S.F., Laurich, C., Lubitz, W., Dawson, J.H., Rother, M., and Frankenberg-Dinkel, N. (2013). A heme-based redox sensor in the methanogenic archaeon *Methanosarcina acetivorans*. J Biol Chem **288** (25): 18458–18472.

Mougel, C., and Zhulin, I.B. (2001). CHASE: an extracellular sensing domain common to transmembrane receptors from prokaryotes, lower eukaryotes and plants. Trends in Biochemical Sciences **26** (10): 582–584.

Mourey, L., Da Re, S., Pédelacq, J.D., Tolstykh, T., Faurie, C., Guillet, V., Stock, J.B., and Samama, J.P. (2001). Crystal structure of the CheA histidine phosphotransfer domain that mediates response regulator phosphorylation in bacterial chemotaxis. J Biol Chem **276** (33): 31074–31082.

Nagasawa, S., Tokishita, S., Aiba, H., and Mizuno, T. (1992). A novel sensor-regulator protein that belongs to the homologous family of signal-transduction proteins involved in adaptive responses in *Escherichia coli*. Mol Microbiol **6** (6): 799–807.

Najnin, T., Siddiqui, K.S., Taha, T., Elkaid, N., Kornfeld, G., Curmi, P.M.G., and Cavicchioli, R. (2016). Characterization of a temperature-responsive two component regulatory system from the Antarctic archaeon, *Methanococcoides burtonii*. Scientific reports **6**: 24278.

Napoli, A., van der Oost, J., Sensen, C.W., Charlebois, R.L., Rossi, M., and Ciaramella, M. (1999). An Lrp-like protein of the hyperthermophilic archaeon *Sulfolobus solfataricus* which binds to its own promoter. J Bacteriol **181** (5): 1474–1480.

Nayak, D.D., and Metcalf, W.W. (2017). Cas9-mediated genome editing in the methanogenic archaeon Methanosarcina acetivorans. Proceedings of the National Academy of Sciences of the United States of America **114** (11): 2976–2981.

Nelson-Sathi, S., Sousa, F.L., Roettger, M., Lozada-Chávez, N., Thiergart, T., Janssen, A., Bryant, D., Landan, G., Schönheit, P., Siebers, B., McInerney, J.O., and Martin, W.F. (2015). Origins of major archaeal clades correspond to gene acquisitions from bacteria. Nature **517** (7532): 77–80.

Nguyen, A.N., Lee, A., Place, W., and Shiozaki, K. (2000). Multistep phosphorelay proteins transmit oxidative stress signals to the fission yeast stress-activated protein kinase. Mol Biol Cell **11** (4): 1169–1181.

Nissle, A. (1917). Die antagonistische Behandlung chronischer Darmstörungen mit Colibakterien. Medizinische Klinik (2): 29–30.

Pappalardo, L., Janausch, I.G., Vijayan, V., Zientz, E., Junker, J., Peti, W., Zweckstetter, M., Unden, G., and Griesinger, C. (2003). The NMR structure of the sensory domain of the membranous two-component fumarate sensor (histidine protein kinase) DcuS of *Escherichia coli*. J Biol Chem **278** (40): 39185–39188.

Parkinson, J.S. (2010). Signaling mechanisms of HAMP domains in chemoreceptors and sensor kinases. Annu Rev Microbiol **64**: 101–122.

Parkinson, J.S., and Kofoid, E.C. (1992). Communication modules in bacterial signaling proteins. Annu Rev Genet **26**: 71–112.

Pas, J., Grotthuss, M. von, **Wyrwicz, L.S., Rychlewski, L., and Barciszewski, J.** (2004). Structure prediction, evolution and ligand interaction of CHASE domain. FEBS Letters **576** (3): 287–290.

Paul, R., Jaeger, T., Abel, S., Wiederkehr, I., Folcher, M., Biondi, E.G., Laub, M.T., and Jenal, U. (2008). Allosteric regulation of histidine kinases by their cognate response regulator determines cell fate. Cell **133** (3): 452–461.

Pérez-Rueda, E., and Collado-Vides, J. (2001). Common history at the origin of the position-function correlation in transcriptional regulators in archaea and bacteria. J Mol Evol **53** (3): 172–179.
Podgornaia, A.I., and Laub, M.T. (2013). Determinants of specificity in two-component signal transduction. Curr Opin Microbiol **16** (2): 156–162.
Posas, F., Wurgler-Murphy, S.M., Maeda, T., Witten, E.A., Thai, T.C., and Saito, H. (1996). Yeast HOG1 MAP Kinase Cascade Is Regulated by a Multistep Phosphorelay Mechanism in the SLN1–YPD1–SSK1 "Two-Component" Osmosensor. Cell **86** (6): 865–875.
Quax, T.E.F., Altegoer, F., Rossi, F., Li, Z., Rodriguez-Franco, M., Kraus, F., Bange, G., and Albers, S.-V. (2018). Structure and function of the archaeal response regulator CheY. Proceedings of the National Academy of Sciences of the United States of America **115** (6): E1259-E1268.
Rasmussen, A.A., Wegener-Feldbrügge, S., Porter, S.L., Armitage, J.P., and Søgaard-Andersen, L. (2006). Four signalling domains in the hybrid histidine protein kinase RodK of *Myxococcus xanthus* are required for activity. Mol Microbiol **60** (2): 525–534.
Reinelt, S., Hofmann, E., Gerharz, T., Bott, M., and Madden, D.R. (2003). The structure of the periplasmic ligand-binding domain of the sensor kinase CitA reveals the first extracellular PAS domain. J Biol Chem **278** (40): 39189–39196.
Rorbert B. Bourret, Katherine A. Borkovich, and and Melvin I. Simon (1991). SIGNAL TRANSDUCTION PATHWAYS INVOLVING PROTEIN PHOSPHORYLATION IN PROKARYOTES. **[Zeitschrift fehlt!]** (60): 401–441.
Rudolph, J., and Oesterhelt, D. (1995). Chemotaxis and phototaxis require a CheA histidine kinase in the archaeon *Halobacterium salinarium*. The EMBO Journal **14** (4): 667–673.
Sakakibara, H. (2006). Cytokinins: activity, biosynthesis, and translocation. Annu Rev Plant Biol **57**: 431–449.
Samanovic, M.I., Hsu, H.-C., Jones, M.B., Jones, V., McNeil, M.R., Becker, S.H., Jordan, A.T., Strnad, M., Xu, C., Jackson, M., Li, H., and Darwin, K.H. (2018). Cytokinin Signaling in *Mycobacterium tuberculosis*. mBio **9** (3).
Sanders, D.A., Gillece-Castro, B.L., Stock, A.M., Burlingame, A.L., and Koshland, D.E. (1989). Identification of the site of phosphorylation of the chemotaxis response regulator protein, CheY. Journal of Biological Chemistry **264** (36): 21770–21778.
Sauer, R.T., Yocum, R.R., Doolittle, R.F., Lewis, M., and Pabo, C.O. (1982). Homology among DNA-binding proteins suggests use of a conserved super-secondary structure. Nature **298** (5873): 447–451.
Schaller, G.E., and Bleecker, A.B. (1995). Ethylene-binding sites generated in yeast expressing the *Arabidopsis* ETR1 gene. Science **270** (5243): 1809–1811.
Soler, N., Marguet, E., Verbavatz, J.-M., and Forterre, P. (2008). Virus-like vesicles and extracellular DNA produced by hyperthermophilic archaea of the order *Thermococcales*. Res Microbiol **159** (5): 390–399.
Soppa, J. (1999). Transcription initiation in Archaea: facts, factors and future aspects. Mol Microbiol **31** (5): 1295–1305.
Sourjik, V., and Schmitt, R. (1996). Different roles of CheY1 and CheY2 in the chemotaxis of *Rhizobium meliloti*. Mol Microbiol **22** (3): 427–436.

Sourjik, V., and Schmitt, R. (1998). Phosphotransfer between CheA, CheY1, and CheY2 in the chemotaxis signal transduction chain of *Rhizobium meliloti*. Biochemistry **37** (8): 2327–2335.

Sowers, K.R., Baron, S.F., and Ferry, J.G. (1984). *Methanosarcina acetivorans sp*. nov., an Acetotrophic Methane-Producing Bacterium Isolated from Marine Sediments. Appl Environ Microbiol **47** (5): 971–978.

Spudich and Stoeckenius (1980). Light-regulated Retinal-dependent Reversible Phosphorylation of *Halobacterium* Proteins. J Biol Chem (Vol.255 No.12): 5501–5503.

Stancik, I.A., Šestak, M.S., Ji, B., Axelson-Fisk, M., Franjevic, D., Jers, C., Domazet-Lošo, T., and Mijakovic, I. (2018). Serine/Threonine Protein Kinases from Bacteria, Archaea and Eukarya Share a Common Evolutionary Origin Deeply Rooted in the Tree of Life. J Mol Biol **430** (1): 27–32.

Steven Hanks and Tony Hunter (1995). The eukaryotic protein kinase superfamily: kinase (catalytic) domain structure and classification[1]. Academic Press, London.

Stock, A.M., Robinson, V.L., and Goudreau, P.N. (2000). Two-component signal transduction. Annu Rev Biochem **69**: 183–215.

Stock, J.B., Ninfa, A.J., and Stock, A.M. (1989a). Protein phosphorylation and regulation of adaptive responses in bacteria. Microbiol Rev **53** (4): 450–490.

Stock, J.B., Ninfa, A.J., and Stock, A.M. (1989b). Protein Phosphorylation and Regulation of Adaptive Responses in Bacteria. Microbiol. Mol. Biol. Rev. (Vol. 53, No. 4): 450–490.

Stock, J.B., Surette, M.G., Levit, M., and Park, P. (1995). Two-Component Signal Transduction Systems: Structure-Function Relationships and Mechanisms of Catalysis. In Two-Component Signal Transduction, J.A. Hoch and T.J. Silhavy, eds (Washington, DC, USA: ASM Press), pp. 25–51.

Studier, F.W., and Moffatt, B.A. (1986). Use of bacteriophage T7 RNA polymerase to direct selective high-level expression of cloned genes. J Mol Biol **189** (1): 113–130.

Tasler, R., Moises, T., and Frankenberg-Dinkel, N. (2005). Biochemical and spectroscopic characterization of the bacterial phytochrome of *Pseudomonas aeruginosa*. FEBS J **272** (8): 1927–1936.

Tatusov, R.L., Galperin, M.Y., Natale, D.A., and Koonin, E.V. (2000). The COG database: a tool for genome-scale analysis of protein functions and evolution. Nucleic Acids Res **28** (1): 33–36.

Taylor, B.L., and Zhulin, I.B. (1999). PAS Domains: Internal Sensors of Oxygen, Redox Potential, and Light. Microbiol. Mol. Biol. Rev. **63** (2): 479–506.

Teale, F.W.J. (1959). Cleavage of the haem-protein link by acid methylethylketone. Biochimica et Biophysica Acta **35**: 543.

Uhl, M.A., and Miller, J.F. (1996). Integration of multiple domains in a two-component sensor protein: the *Bordetella pertussis* BvgAS phosphorelay. The EMBO Journal **15** (5): 1028–1036.

Ulrich, L.E., Koonin, E.V., and Zhulin, I.B. (2005). One-component systems dominate signal transduction in prokaryotes. Trends in Microbiology **13** (2): 52–56.

Vivek Anantharaman and L. Aravind (2001). The CHASE domain: a predicted ligand-binding modulein plant cytokinin receptors and other eukaryotic and bacterial receptors. Trends in Biochemical Sciences (26).

Wagner, A., Whitaker, R.J., Krause, D.J., Heilers, J.-H., van Wolferen, M., van der Does, C., and Albers, S.-V. (2017). Mechanisms of gene flow in archaea. Nat Rev Microbiol **15** (8): 492–501.

Wagner, S., Klepsch, M.M., Schlegel, S., Appel, A., Draheim, R., Tarry, M., Högbom, M., van Wijk, K.J., Slotboom, D.J., Persson, J.O., and Gier, J.-W. de (2008). Tuning *Escherichia coli* for membrane protein overexpression. Proceedings of the National Academy of Sciences of the United States of America **105** (38): 14371–14376.

Wolanin, P.M., and Stock, J.B. (2003). Transmembrane Signaling and the Regulation of Histidine Kinase Activity. In Histidine Kinases in Signal Transduction (Elsevier), pp. 73–122.

Woodward, J.J., Martin, N.I., and Marletta, M.A. (2007). An *Escherichia coli* expression-based method for heme substitution. Nat Methods **4** (1): 43–45.

Zhang, J., Kang, Z., Chen, J., and Du, G. (2015). Optimization of the heme biosynthesis pathway for the production of 5-aminolevulinic acid in Escherichia coli. Scientific reports **5**: 8584.

Zhang, J.K., Pritchett, M.A., Lampe, D.J., Robertson, H.M., and Metcalf, W.W. (2000). In vivo transposon mutagenesis of the methanogenic archaeon *Methanosarcina acetivorans* C2A using a modified version of the insect mariner-family transposable element Himar1. Proceedings of the National Academy of Sciences of the United States of America **97** (17): 9665–9670.

Zhang, J.K., White, A.K., Kuettner, H.C., Boccazzi, P., and Metcalf, W.W. (2002). Directed mutagenesis and plasmid-based complementation in the methanogenic archaeon Methanosarcina acetivorans C2A demonstrated by genetic analysis of proline biosynthesis. J Bacteriol **184** (5): 1449–1454.

Zhang, L. (2011). Heme biology: The secret life of heme in regulating diverse biological processes (Singapore, Hackensack, NJ: World Scientific).

Zhang, W., and Shi, L. (2005). Distribution and evolution of multiple-step phosphorelay in prokaryotes: lateral domain recruitment involved in the formation of hybrid-type histidine kinases. Microbiology (Reading) **151** (Pt 7): 2159–2173.

Zschiedrich, C.P., Keidel, V., and Szurmant, H. (2016). Molecular Mechanisms of Two-Component Signal Transduction. J Mol Biol **428** (19): 3752–3775.

Zürcher, E., and Müller, B. (2016). Cytokinin Synthesis, Signaling, and Function--Advances and New Insights. Int Rev Cell Mol Biol **324**: 1–38.

8 Curriculum vitae

Personal dates

Name:	Anne Sexauer
Date of birth:	08.06.1988
Place of birth	Emmendingen
Adress:	Hauptstrasse 25, 79346 Endingen a.K.
Mailadress:	anne.sexauer@yahoo.de
Nationality:	german

Education

07/2005-06/2008	Graduation of german high school diploma with nutritional science specialization (Abitur) at St. Ursula Schulen in Freiburg, Germany
08/2008-03/2009	theological studies at the private school in Ostermoordorf
04/2009-10/2012:	Bachelor of Science (B. Sc.) in Biology at the TU Kaiserslautern, Germany
10/2012-06/2015:	Master of Science (M. Sc.) in Microbial and Plant Biotechnology at the TU Kaiserslautern, Germany
06/2015-2021:	PhD thesis in the department of Microbiology at the TU Kaiserslautern, Germany

Publications:

Laux, A., Sexauer, A., Sivaselvarajah, D., Kaysen, A., and Brückner, R. (2015). Control of competence by related non-coding csRNAs in *Streptococcus pneumoniae* R6. Frontiers in genetics 6: 246.

Meiers, M., Laux, A., Eichinger, D., Sexauer, A., Marx, P., Bertram, R., and Brückner, R. (2017). A tetracycline-inducible integrative expression system for *Streptococcus pneumoniae*. FEMS Microbiology Letters 364 (5)

9 Supplementary data

9.1 BLASTp analysis in *Methanosarcina spec.*

```
CLUSTAL O(1.2.4) multiple sequence alignment


WP_048122296.1      MNVSRKILAIIYIIFALLISVVIFASQSILGSTFSDLQKKEATDNVEKIENMIDLQILQL    60
WP_048137850.1      MNVSRKIFVIIYIIFALLTSLVIFASQNILYSSFSDLEEKEAIGTVENIHNVIDFQIIQL    60
WP_048171877.1      MNVSRKIFVIIYIIFALLTSLVIFASQNILYSSFSDLEEKEAIGTVENIHNVIDFQIIQL    60
WP_048160861.1      MNVSRKIFVIIYIIFALLTSLVIFASQNILYSSFSDLEEKEAIGTVENIHNVIDFQIIQL    60
MA4377              MNVSRKILVIIYIIFALLTSVVIFASQNILDSSFSGLEEKEAIENVESVHNVIDFQIIQL    60
WP_011024256.1      MNVSRKILVIIYIIFALLTSVVIFASQNILDSSFSGLEEKEAIENVESVHNVIDFQIIQL    60
WP_048174065.1      MNVSKKIFVIIYIIFALLTSVVIFASQNILDSSFSSLEEKEAIENVESVQNVIHFQIIQL    60
WP_048185078.1      MNVSKKIFVIIYIIFALLTSVVIFASQNILDSSFSSLEEKEAIENVESVQNVIHFQIIQL    60
                    ****:**:.********* *:******.** *:**.*::***  .**.:.*:*.:**:**


WP_048122296.1      EKINSDLSSRDDVRNLMLNQGLQNLSSGTPLGDIFSISGCDFIFLVNHSGYIVYSEISDP    120
WP_048137850.1      DETNSALSSREDIRAFMLSENQEDL-GRTVLTDLFTLSGCDFIFFVNSSGHIIYSQVSDS    119
WP_048171877.1      DETNSALSSREDIRAFMLSENQEDL-GRTVLTDLFTLSGYDFIFFVNSSGDIIYSQVSDS    119
WP_048160861.1      DETNSALSSREDIRAFMLSENQEDL-GRTVLTDLFTLSGYDFIFFVNSSGDIIYSQVSDS    119
MA4377              DETSSALVSREDVRAFMVSENPKDL-GGTLLTDLFTLSGCDFVFFVNSSGTMIYSQVSDS    119
WP_011024256.1      DETSSALVSREDVRAFMVSENPKDL-GGTLLTDLFTLSGCDFVFFVNSSGTMIYSQVSDS    119
WP_048174065.1      EETNSALASREDIRAFIVSENPEDL-GGTLLSDLFILNGCDFVFFVNSSGTMIYSQVSDS    119
WP_048185078.1      EETNSALASREDIRAFIVSENPEDL-GGTLLSDLFILNGCDFVFFVNSSGTMIYSQVSDS    119
                    :: .* * **:*:* :::.:. ::* . * * *:* :.* **:*:** ** ::**::**


WP_048122296.1      EPSTSASTLNVSTVTVSTVNASTVNASTVNASYLPIVRQRINDGSLLCKETETSLNGLFL    180
WP_048137850.1      IYASNA----------------------SNDSIIPEINQQINAGSLLCGGEMSPLNGMLL    157
WP_048171877.1      INAGNA----------------------SNDSLIPEINHKINAGSLLCRGETSSLNGMLL    157
WP_048160861.1      INAGNA----------------------SNDSIIPEINHKINAGSLLCRGETSSLNGMLL    157
MA4377              KNASDA----------------------SSDLIITEIDQKINEGDLLCRERLSPLSGILL    157
WP_011024256.1      KNASDA----------------------SSDLIITEIDQKINEGDLLCRERLSPLSGILL    157
WP_048174065.1      KNSSNV----------------------SSDLIIHEFYRKINEGDLLFRERLSPLSGLLL    157
WP_048185078.1      KNASNV----------------------SSDLIIHEFYQKINEGDLLFRERLSPLSGLLL    157
                      : ..                        .   :  . ::** *.**     : *.*::*


WP_048122296.1      LKNGPAIISSQPVFAAPDNNESSGTIILGKYLDSSFIESVQESTGSTFALYSFNNASSDL    240
WP_048137850.1      LKNGPAIVSCRPVSAAYDNREIIGTIILGMNLDSGFVESIQKITGNPVLLYSPDSVPPDF    217
WP_048171877.1      LKNGPAIVSCRPVSAVYDNREIIGTIILGMNLDSGFVESIQKITGNPVLLYSPDNLPPDF    217
WP_048160861.1      LKNGPAIVSCRPVSAAYDNREIIGTIILGMNLDSSFVESIQKITGNPVLLYSPDSVPPDF    217
MA4377              LENGPVIVSCRPVSAALDNSKMIGTIVLGKKLDSDFVDSIQKITGNPVLLYGPDNAPPEF    217
WP_011024256.1      LENGPVIVSCRPVSAALDNSKMIGTIVLGKKLDSDFVDSIQKITGNPVLLYGPDNAPPEF    217
WP_048174065.1      LENGPVIVSCCPVSAAPDNSETIGTIVLGKKLDSGFVESIQKITGNPVLFYGPDNAPPEF    217
WP_048185078.1      LENGPVIVSCCPVSAAPDNSETIGTIVLGKKLDSGFVESIQKITGNPVLFYGPDNAPPEF    217
                    *:***.*:*. ** *. ** :  ***:**  ***.*::*:*: **. . :*. :.   ::


WP_048122296.1      LQAFFENPGPNFTYT--VTGEHVICYSVLEDLSGSPAIVIQTDADSSIYAEGQKALRYIV    298
WP_048137850.1      QQVFFENGNESFTHI--VEGDRLAGYYIHEDLNGNPTVMVRADADRNIYAEGRKSLKYIV    275
WP_048171877.1      QQAFFENGNESFTHI--VEGNRLAGYYIHEDLYGNPTVMVRADADRNIYAEGRKSLKYIV    275
WP_048160861.1      QQAFFENGNESFTHI--VEGNRLAGYYIHEDLYGNPTVMVRADADRNIYAEGRKSLKYIV    275
MA4377              EHVFSENGSENFTQLVDVEGDRLAGYFIHRDINGNPTIMVRTTADRNIYEEGRKSLRYIV    277
WP_011024256.1      EHVFSENGSENFTQLVDVEGDRLAGYFIHRDINGNPTIMVRTTADRNIYEEGRKSLRYIV    277
WP_048174065.1      HQAFLENGNENLTHLVDVEGDRLAGYFIHRDINGNPAIMVRTTADRNIYEEGRKSLKYIV    277
WP_048185078.1      HQAFLENGNENLTHLVDVEGDRLAGYFIHRDINGNPAIMVRTAADRNIYEEGRKSLKYIV    277
                     :.* ** . .:*    * *:::  * : .*: *.*:::::: ** .** **:*:*:***


WP_048122296.1      FFLLFAGLTIGASCKFLLDREVVSRIVAIDNFVEKVRLNENFSERFPMDGDDELSRLSEG    358
WP_048137850.1      LFLLFSGLMVGAVCKFLLDREVVSRIVAIDNFVEKVGKDESFSAHCIMNGDDELSRLTEG    335
WP_048171877.1      LFLLFSGLMVGAVCKFLLDREVVSRIVAIDNFVEKVGKDESFSAHCIMNGDDELSRLTEG    335
WP_048160861.1      LFLLFSGLMVGAVCKFLLDREVVSRIVAIDNFVEKVGKDESFSAHCIMNGDDELSRLTEG    335
MA4377              LFLLFSGLMVGAGCKFLLDREVVSRLVAIDSFVDRVGKDEDFSAHCIMEGDDELSRLTEG    337
WP_011024256.1      LFLLFSGLMVGAGCKFLLDREVVSRLVAIDSFVDRVGKDEDFSAHCIMEGDDELSRLTEG    337
WP_048174065.1      FFLLFSGLMVGAGCKFLLDREVVSRLVAIDTFVDKVGKDEDFSAHCIMEGDDELSRLTEG    337
WP_048185078.1      FFLLFSGLMVGAGCKFLLDREVVSRLVAIDTFVDKVGKDEDFSAHCIMEGDDELSRLTEG    337
                    :****:** :** ************:****.**:*  :*.** :  *:********:**


WP_048122296.1      INQTLDRLKTTSNEFKAQEHEKKLILDSLSELVVFMDSDLKIIWLNKAALDYMGMKMDDV    418
WP_048137850.1      INRMLDRLKINSDKSKAQEHEKRVILNSLSELVIFMDIELRIVWANRASLDHAGLKLENI    395
WP_048171877.1      INRMLDRLKINSDKSKAQEHEKRVILNSLSELVIFMDIELRIVWANRASLDHAGLKLENI    395
WP_048160861.1      INRMLDRLKINSDKSKAQEHEKRVILNSLSELVIFMDIELRIVWANRASLDHAGLKLENI    395
MA4377              INRMLDRLRLNSDKVKAQEHEKKVILNSLSELVIFMDLELKIVWANRASLDYAGLKLENI    397
WP_011024256.1      INRMLDRLRLNSDKVKAQEHEKKVILNSLSELVIFMDLELKIVWANRASLDYAGLKLENI    397
WP_048174065.1      INRMLDRLKLNSDKVKAQEHEKKVILNSLSELVIFMDLELKIVWANRASLDYAGLKLENI    397
WP_048185078.1      INRMLDRLKLNSDKVKAQEHEKKVILNSLSELVIFMDLELKIVWANRASLDYAGLKLENI    397
                    **: ****: .*:: ********::**:******:*** :*:*:* *:*:**: *:*::::


WP_048122296.1      IGQHYQDLYILYKENPGKSPVLKALESGNEEFGEVVTQDGKVWTITAIPIKNEDSRITGI    478
WP_048137850.1      IGHRYEEFSPMSDAVSGESFAQKALESGNEEFGEVVTPDGKVWMIRANLIKDNNGRVTGV    455
WP_048171877.1      IGHRYEEFSPMSDAVSGESFAQKALESGNEEFGEVVTPDGKVWMIRANLIKDNNGRVTGV    455
WP_048160861.1      IGHRYEEFSPMSDAVSGESFAQKALESGNEEFGEVVTPDGKVWMIRANLIKDNNGRVTGV    455
MA4377              VGHSYEKLSPISDAVSGRALAQKALESGNEETGEVVTPDGKIWTIRMNLIKDEDGKVTGF    457
WP_011024256.1      VGHSYEKLSPISDAVSGRALAQKALESGNEETGEVVTPDGKIWTIRMNLIKDEDGKVTGF    457
```

```
WP_048174065.1      IGHSYEELSPMSDAVSGRALAQKALESGKENTGEVATPDGKVWMIRMNLIKDEEGKVTGF    457
WP_048185078.1      IGHSYEELSPMSDAVSGRALAQKALESGKENTGEVATPDGKVWMIRMNLIKDEKGKVTGF    457
                    :*: *:.:  : .   *.: . ******:*: ***.* ***:* *    **::..::**.

WP_048122296.1      LKTGFDITVHRRSEEKLIQAKLEAEEANNSKSEFLTNVSHELRTPLNSIIGFSDILLDKV    538
WP_048137850.1      LQTGLDITAYKRSEEKLLQAKLEAEAASCTKSEFLANMSHELRTPLNSIIGFSDILLERV    515
WP_048171877.1      LQTGLDITAYKRSEEKLLQAKLEAEAASCTKSEFLANMSHELRTPLNSIIGFSDILLERV    515
WP_048160861.1      LQTGLDITAYKRSEEKLLQAKLEAEAASCTKSEFLANMSHELRTPLNSIIGFSDILLERV    515
MA4377              LQTGLDITAHRRSEEKLLQAKLEAEAASCTKSEFLANMSHELRTPLNSIIGFSDILIERV    517
WP_011024256.1      LQTGLDITAHRRSEEKLLQAKLEAEAASCTKSEFLANMSHELRTPLNSIIGFSDILIERV    517
WP_048174065.1      LQTGLDITAHRRSEEKLLQAKLEAEAASCTKSEFLANMSHELRTPLNSIIGFSDILIERV    517
WP_048185078.1      LQTGLDITAHRRSEEKLLQAKLEAEAASCTKSEFLANMSHELRTPLNSIIGFSDILIERV    517
                    *:**:***.::******:******* *. :*****:*:******************:::*

WP_048122296.1      FGDLNEKQFRYISNISTSGKHLLALINDILDLSKVEAGKMELHYSEFSIDSVFEEVKAVL    598
WP_048137850.1      FGELNGKQLRYVNNISTSGKHLLGLINDILDLSKVEAGKMELHYSEFSIDPVFEEVKATL    575
WP_048171877.1      FGELNGKQLRYVNNISTSGKHLLGLINDILDLSKVEAGKMELHYSEFSIESVFEEVKATL    575
WP_048160861.1      FGELNGKQLRYVNNISTSGKHLLGLINDILDLSKVEAGKMELHYSEFSIESVFEEVKATL    575
MA4377              FGELNEKQLKYVNNISGSGKHLLGLINDILDLSKVEAGKMDLHYSEFTVDSVFEEVKSTL    577
WP_011024256.1      FGELNEKQLKYVNNISGSGKHLLGLINDILDLSKVEAGKMDLHYSEFTVDSVFEEVKSTL    577
WP_048174065.1      FGGLNGKQLKYVNNISVSGKHLLGLINDILDLSKVEAGKMELHYSEFTVDSVFEEVKATL    577
WP_048185078.1      FGGLNGKQLKYVNNISVSGKHLLGLINDILDLSKVEAGKMELHYSEFTVDSVFEEVKATL    577
                    ** ** **::*:.*** ******.****************:*******::: ******:.*

WP_048122296.1      SPLIQVKSLEVTFNVESDVTTLEADRGRLIQILYNLVSNAIKFTPNGGKVSVYCKESGNR    658
WP_048137850.1      SPLTQVKSLEISFKVEPDFAAIQADRNRFIQILYNLVSNAVKFTPEGGKISVHCKKSGNR    635
WP_048171877.1      SPLTQVKSLEISFKVEPDFADIQADKNRFIQILYNLVSNAVKFTPEGGKVSVHCIKSGNR    635
WP_048160861.1      SPLTQVKSLEISFKVESDFADIQADKNRFIQILYNLVSNAVKFTPEGGKVSVHCIKSGNR    635
MA4377              FPLAQAKSLEINFVVGPDFGDIQADRSRLIQILYNLVSNAIKFTPEGGRVSVYCKKSGSR    637
WP_011024256.1      FPLAQAKSLEINFVVGPDFGDIQADRSRLIQILYNLVSNAIKFTPEGGRVSVYCKKSGSR    637
WP_048174065.1      SPLFQAKSLEINFVVGPDFGDIQADRSRIIQILYNLVSNAIKFTPEGGRVSVYCKKSGRR    637
WP_048185078.1      SPLFQAKSLEINFVVGPDFGDIQADRSRIIQILYNLVSNAIKFTPEGGRVSVYCKKSGRR    637
                     ** *.****:.* *  *.  ::**:.*:***********:****:**::**:* :** *

WP_048122296.1      ALISVIDTGIGISAEDQVKLFQPFTQLDASTAKQYCGTGLGLALVKKIVNLHQGDIWVES    718
WP_048137850.1      AIFSVTDTGIGISSEDQKKLFQPFTQIDASSAKQYCGTGLGLALVKKIVHLHQGDIWVES    695
WP_048171877.1      AIFSVKDTGIGISSEDQKKLFQPFTQIDASSAKQYCGTGLGLALVKKIVHLHQGDIWVES    695
WP_048160861.1      AIFSVKDTGIGISSEDQKKLFQPFTQIDASSAKQYCGTGLGLALVKKIVHLHQGDIWVES    695
MA4377              ALFSVTDTGIGISSEDQKKLFQPFTQIDSSSARQYCGTGLGLALVKKIVNLHKGDIWVES    697
WP_011024256.1      ALFSVTDTGIGISSEDQKKLFQPFTQIDSSSARQYCGTGLGLALVKKIVNLHKGDIWVES    697
WP_048174065.1      AIFSVMDTGIGISSEDQKKLFQPFTQIDSSSAKQYCGTGLGLALVKKIVNLHQGDIWVES    697
WP_048185078.1      AIFSVMDTGIGISSEDQKKLFQPFTQIDSSSAKQYCGTGLGLALVKKIVNLHQGDIWVES    697
                    *::** *******:*** ********:*:*:*:*****************:**:*******

WP_048122296.1      DPGKGSNFTFSLPLRKPLELRKASKIGIEDVILEFEMSKAAALSVKENIENSQEEVELPE    778
WP_048137850.1      ELEKGSTFMFIIPLTKPPESRKADTKEIDDLMLEFEMNKAATFSVKECAEDLQDEIELPE    755
WP_048171877.1      ELKKGSTFMFIIPLTKPPESRKADTKDIDDLMLEFEMNKAATFSVKECVEDLQEEIELPE    755
WP_048160861.1      ELKKGSTFMFIIPLTKPPESRKADTREIDDLMLEFEMNKAATFSVKEGVEDLLDEIELPE    755
MA4377              ELEKGSTFMFTIPLTKPPESPKADTKGIEDVMLEFEMSKAAAFSAKECEEALKEELELPE    757
WP_011024256.1      ELEKGSTFMFTIPLTKPPESPKADTKGIEDVMLEFEMSKAAAFSAKECEEALKEELELPE    757
WP_048174065.1      ELEKGSTFMFTIPLTKPLESKKTDTGGIEDVMLEFDMSKVAAFSVKGCEEALKEEIELPE    757
WP_048185078.1      ELEKGSTFMFTIPLTKPLESKKTDTGGIEDVMLEFDMSKVAAFSVKGCEEALKEEIELPE    757
                    :  ***.* * :** ** *  *:..  *:*::***:*.*.*::*.*   *   :*:****

WP_048122296.1      ICPSEKGDVKQELILVVDDDKSSSELLSIILKDAGYSVALLYSGKRVLEVAKSLKPDIIT    838
WP_048137850.1      ILLPEKSIGAQNLVLVVDDEMNSNELISVVLREDGYSTASLYRGKDVLYVAKKLKPYVIT    815
WP_048171877.1      VLLPEKSIGAQNLVLVVDDERNSNELISVVLRDDGYSTASLYRGKDVLNVAKKLKPYVIT    815
WP_048160861.1      ILLPEKSIGAQNLVLVVDDERNSNELISVVLREDGYSTASLYRGKDVLNVAKKLKPYVIT    815
MA4377              ILLPENR-EAQSLVLVVDDDINSNELISVVLREAGYSTASLHNGKDVLEVAKKLKPDVIT    816
WP_011024256.1      ILLPENR-EAQSLVLVVDDDINSNELISVVLREAGYSTASLHNGKDVLEVAKKLKPDVIT    816
WP_048174065.1      IFLPENG-EAQNLVLVVDDDINSNELTSVVLREAGYSTASLYNGKDVLEVAKKLKPDVIT    816
WP_048185078.1      IFLPENG-EAQNLVLVVDDDINSNELTSVVLREAGYSTASLYNGKDVLEVAKKLKPDVIT    816
                    :   *:    *.*:*****: .*.** *::*:: ***.* *: ** ** ***.*** :**

WP_048122296.1      LDVFLPDTNGWLVLRQLQNDPYTASIPVLIISMTNNNELGITLGATYSFAKPVKRIELVN    898
WP_048137850.1      LDVFLPDTNGWGVLRQLKSDPETARIPILIISVTDNNELGIAFGATYSFTKPVKRIELLD    875
WP_048171877.1      LDVFLPDTNGWGVLRQLKSDPETARIPILIISVTDNNELGIAFGATYSFTKPVKRIELLD    875
WP_048160861.1      LDVFLPDTNGWGVLRQLKSDPETARIPILIISVTDNNELGIAFGATYSFTKPVKRIELLD    875
MA4377              LDVLLPDTSGWNVLKQLKSDLDTTSIPVLIISVTDNNELGVALGATYSFTKPVRRVELLD    876
WP_011024256.1      LDVLLPDTSGWNVLKQLKSDLDTTSIPVLIISVTDNNELGVALGATYSFTKPVRRVELLD    876
WP_048174065.1      LDVLLPDISGWNVLKQLKSDLDTTSIPVLIISVTDNNELGVALGATYSFTKPVRRVELLD    876
WP_048185078.1      LDVLLPDISGWNVLKQLKSDLDTTSIPVLIISVTDNNELGVALGATYSFTKPVRRVELLD    876
                    ***:*** .** **:**:.*  *: **:****:*:*****:::******:***:*:**::

WP_048122296.1      SLREITGKFRFESPKVLIVDDDENTVELLSSMIEPEGFEVIKAYSGREGLQNLFLEHQPD    958
WP_048137850.1      SLREITGKFRFEEPRILIIDDDDNAVELLSSMIEPEGFEVVKAYSGQEGLDSLFSEQQPD    935
WP_048171877.1      SLREITGKLRFEEPRILIIDDDDNAVELLSSMIEPEGFEVVKAYSGQEGLDSLFSEQQPD    935
WP_048160861.1      SLREITGKLRFEEPRILIIDDDDNAVELLSSMIEPEGFEVVKAYSGQEGLESLFSEQQPD    935
MA4377              SLREITGKFSFDEPKVLIIDDDENAVELLSSMIESEGFEIVKAYSGQAGLDKLFSEQQPD    936
WP_011024256.1      SLREITGKFSFDEPKVLIIDDDENAVELLSSMIESEGFEIVKAYSGQAGLDKLFSEQQPD    936
WP_048174065.1      SLREITGKFSFDEPKVLIIDDDENAVELLSSMIESEGFEIVKAYSGQEGLDKLFSGQQPD    936
WP_048185078.1      SLREITGKFSFDEPKVLIIDDDENAVELLSSMIESEGFEIVKAYSGQEGLDKLFSGQQPD    936
                    ********: *:.*::**:***:*:********* ****::*****: **:.**  :***

WP_048122296.1      ILILDLMMPGISGFDVISSMRADVRTKNIPLIVCTSGELTEKNLEELNSELKGHLISILK    1018
WP_048137850.1      ILILDLLMPGISGFEVISRMRADEKTKDIPLIVCTAGEFTEKNIEELNGELKERFISILK    995
WP_048171877.1      ILILDLLMPGISGFEVISRMRADEKTKDIPLIVCTAGEFTEKNIEELNGELKERLISILK    995
WP_048160861.1      ILILDLLMPGISGFEVISRMRADEKTKDIPLIVCTAGEFTEKNIEELNGELKERLISILK    995
MA4377              ILILDLLMPEISGFEIISRLRDGEQTKDIPLIVCTAGEFTEKNIEKLNGELKGHLISIMK    996
WP_011024256.1      ILILDLLMPEISGFEIISRLRDGEQTKDIPLIVCTAGEFTEKNIEKLNGELKGHLISIMK    996
```

```
WP_048174065.1      ILILDLLMPEISGFEVISYLRAGEQTKDIPLILCTAGESTEKNIEELNGELKGHLISIMK    996
WP_048185078.1      ILILDLLMPEISGFEVISYLRAGERTKDIPLILCTAGESTEKNIEELNGELKGHLISIMK    996
                    ******:** ****::** :* . :**:****:**:** ****:*:**.*** ::***:*

WP_048122296.1      KGTFGRKELINRIKQLTMLKRRNDEKNPDCRR       1050
WP_048137850.1      KGTFGRKELINRIKQLAMLKRREDERNSYCRR       1027
WP_048171877.1      KGTFGRKELINRIKQLAMLKRREDERNSYCRR       1027
WP_048160861.1      KGTFGRKELINRIKQLAMLKRREDERNSYCRR       1027
MA4377              KGTFGRKELINRIKQLAMLKRREDERNSYCRR       1028
WP_011024256.1      KGTFGRKELINRIKQLAMLKRREDERNSYCRR       1028
WP_048174065.1      KGTFGRKELINRIKQLAMLKRREDERNSYCRR       1028
WP_048185078.1      KGTFGRKELINRIKQLAMLKRREDERNSYCRR       1028
                    ***************:*****:**:*  ***
```

Figure S5.1 BLASTp in *Methanosarcina spec*. Domain sequences were predicted with the PROTEIN motif tool. Blue: CHASE4 domain; Light Green: HAMP; Red: PAS; Green-blue: DHp domain; Dark Green: CA-domain; Violet: R1 domain; Grey: R2 domain. In yellow highlighted and in fat formatted amino acids were substituted.

9.2 Oligomerization state of histidine variants

All histidine variants show the same elution volume from the SEC which corresponds to ~120 kDa. The same sample used for SEC was employed to autoradiography (Figure 3.7).

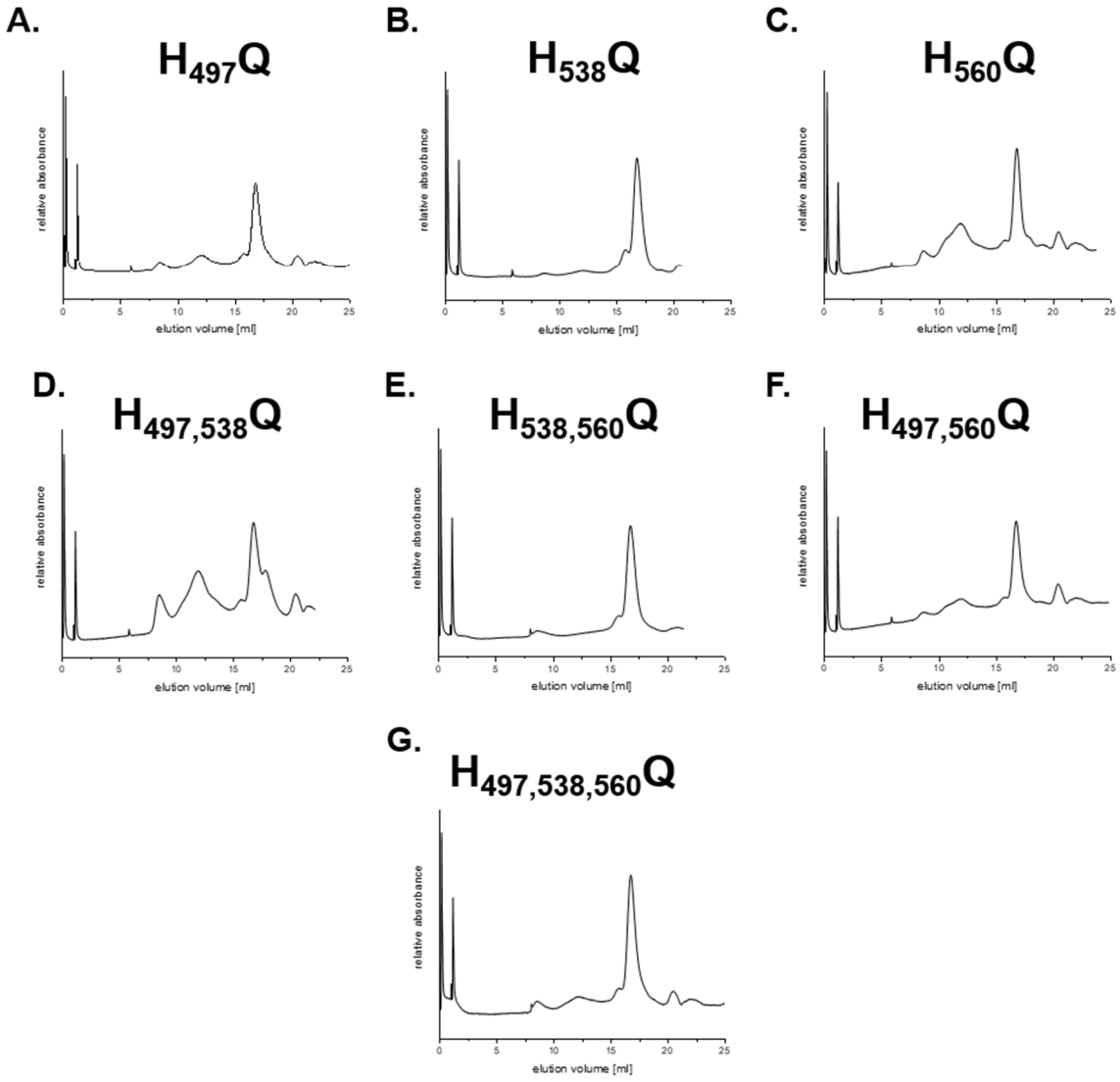

Figure S5.2 SEC profile of all histidine variants of PK. All samples were dialyzed in $NaPOH_4$ pH 7.0 buffer concentrated before loading on Superose^{TM} 6 10/300 GL column. Estimated oligomerization state for loaded histidine variants are: $PKH_{497}Q$, 120 kDa; $PKH_{538}Q$, 120 kDa; $PKH_{560}Q$, 117 kDa; $PKH_{497,538}Q$, 121 kDa; $PKH_{497,560}Q$, 122 kDa, $PKH_{538,560}Q$, 122 kDa; $PKH_{497,538,560}Q$, 123 kDa.

9.3 Activity of MA4377 is redox independent

Kinase assays were performed under oxidized and reduced conditions according to the kinases MsmS and RdmS that might be redox sensitive. Truncated version PK of MA4377 and histidine variants showed activity independent of the redox state (Figure S5.3). Under oxidizing conditions PK is forming oligomers probably due to forming disulfide bonds and shows autophosphorylation activity. Performing kinase assays under reduced conditions reveals kinase activity of PK as monomer. Strikingly is that MA4377 is active weather forming oligomers under oxidizing conditions or being present as monomer under reduced conditions. As the condition inside the cell should be reduced a monomeric active form of MA4377 is reasonable, which is also verified by SEC analysis independent of ATP availability.

To be certain that the phosphorylation under both conditions is specific, kinase assays with histidine variants of PK were performed. Determination of the PK $H_{497}Q$ variant that is unable to autophosphorylate as the phosphorylation site is substituted by glutamate showed no signal under reduced conditions. Interestingly, the same variant showed activity under oxidizing conditions (Figure S5.3.C). The same activity behavior was detected with a variant of both histidine residues $H_{497,538}Q$ (Figure S5.3.D).

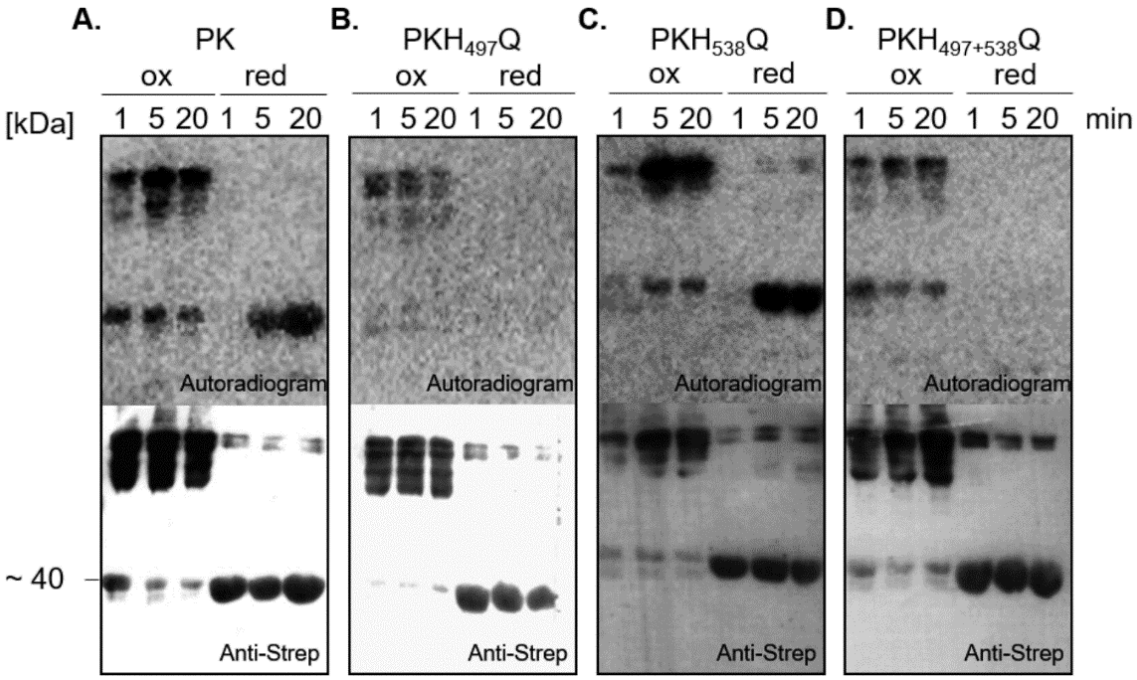

Figure S5.3. Autophosphorylation assay of histidine variants under oxidized and reduced conditions from *E. coli* BL21 (DE3). 10 µM of purified **A.** PK and the histidine variants **B.** $PKH_{497}Q$ **C.** $PKH_{538}Q$ **D.** $PKH_{497+538}Q$

were phosphorylated with [γ-^{32}P]-ATP and samples were taken after 1, 5 and 20 min. Oxidized (ox) conditions contain 4x SDS sample buffer lacking β-mercaptoethanol. Samples under reduced (red) conditions contained DTT (2mM), were flushed with N_2 and stopped with buffer containing β-mercaptoethanol. All samples were resolved on SDS-PAGE and subjected to autoradiography. Proteins were transferred to PVDF membrane and detected by anti-Strep-Tactin®-AP-conjugate.

Under oxidizing conditions oligomeric state of PK is probably formed by disulfide bonds which could not subsequently be verified via SEC profile (Figure S5.4.A1). Adding ATP which is important to activate the kinase activity and therefore important for dimerization could not reveal the oligomeric state of PK (Figure S5.4.A2). Instead all SEC profile of truncated MA4377 versions reveal a long stretched dimer formation. So far, no difference in elution profile under oxidized and reduced condition could be determined. However, it is questionable why a kinase should be active under oxidizing conditions.

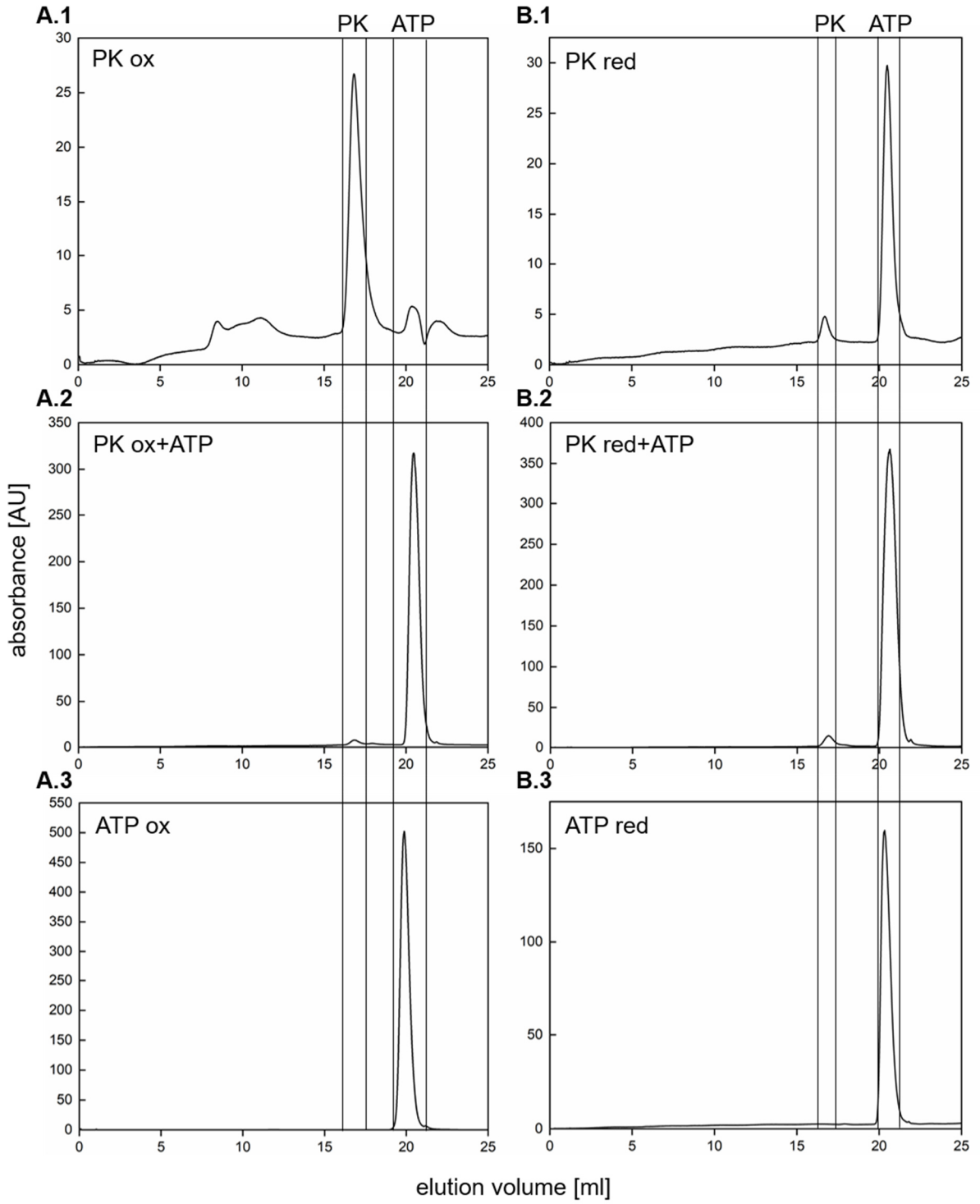

Figure S5.4. SEC profile of PK under oxidized and reduced conditions. Elution profile of purified PK produced in *E. coli* BL21 (DE3) via size exclusion chromatography under oxidized conditions. The protein was separated via a Superose™ 6 10/300 GL column (GE Healthcare) and equilibrated with $NaHPO_4$ buffer pH 7.0. Absorbance of the eluted protein was monitored at a wavelength of 280 nm. **A.1** Elution profile of PK under oxidized condition. **A.2** Elution profile of PK under oxidized condition with ATP (10 mM). **A.3** Elution profile of ATP (10 mM) as reference**. B.** Elution profile of purified PK produced in *E. coli* BL21 (DE3) via size exclusion chromatography under reduced conditions. The protein was separated via a Superose™ 6 10/300 GL column (GE Healthcare) and equilibrated with sonicated $NaPOH_4$ buffer pH 7.0 containing 2 mM DTT. Absorbance of the eluted protein was monitored at a wavelength of 280 nm. **B.1** Elution profile of PK under reduced condition. **B.2** Elution profile of PK under reduced condition with ATP (10 mM). **B.3** Elution profile of ATP (10 mM) as reference.

As reference the transcription factor MA4375, which possesses no autophosphorylation activity, was employed to radioactivity under the same oxidizing and reducing conditions like PK and the histidine residues (Figure 5.5). TF is not able phosphorylate itself but shows a radioactive signal under oxidizing conditions.

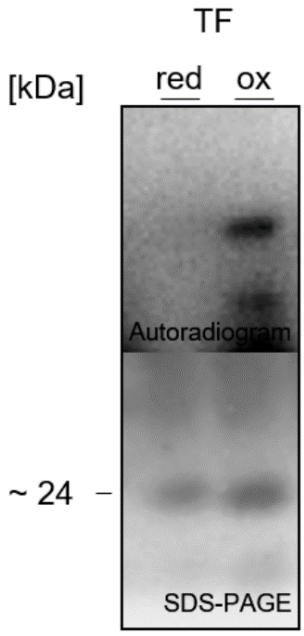

Figure S5.5. Autophosphorylation assay of TF under oxidized and reduced conditions from *E. coli* BL21 (DE3). 10 µM of purified His-tagged TF was phosphorylated with [γ-^{32}P]-ATP and samples were taken after 10 min. Oxidized (ox) conditions contain 4x SDS sample buffer lacking β-mercaptoethanol. Samples under reduced (red) conditions contained DTH, were flushed with N_2 and stopped with buffer containing β-mercaptoethanol. All samples were resolved on SDS-PAGE and subjected to autoradiography. Protein were transferred to PVDF membrane and detected by anti-Strep-Tactin®-AP-conjugate.

Probably disulfide bonds or other factors can lead to an unspecified binding of the radiolabeled γ-[P^{32}]-ATP which results in an unspecific signal and therefore reveal autophosphorylation activity which might be an artifact.

9.4 Removal of excessive [γ-^{32}P]-ATP

The kinase assay revealed that adding the truncated version PKR1R2 to the autophosphorylated PK, is not able to get autophosphorylated itself, after removing excessive [γ-^{32}P]-ATP with illustra™ MicroSpin™ G-50 columns (VWR) (Figure S5.6).

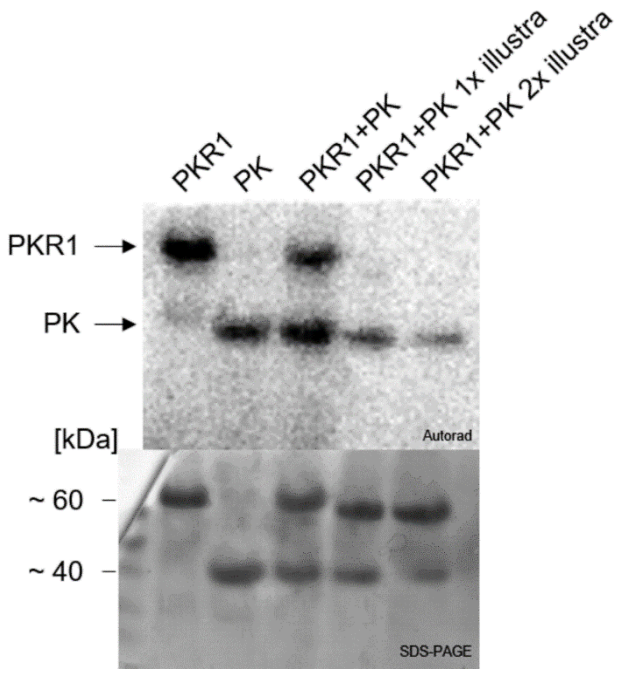

Figure S5.6 Removal of excessive [γ-^{32}P]-ATP with illustra™ MicroSpin™ G-50 columns (VWR). PKR1 (12.1 µg), PK (10 µM), PK+PKR1 show autophosphorylation activity as references. Excessive [γ-^{32}P]-ATP of autophosphorylated PK is removed 1x or 2x with illustra™ MicroSpin™ G-50 columns (VWR). All reactions were stopped after different time points and 10 µl sample resolved on SDS-PAGE, subjected to autoradiography (Autorad.) and Coomassie blue staining to show protein loading (SDS-PAGE).